Universidad de los Andes
Colombia

Solvation and Molecular Encapsulation by Ionic Resorcin[4]arenes in Polar Media

Dissertation zur Erlangung des Doktorgrades der Naturwissenschaften (Dr. rer. nat.) der Naturwissenschaftlichen Fakultät IV Chemie und Pharmazie der Universität Regensburg, Deutschland

Tesis Doctoral para optar al grado de Doctor en Ciencias (Dr. Sc.) otorgado por la Universidad de los Andes, Colombia

vorgelegt von

Nicolás Moreno Gómez

aus Bogota, Kolumbien

Bogota 2018

Declaration

This doctoral thesis was accomplished at the Laboratory of Solutions Thermodynamics of the Universidad de los Andes, Colombia, and the Institute of Physical and Theoretical Chemistry at the University of Regensburg. between August 2013 and May 2018 under the supervision of Prof. Dr. Edgar F. Vargas and Prof. Dr. Richard Buchner. It was developed under the framework of the Joint Cotutelle Agreement between both Universities.

Dissertation submission:	4.6.2018
Dissertation defense:	3.8.2018
Thesis Supervisors:	Prof. Dr. Edgar F. Vargas
	Prof. Dr. Richard Buchner
Examination Committee:	Prof. Dr. Edgar F. Vargas
	Prof. Dr. Richard Buchner
	Prof. Dr. Dominik Horinek
	Prof. Dr. Wolfram Baumann
	Prof. Carmen María Romero, M.Sc.
Committee Chairman:	Prof. Dr. Elizabeth Jimenez

Acknowledgment

The present work was only possible due to the mutual interest in the promotion of high quality research in Chemistry shared by Uniandes and UniRegensburg. I am deeply grateful with the Chemistry Department at Uniandes for granting me an *Asistencia Graduada*, with the Science Faculty for the financial support to elaborate and present the results obtained in this thesis at International Conferences via *Proyectos Semilla* and lastly with *Apoyo Financiero* at Uniandes and the *Internationales Promotionsprogramm der Universität Regensburg*, iPUR, for funding my stays in Regensburg.

Contents

Chapter 1

Introduction

Supramolecular chemistry is perhaps the best tool chemists have today to carry out processes with high efficiency at a molecular level. Arguably, the major goal of this field is to create synthetic receptors with high affinity and high selectivity towards the binding guests[1]. Since its establishment about 30 years ago, supramolecular chemistry has developed various families of synthetic receptors along with some rules that serve as guidelines for their design[2]. Traditionally, the design of receptors has been based on the complementarity between host and guest, neglecting that molecular recognition processes are strongly affected by solvation[2].

The relevance of solvation in supramolecular chemistry has been not fully addressed as reflected by the principle of preorganization[3]. This concept states that when low solvation is present, more stable complexes may be obtained. This idea leads to the development of supramolecular ensembles which serves mostly in non-polar media, were solute-solvent interactions are not too strong. The way how this principle works is illustrated by considering the process to form a host-guest complex in solution[4]. After assuming that both host and guest have structural complementarity, the process will be thus limited by the strength of solute-solvent interactions. Since this kind of interactions depends on the nature of the chemical structure of the solvent and solute molecules, different strengths of association should be expected in different solvents for the same host-guest system. This is reflected by thermodynamic quantities representing the process, where differences in free energy between the solvated forms of the host, guest, and host-guest complex determine the ΔG of complexation[3].

Interestingly, the change of association constants in different solvents showed that association via reversible interactions may be promoted by different driving forces. While association using hydrogen bonding decreases with solvent polarity, solvophobic driven association increases[3,4,5]. This opposite behavior can be explained by the two solvation mechanisms, namely solvophilic and solvophobic solvation. The first one makes references to the direct interaction of the solute with the solvent via electrostatic interactions[6], while the second refers to exclusion of some space accessible otherwise to the solvent molecules by the presence of a solute particle[6] causing a reorganization of solvent structure surrounding the solvophobic moiety of the solute[4].

When solvation is not large, as in non polar media, supramolecular chemist has take advantage of the structural features to obtain systems based on specific inter-

actions, like hydrogen bonding, to promote molecular recognition and self-assembly processes[7]. However, in polar media the situation is different. Polar, and in particular protic solvents, weaken interactions between receptor and guest molecules, narrowing the options to the significantly weaker hydrophobic interactions[7]. Nevertheless, numerous examples encountered in nature suggest that supramolecular chemistry in water is possible[1,7]. If receptors are going to be active in water, which is an indispensable requirement for practical applications, such as detection and quantification of species in medicinal diagnostics or of pollutants in the environment[8], solvation should be considered during their design. Since most of the currently known synthetic receptors were specifically designed for environments exhibiting weak solvation, they cannot be directly used in polar media. However, the development of synthetic receptors for aqueous environments represents a special challenge. First, the host needs to be soluble in water, a basic requirement which severely limits the type of building blocks which can be used for receptor construction, and, second, special interactions and approaches have to be chosen to overcome the competitive interactions of the water with host and guest species[1]. Thus, to properly fulfill the requirements for the design of receptors in water, understanding water-receptor interactions is of crucial importance.

Ionic resorcin[4]arenes are a type of receptors helpful in the study of supramolecular chemistry in polar media, since they have shown the use of electrostatic interaction to form ionic associates and host-guest complexes[9,10]. Among the different reported examples, for this work is of interest the heterodimer formed by two opposite charged *C*-methylresorcin[4]arenes[10], one negatively charged with -SO_3^- groups and the other positively charged with -$(CH_3)_2NH^+$ residues, since a previous study[10] showed that despite the formation of the capsule resembling shaped heterodimer, the inclusion of a guest or "encapsulation" was not possible to achieve. Although it was no stated by the authors[10], this scenario represents the problem described above which despite of considering the structural complementaries, solvents effects prevented the formation of the desired supramolecular ensemble. Therefore, the present work tries to contribute to the understanding of the problem of solvation and molecular encapsulation using ionic resorcin[4]arenes by studying the solvation of the involved ionic *C*-methylresorcin[4]arenes in the heterodimer and their interactions in polar media.

Bibliography

[1] Oshovsky, G. V.; Reinhoudt, D. N.; Verboom, W. *Angew. Chem. Int. Ed.* **2007**, *46*, 2366–2393.

[2] Kataev, E. A.; Mueller, C. *Tetrahedron* **2014**, *70*, 137–167.

[3] Wittenberg, J. B.; Isaacs, L. In *Supramolecular Chemistry: From Molecules to Nanomaterials*; Steed, J. W., Gale, P. A., Eds.; Wiley Online Library, 2012; pp 25–44.

[4] Rekharsky, M.; Inoue, Y. In *Supramolecular Chemistry: From Molecules to Nanomaterials*; Steed, J. W., Gale, P. A., Eds.; Wiley Online Library, 2012; pp 117–134.

[5] Smithrud, D. B.; Diederich, F. *Journal of the American Chemical Society* **1990**, *112*, 339–343.

[6] Kalugin, O. N.; Adya, A. K.; Volobuev, M. N.; Kolesnik, Y. V. *Physical Chemistry Chemical Physics* **2003**, *5*, 1536–1546.

[7] Davis, A. P.; Kubik, S.; Dalla Cort, A. *Organic & biomolecular chemistry* **2015**, *13*, 2499–2500.

[8] Kubik, S. *Chem. Soc. Rev.* **2010**, *39*, 3648–3663.

[9] Kazakova, E. K.; Makarova, N. A.; Ziganshina, A. U.; Muslinkina, L. A.; Muslinkin, A. A.; Habicher, W. D. *Tetrahedron Letters* **2000**, *41*, 10111–10115.

[10] Morozova, Y. E.; Shalaeva, Y. V.; Makarova, N. A.; Syakaev, V. V.; Kazakova, E. K.; Konovalov, A. I. *Russ. Chem. Bull.* **2009**, *58*, 95–100.

Chapter 2

Synthesis of Ionic Resorcin[4]arenes

2.1 Introduction

Resorcin[4]arenes can be considered an appropriate model solute to study the fundamentals behind supramolecular chemistry in solution. They are molecules with an important place among macrocycles due to their structure, which gives them different supramolecular capabilities. The possibility to act as a host and to form well-defined supramolecular ensembles are the two most common abilities[(1)]. Other less known, but of importance, is their ability to form colloidal aggregates[(2)]. The diversity of behaviors is related to the synthetic versatility of resorcin[4]arenes since the preparation and further modifications can be made with relative simplicity[(3,4)]. Additionally, the structural properties of resorcin[4]arenes (Figure 2.1) have permitted them the ability to form capsule-like structures[(1,5)] and to be used as scaffolds towards more complex structures[(6)].

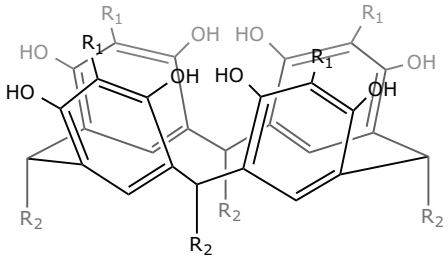

Figure 2.1: General structure of the Resorcin[4]arenes.

Although not completely clear, the main aspects responsible for the supramolecular behavior of resorcin[4]arenes are its residues (R_1 and R_2 in Fig 2.1), conformational properties and solvation in solution. The first one can be exemplified by the results of Korshin et al.[(7)], which show that the usage of ionic moieties not only increases the solubility in polar media, but also confers the possibility of ionic interactions. The second one, the conformation, is of importance because the resorcin[4]arene structure may exist in different conformations and configurations[(4)], see Figure 2.2. This diversity arises from the fact that the methine carbons, which serve as a bridge between aromatic units and the R_2 substituent, are stereogenic centers that allow the existence of four different diastereomers. Moreover, the conformation

in solution depends on the synthesis conditions of the resorcin[4]arene as well as on the nature of the medium (solvation)[8]. These aspects are relevant to understand the dependence of the interaction with the solvent, as seen in other systems[9,10,11], for example, resorcin[4]arenes with aliphatic moieties have shown that in protic solvents boat conformations are preferred, whereas in aprotic media an "averaged" crown conformation is observed[12].

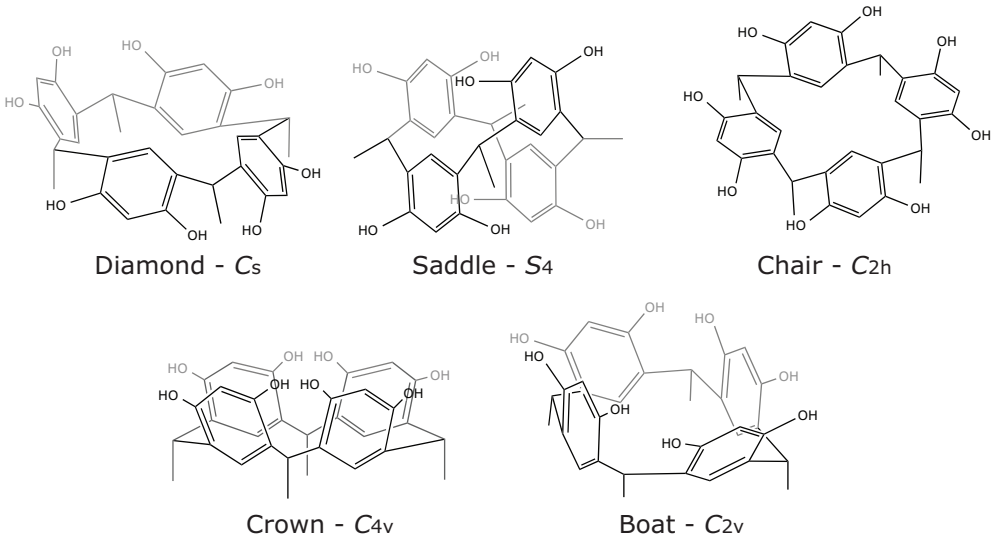

Figure 2.2: Most common Resorcin[4]arenes conformations using the methylresorcin[4]arene, Fig. 2.1 with R_1= -H and R_2= -CH_3, as example for clarity

One drawback of the elemental resorcin[4]arene structure is the limited solubility in water[13], where many interesting supramolecular phenomena takes place. This limitation can be addressed by including ionic moieties[7,14,15]. With this in mind, this chapter presents the synthetic process to the preparation of two ionic *C*-methylresorcin[4]arenes with appreciable solubility to be studied as a function of concentration with different techniques. Two substitutions that prove to be useful for this purpose are sulphonation (Fig 2.1, R_1=-CH_2SO_3Na) and aminomethylation with subsequent formation of the hydrochloride salt (Fig. 2.1, R_1=-$CH_2(CH_3)_2NHCl$). In the next sections, the details for the preparation of two ionic resorcin[4]arenes soluble in water, namely *C*-methylresorcin[4]arene sodium tetrasulphonate and *C*-methylresorcin[4]arene tetraminomethylated hydrochloride are presented with the corresponding product characterization.

2.2 Synthesis of ionic Resorcin[4]arenes

Preparation of ionic resorcin[4]arenes consists of a two-step procedure. First the elementary structure (Fig. 2.1) is prepared via acid catalyzed condensation of resorcinol with an aldehyde[4,8,16]. Afterward, the introduction of ionic moieties in the upper rim of the resorcin[4]arene structure (R_1, Fig. 2.1) is done using formaldehyde and the corresponding substituent.

2.2.1 Synthesis of *C*-methylresorcin[4]arene

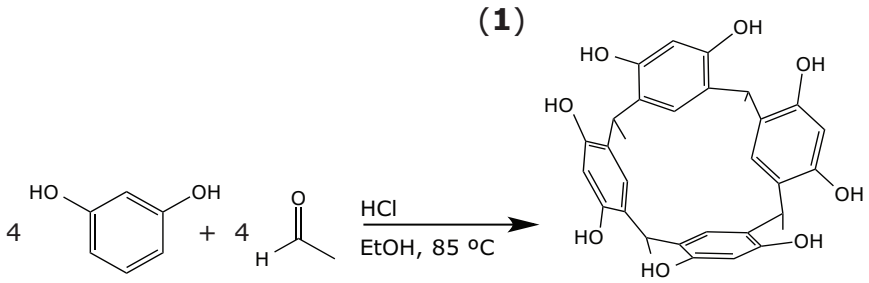

Figure 2.3: Synthesis of the *C*-methylresorcin[4]arene via acid catalyzed condensation of Resorcinol and Acetaldehyde

Synthesis of the common basic structure **1** (*C*-methylresorcin[4]arene; 2,4,6,8-tetramethyl-1,3,5,7(1,3)-tetrabenzenacyclooctaphan-$1^4, 1^6, 3^4, 3^6, 5^4, 5^6, 7^4, 7^6$-octanol, CAS 65338-98-9) was achieved by following the procedure described by Tunstad[16] (described in Figure 2.3): To a solution of resorcinol (CAS 108-46-3, Alfa Aesar 99%, 0.25 mol) in ethanol (CAS 64-17-5, Alfa Aesar HPLC Grade, 300 mL), concentrated hydrochloric acid (HCl, CAS 7647-01-0, Sigma-Aldrich 37%, 0.47 mol) was added and the solution cooled to 0 ℃ before adding acetaldehyde (CAS 75-07-0, Panreac 99%, 0.25 mol) drop-wise over a period of 45 min. The reaction mixture was refluxed for 8 h and then poured carefully into 600 mL ice-cold water. The precipitated solid was filtered, recrystallized from water, and dried at 65 ℃ for 18 h. The product was obtained as a pale-yellow powder in 85 % yield.

2.2.2 Synthesis of *C*-methylresorcin[4]arene tetraminomethylated hydrochloride ($\mathrm{TAM} \cdot (\mathrm{HCl})_4$)

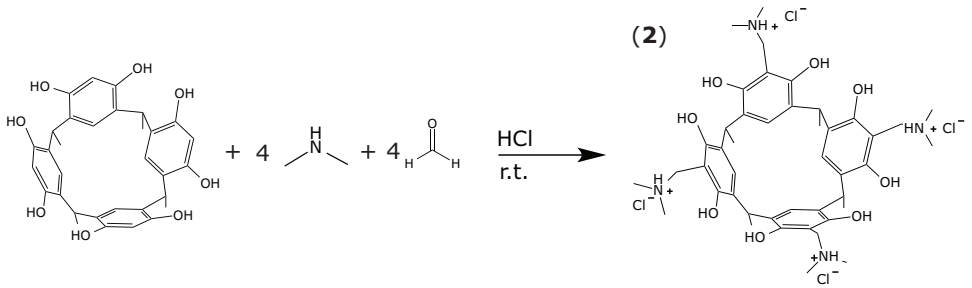

Figure 2.4: Synthesis of the Tetraminomethylated *C*-methylresorcin[4]arene hydrochloride, $\mathrm{TAM} \cdot (\mathrm{HCl})_4$.

Tetraminomethylated *C*-methylresorcin[4]arene, (**2**) ($\mathrm{TAM} \cdot (\mathrm{HCl})_4$, 1,1',1",1"'-($1^4, 1^6, 3^4, 3^6, 5^4, 5^6, 7^4, 7^6$-octahydroxy-2,4,6,8-tetramethyl-1,3,5,7(1,3)- tetrabenzenacyclooctaphane-$1^5, 3^5, 5^5, 7^5$-tetrayl)tetrakis(*N*, *N*-dimethylmethanaminium) chloride) was obtained by modifying the procedures of Matsushita[17] and Morozova[15]. Here, the *C*-methylresorcin[4]arene (18 mmol) was dissolved in 33 mL of a 1:1 mixture of ethanol and toluene (CAS 108-88-3, Sigma-Aldrich 99.8%). Then a mixture of 9.7 mL formaldehyde dissolved in methanol (37-38% w/w, CAS 50-00-0, Panreac) and 11.4 mL aqueous dimethylamine (40% w/w, CAS 124-40-3, Sigma-Aldrich) was added. The reaction mixture was stirred at room temperature for 8 h and then

concentrated hydrochloric acid added drop-wise until the gas evolution stopped. Of the formed two-phase mixture, the upper toluene-rich translucent phase was discarded. The lower phase was poured into cold ethanol (150 mL) and allowed to stand overnight. The precipitated solid was filtered and collected. In cases where the product did not precipitate, the solvent was removed with a rotary evaporator and the residue dried at 60 ℃ overnight. The pulverized material was purified by Soxhlet extraction with ethanol and subsequent solvent remove. The final product, obtained as a pale-pink powder in 65 % yield, was dried at 60 ℃ for 18 h.

2.2.3 Synthesis of *C*-methylresorcin[4]arene sodium tetrasulphonate (Na_4TES)

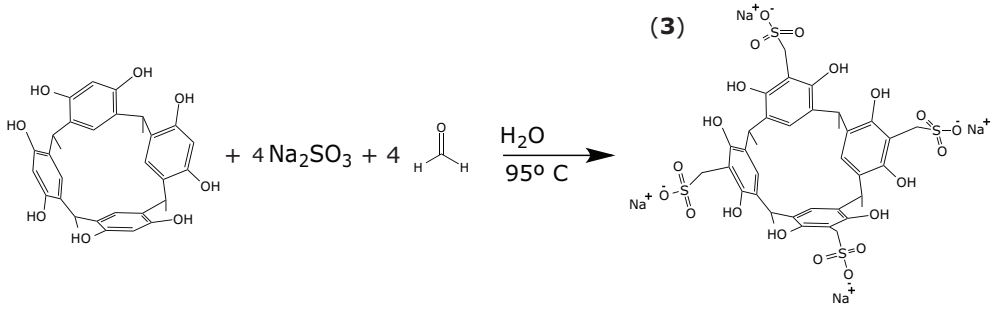

Figure 2.5: Synthesis of the *C*-methylresorcin[4]arene sodium tetrasulphonate, Na_4TES.

Functionalization of **1** with sulfonate groups was done following Kazakova et al reported procedure[14]. The obtained compound **3** (Na_4TES, Sodium ($1^4, 1^6, 3^4, 3^6, 5^4, 5^6, 7^4, 7^6$-octahydroxy-2,4,6,8-tetramethyl-1,3,5,7(1,3)-tetrabenzenacyclooctaphane $1^5, 3^5, 5^5, 7^5$tetrayl) tetramethanesulfonate) was synthesized by dissolving The *C*-methylresorcin[4]arene (**1**, 1.3 mmol) in a mixture of Sodium Sulfite (CAS 7757-83-7, Sigma-Aldrich 98%, 5.2 mmol), Formaldehyde (37%, 0.4 mL) and Water (4 mL). The mixture was heated to $90-95°$ for 4h. After cooling down to room temperature, HCl (37%, 0.3 mL) was added. Then, acetone (20 mL) was added to the mixture causing the precipitation of the sulfonated resorcin[4]arene. The compound was recrystallized from Acetone(90% v/v)/Water mixtures. The final product, obtained as a pale-red powder in 50 % yield, was dried at 60 ℃ for 18 h.

2.3 Characterization

Characterization was done using solution Nuclear Magnetic Resonance, NMR, and Mass spectrometry. Proton NMR, ^{1}HNMR, is a convenient way to characterize resorcin[4]arenes. Considering that resorcin[4]arenes display different conformations (Figure 2.2), its assignment can be done using the signal pattern of the ^{1}H-NMR spectrum[12]. As shown in Figure 2.6 the number of signals coincide with the number of hydrogen nuclei in a single unit of resorcin[4]arene, indicating that the most probable configuration is the all-*cis* crown conformation (C_{4v}) as product of the equilibrium between boat conformations[12]. Comparison with previously reported

spectra[15] shows good agreement. Similar results were obtained both in Deuterated Water (D_2O) and deuterated Dimethylsulfoxide (DMSO-d_6). Additional analysis of the ^{13}C-NMR confirms the connectivity of the structures.

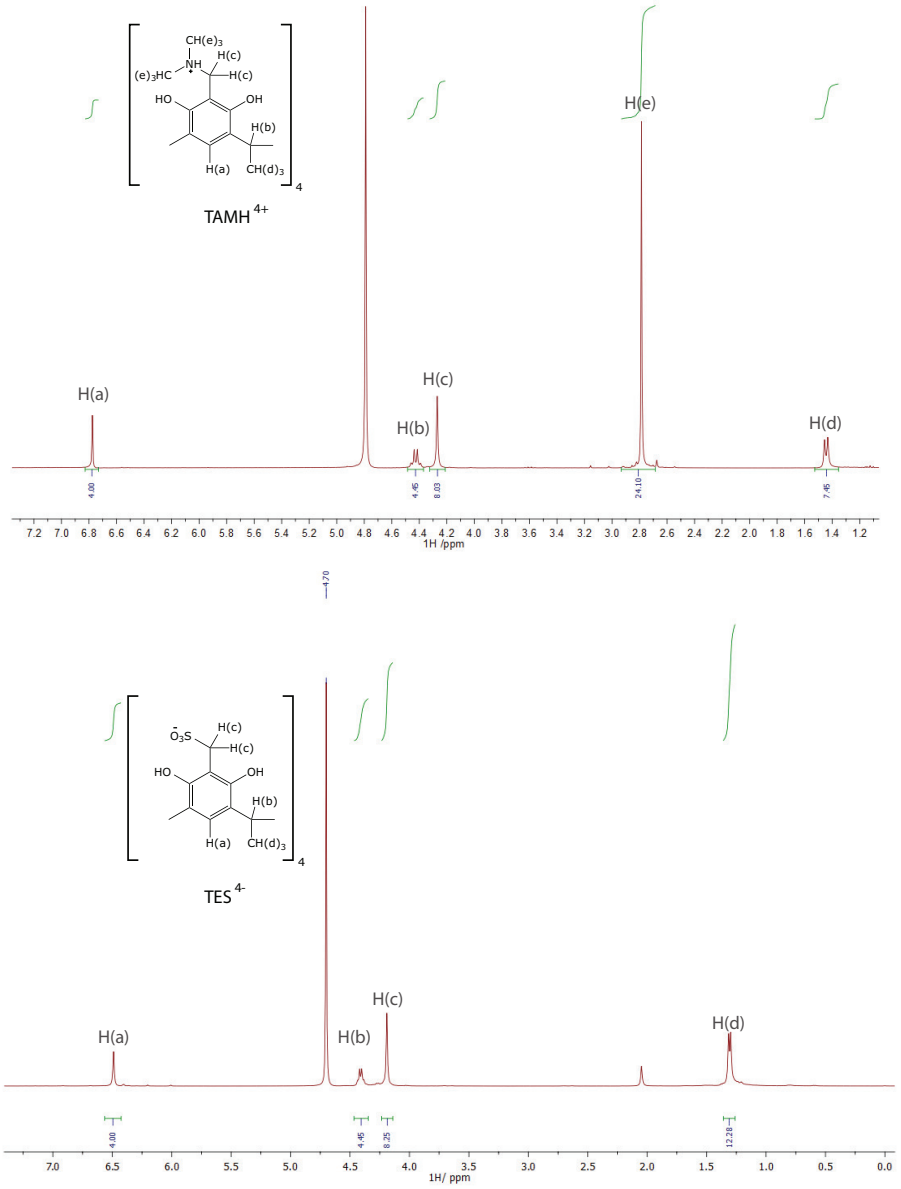

Figure 2.6: ^{1}H-NMR spectrum of TAM $\cdot$ $(HCl)_4$ and Na_4TES in deuterated water (D_2O). The presence of only five signals suggest an averaged crown conformation (C_{4V}, Fig.2.2)[12].

***C*-methylresorcin[4]arene, (1)**: ^{1}H NMR (400 MHz, DMSO-d_6) δ (ppm) 8.45 (s, 8H, O**H**), 6.64 (s, 4H, C**H**-Ar, meta to OH), 6.02 (s, 4H, C**H**-Ar, ortho to OH), 4.33 (d, J = 7.1 Hz, 4H, C**H**), 1.17 (d, J = 7.0 Hz, 12H, C**H**$_3$). ^{13}C NMR (101 MHz, DMSO-d_6) δ (ppm) 152.0 (**C**-Ar), 125.4 (**C**H-Ar, meta to OH), 123.2 (**C**-Ar), 102.2 (**C**H-Ar, ortho to OH), 28.7 (**C**H), 21.76 (**C**H$_3$).

***C*-methylresorcin[4]arene tetraminomethylated hydrochloride, (2), (TAM·(HCl)$_4$)**: ^{1}H NMR (400 MHz, DMSO-d_6) δ (ppm) 9.26 (br s, 8H, O**H**), 7.36 (s, 4H, C**H**-Ar, metha to OH), 4.69 (d, J = 6.5 Hz, 4H, C**H**), 4.26 (s, 8H, C**H**$_2$), 3.41 (br s, 4H, N**H**), 2.66 (s, 24H, N-C**H**$_3$), 1.61 (d, J = 6.1 Hz, 12H, CH3). ^{13}C NMR (101 MHz, DMSO-d_6) δ (ppm) 150.9 (**C**-Ar), 127.0 (**C**-Ar), 126.5 (**C**H-Ar), 108.2 (**C**-Ar), 50.8 (**C**H$_2$), 42.2 (N-**C**H$_3$), 29.9 (**C**H), 20.3 (**C**H$_3$).

***C*-methylresorcin[4]arene sodium tetrasulphonate, (3), (Na$_4$TES)**: ^{1}H NMR (400 MHz, D$_2$O) δ (ppm) 6.62 (s, 4H, C**H**-Ar), 4.54 (q, J = 6.6 Hz, 4H, C**H**), 4.31 (s, 8H, C**H**$_2$), 1.44 (d, J = 6.4 Hz, 12H, C**H**$_3$). ^{13}C NMR (101 MHz, D$_2$O) δ (ppm) 150.2 (**C**-Ar), 127.5 (**C**-Ar), 124.9 (**C**H-Ar), 110.0 (C-Ar ortho to OH), 47.1 (**C**H$_2$), 31.7 (**C**H), 19.4 (**C**H$_3$).

Confirmation of resorcin[4]arenes TAM · (HCl)$_4$ and Na$_4$TES was also achieved using mass spectrometry. The instrument used was an HPLC Agilent 1260 infinity with a Q-ToF (6520) detector. Figure 2.7 confirms the formation of the Na$_4$TES with the signal m/z = 941.07 which correspond to the ion $[NaC_{36}H_{38}O_{20}S_4]^-$. In the same way, Figure 2.7 also show the preparation of TAM · (HCl)$_4$ with the signal at m/z = 919.08 which is close to the calculate compound mass of 918.82 g mol^{-1}.

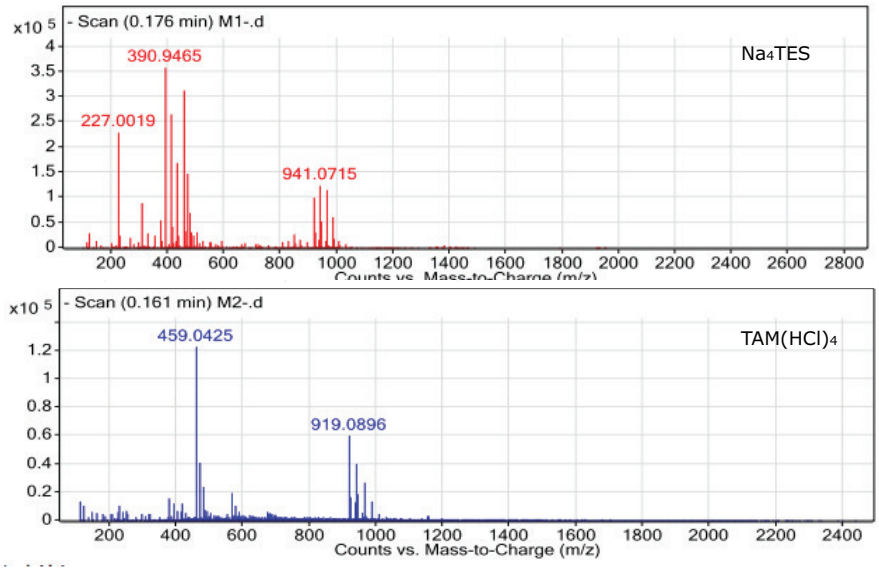

Figure 2.7: ESI Mass spectra of Na$_4$TES and TAM · (HCl)$_4$

Purity was evaluated using High-Performance Liquid Chromatography (Hewlett Packard 1100 HPLC with quaternary pump) using manual injection and using a variable wavelength detector (VWD). The column used is ProntoSil 200-5-C18 ace -EPS 5.0 (250 mm x 4.6 mm; 5.0 μm; 200 Å). Samples were dissolved in water and the mobile phase consisted in mixtures of Acetonitrile (A) and Phosphate buffer 25 mM pH = 7 (B). Elution was done with the following Gradient: 0-6 min 30% B and 6-10 min 30-50% B. Detection was done at wavelength of 277 nm. Chromatograms in figure 2.8 showed that Na$_4$TES is detected with a retention time of 5.6 min and TAM · (HCl)$_4$ with 6.0 min. The Na$_4$TES chromatogram showed an additional peak at 4.9 min which is also detected in a blank run, thus it can not be attributed

as a major impurity of the compound, and area comparison indicates a purity of 0.99. In the case of $TAM \cdot (HCl)_4$, a peak with a tail that is not present in the blank run. If this tail found in $TAM \cdot (HCl)_4$ chromatogram is attributed to different configurations, the calculated chromatographic purity is 0.99 for $TAM \cdot (HCl)_4$. Additional determinations using quantitative NMR (qNMR)[18] with Maleic Acid (CAS 110-16-7, 0.99, Sigma-Aldrich) as internal standard give a mass fraction purity of 0.99.

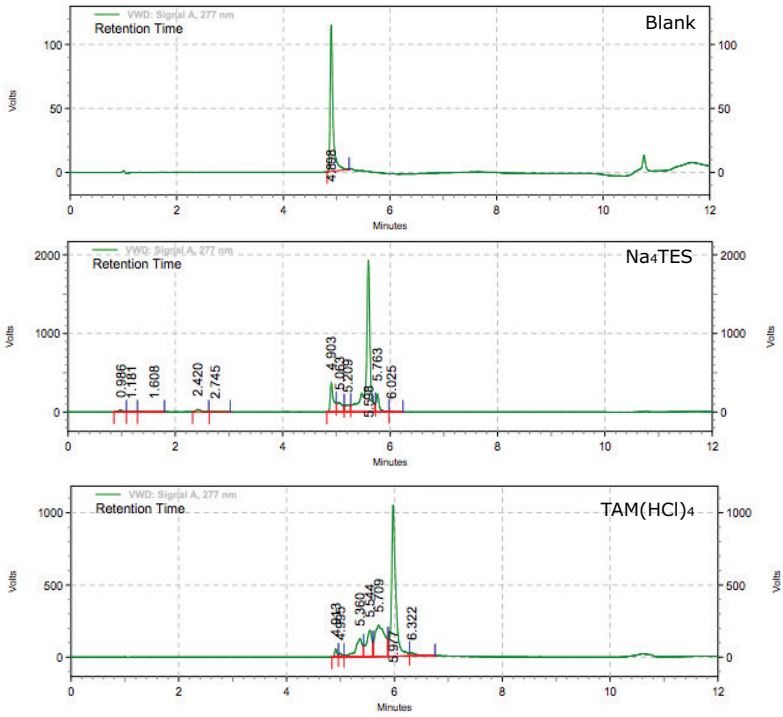

Figure 2.8: HPLC-DAD Chromatograms of Na_4TES and $TAM \cdot (HCl)_4$ using a mixture of Acetonitrile-Phospate Buffer (25 mM, pH = 7) as mobile phase.

It has been reported than resorcin[4]arenes may form solvates after recrystallization[19,20]. For this reason, thermogravimetric analysis (TGA) was carried out using a Netzch STA 409 thermobalance in a temperature range from 283 K up to 974 K at rate of 10 K/min. Analysis of the TG thermogram suggests a mass loss of 5 % for Na_4TES and 4% for $TAM \cdot (HCl)_4$. This mass reduction is coherent with the presence of hydrates: $TAM \cdot (HCl)_4 \cdot 2H_2O$ and $Na_4TES \cdot 3H_2O$. However, hydrates formation was prevented by further recrystallization and longer drying periods with vacuum and proper storage. This was reflected in the TG by decreasing the mass loss percentage (1.7% for Na_4TES, 2.2% for $TAM \cdot (HCl)_4$). Additional drying in the presence of of phosphorous pentoxide reduce humidity as shown by analysis using Coulometric Karl-Fisher titration, which yield a humidity less than 0.1%.

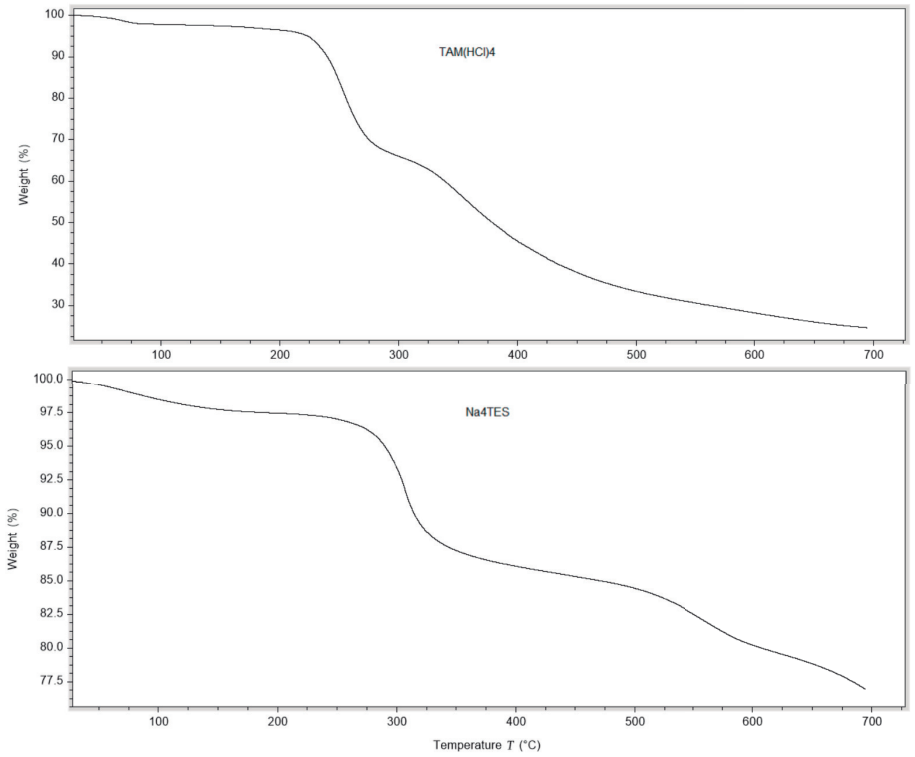

Figure 2.9: Thermogravimetric Analysis of TAM · $(HCl)_4$ (top) and Na_4TES (down) *C*-methylresorcin[4]arenes.

Bibliography

[1] Avram, L.; Cohen, Y.; Rebek Jr, J. *Chemical Communications* **2011**, *47*, 5368–5375.

[2] Helttunen, K.; Shahgaldian, P. *New Journal of Chemistry* **2010**, *34*, 2704–2714.

[3] Cram, D. J.; Karbach, S.; Kim, H. E.; Knobler, C. B.; Maverick, E. F.; Ericson, J. L.; Helgeson, R. C. *Journal of the American Chemical Society* **1988**, *110*, 2229–2237.

[4] Jain, V.; Kanaiya, P. *Russian Chemical Reviews* **2011**, *80*, 75–102.

[5] MacGillivray, L. R.; Atwood, J. L. *Nature* **1997**, *389*, 469.

[6] Sliwa, W.; Kozlowski, C. *Calixarenes and Resorcinarenes. Synthesis, Properties and Applications*; Wiley Online Library, 2009.

[7] Korshin, D. E.; Kashapov, R. R.; Murtazina, L. I.; Mukhitova, R. K.; Kharlamov, S. V.; Latypov, S. K.; Ryzhkina, I. S.; Ziganshina, A. Y.; Konovalov, A. I. *New Journal of Chemistry* **2009**, *33*, 2397–2401.

[8] Timmerman, P.; Verboom, W.; Reinhoudt, D. N. *Tetrahedron* **1996**, *52*, 2663–2704.

[9] Smithrud, D. B.; Diederich, F. *Journal of the American Chemical Society* **1990**, *112*, 339–343.

[10] Diehl, K. L. et al. *Synthetic Receptors for Biomolecules: Design Principles and Applications*; The Royal Society of Chemistry, 2015; pp 39–85.

[11] Sommer, F.; Marcus, Y.; Kubik, S. *ACS Omega* **2017**, *2*, 3669–3680.

[12] Abis, L.; Dalcanale, E.; Du vosel, A.; Spera, S. *Journal of the Chemical Society, Perkin Transactions 2* **1990**, 2075–2080.

[13] Franco, L. S.; Salamanca, Y. P.; Maldonado, M.; Vargas, E. F. *Journal of Chemical & Engineering Data* **2009**, *55*, 1042–1044.

[14] Kazakova, E. K.; Makarova, N. A.; Ziganshina, A. U.; Muslinkina, L. A.; Muslinkin, A. A.; Habicher, W. D. *Tetrahedron Letters* **2000**, *41*, 10111–10115.

[15] Morozova, Y. E.; Shalaeva, Y. V.; Makarova, N. A.; Syakaev, V. V.; Kazakova, E. K.; Konovalov, A. I. *Russ. Chem. Bull.* **2009**, *58*, 95–100.

[16] Tunstad, L. M.; Tucker, J. A.; Dalcanale, E.; Weiser, J.; Bryant, J. A.; Sherman, J. C.; Helgeson, R. C.; Knobler, C. B.; Cram, D. J. *The Journal of Organic Chemistry* **1989**, *54*, 1305–1312.

[17] Matsushita, Y.; Matsui, T. *Tetrahedron letters* **1993**, *34*, 7433–7436.

[18] Bharti, S. K.; Roy, R. *TrAC Trends in Analytical Chemistry* **2012**, *35*, 5–26.

[19] Pietraszkiewicz, O.; Utzig, E.; Zielenkiewicz, W.; Pietraszkiewicz, M. *Journal of thermal analysis and calorimetry* **1998**, *54*, 249–255.

[20] Sanabria, E.; Esteso, M. A.; Pérez-Redondo, A.; Vargas, E.; Maldonado, M. *Molecules* **2015**, *20*, 9915–9928.

Chapter 3

Solvation and Counter-Ion Binding of Ionic Resorcin[4]arenes

3.1 Introduction

Broad-band dielectric relaxation spectroscopy (DRS) probes polarization as the response of the sample to a time-dependent electric field. For electrolyte solutions, polarization essentially originates from the orientational fluctuations of permanent dipoles, intramolecular polarizability and ion motion[(1)]. Consequently, analysis of polarization may yield information of the species in the solution via interpretation of dipole interactions and dynamics. To obtain this information, DRS records the response of the sample to an external electric field in terms of the complex permittivity spectrum, $\hat{\varepsilon}(\nu)$:

$$\hat{\varepsilon}(\nu) = \varepsilon'(\nu) - \mathrm{i}\varepsilon''(\nu) \tag{3.1}$$

which detects all processes associated with dipole-moment fluctuations[(2)]. This complex quantity is composed by its real part the relative permittivity, $\varepsilon'(\nu)$, and the imaginary part ($\mathrm{i}^2 = -1$), $\varepsilon''(\nu)$, the dielectric loss at frequency ν. Analysis of $\hat{\varepsilon}(\nu)$ is usually done with empirical models of dielectric relaxation[(2)]. Combination of a suitable number of these models will describe the recorded dielectric relaxation. In the simplest case, the contribution may have a Lorentzian bandshape, although distortions might be expected. In each case, the contribution uses a different amount of parameters to describe its shape, where the mode amplitude, S_j and the relaxation time, τ_j, are the ones responsible for representing the relaxation strength and position respectively ($\tau_j = 1/2\pi\nu_j$). When distortions are present, shape parameters, α and β, can be included to represent symmetrical and unsymmetrical mode broadening respectively. Once the model is decided, the following analysis of τ_j and S_j can provide information about the phenomena at the molecular level. In the case of τ_j, they directly represent cooperative dynamics rather than individual dipoles[(3)]. However, when the dielectric relaxation is dominated by rotational diffusion, like in the case of dipolar aprotic solvents or ion pairs[(3)], motion of individual dipoles may be detected. In the case of S_j, access to information at a molecular level is only possible using microscopical models of dielectric relaxation. They allow for systems exhibiting more than one dispersion step to connect each mode S_j with the concentration of a relaxing species with an effective dipole moment, μ_{eff}; which is the

gas phase dipole moment corrected for medium induced polarization (reaction-field) and for dipole correlations[4,5].

Since the presence of a solute causes shifts in the solvent relaxation time and strength[3], DRS can be used to study solvation. The first way is by considering the change of solvent dynamics reflected in the relaxation time,τ_j. For example, hydrophobic hydration, which is typically present in aqueous solutions of solutes with hydrophobic moieties can be identified by the slower dynamics of water molecules surrounding the solute[6]. Additionally, if the timescale of this slow water is within the covered frequency range a new independent relaxation mode can be expected[3]. On the contrary, if the timescale falls outside the covered region, as in the case of ion hydration where the strong ion-solvent interactions may completely immobilize interacting water molecules, such interaction is invisible to DRS. In this case, solvation is indirectly evidenced by the reduction in the concentration of solvent molecules, behaving as bulk and is reflected in a reduction of the pure solvent relaxation strength, S_j. In the microwave region, $0.1 \leq \nu/\mathrm{GHz} \leq 89$, of the present experiments solute and solvent dynamics are probed on the pico- to nanosecond timescale, providing thus otherwise inaccessible information on solute-solvent and solute-solute interactions[1,3].

DRS also has the capacity to elucidate ionic association in electrolytes solutions[3]. This phenomenon is encountered in electrolyte solutions where the solvent has a low permittivity or in solutions with highly charged ions[7]. However, detection and further ion associate identification depend on the technique[8]. Since the resulting species from the ion interaction has a dipole moment that arises from the interaction of opposite charges, DRS results very convenient to their analysis[3,8], even in weakly interacting ions. Additionally, because the rotational correlation time depends on the size of ionic aggregate, further discrimination between multiple species may be possible[1,3]. However, its detection depends if their lifetime is at least comparable to their rotational correlation time[3].

Solvation and ionic interactions are two important aspects to be considered in the study of supramolecular chemistry in polar solvents. For this reason, as a first approach to the study of solutions of ionic resorcin[4]arenes Na_4TES and $\mathrm{TAM} \cdot (\mathrm{HCl})_4$ in aqueous and DMSO solutions using DRS at 298.15 K are presented in the following sections. From the obtained spectra, analysis of the resolved parameters allowed to elucidate differences in solvation and ion association that arise from structural differences.

3.2 Experimental

3.2.1 Sample preparation

Prior sample preparation, solutes $\mathrm{TAM} \cdot (\mathrm{HCl})_4$ and Na_4TES were dried for 72 h at 60 °C under reduce pressure ($\sim$ 2 x 10^{-6} bar) using P_2O_5 (Sicapent, Merck, Germany) as desiccant. Dried salts where stored in a glove box under a nitrogen atmosphere prior its use. Water content was verified using Coulometric Karl-Fisher titration, obtaining less than 100 ppm of water content. Samples were prepared

gravimetrically without buoyancy correction. Aqueous solutions used degassed water (Millipore, specific resistance 18 $\leq$ MΩ cm) and solutions in DMSO (Sigma Aldrich, $\geq$ 99.9%) were prepared inside the glove box to prevent water gain.

3.2.2 Dielectric spectroscopy

Dielectric spectra of solutions of $TAM \cdot (HCl)_4$ and Na_4TES were recorded at 298.15 K in the concentration range of $0.01 \leq m/$ mol kg$^{-1} \leq 0.25$ and $0.01 < m/$ mol kg$^{-1} < 0.25$, respectively, covering frequencies $0.02 \leq \nu/\text{GHz} \leq 89$. For $\nu \leq 50$ GHz, a coaxial cut-off cell (0.02-1.00 GHz), and two reflection cells (0.2-50 GHz) were used in conjunction with a vector network analyzer[9], whereas a waveguide interferometer covered the higher frequencies[10]. The quantity directly accessible with these instruments is the total dielectric response of the sample, $\hat{\eta}(\nu) = \hat{\varepsilon}(\nu) + \kappa/(2\pi\nu\varepsilon_0)$, where ε_0 is the permittivity of vacuum and $\hat{\varepsilon}(\nu) = \varepsilon'(\nu) - i\varepsilon''(\nu)$ the complex permittivity, with relative permittivity, $\varepsilon'(\nu)$, and dielectric loss, $\varepsilon''(\nu)$; $i^2 = -1$[11]. Density data required for converting m into c were measured with a vibrating-tube densimeter (Anton-Paar, DMA 5000M) at (298.15 ± 0.02) K. The dc conductivities, κ, required for converting $\hat{\eta}(\nu)$ to $\hat{\varepsilon}(\nu)$ were determined as described elsewhere[12].

3.2.3 Model Assessment

Analysis of the obtained spectra was done by fitting to different sets consisting of n dispersion steps described by the Havriliak-Negami equation:

$$\hat{\varepsilon}(\nu) = \sum_{j=1}^{n} \frac{S_j}{[1 + (i2\pi\nu\tau_j)^{1-\alpha_j}]^{\beta_j}} + \varepsilon_\infty \tag{3.2}$$

Each dispersion step, j, characterized by its amplitude, S_j, and relaxation time, τ_j, was modeled by a Havriliak-Negami (HN) equation with relaxation time distribution parameters $0 \leq \alpha_j < 1$ and $0 < \beta_j \leq 1$ or its simplified variants, the Cole-Davidson (CD, $\alpha_j = 0$), Cole-Cole (CC, $\beta_j = 1$) or Debye (D, $\alpha_j = 0$ & $\beta_j = 1$) equations[2]. Theoretically the infinite-frequency permittivity ε_∞, arises from intramolecular polarizability only. However, due to the limited frequency range of the present study, intermolecular vibrations and librations of solvent at $\nu > 100$ GHz contribute to the measured spectra; for example, the fast water relaxation at ~ 500 GHz[13]. Accordingly, in most trial fits ε_∞ was treated as an adjustable parameter. The static permittivity of the sample is given by $\varepsilon = \sum_j S_j + \varepsilon_\infty$. The tested models were assessed according to the criteria described in detail by Stoppa et al.[14].

3.3 Results and Discussion

The resolved relaxation parameters ε, S_j, τ_j and ε_∞ obtained from the fits of the spectra using eq. (3.2) are presented in supporting tables A.1-A.4. These tables also contain the experimental data of ρ and κ. Figure 3.1 shows typical recorded parts of the complex permittivity, $\hat{\varepsilon}$, spectra as function of molar concentration, c. As it can be seen, the static permittivity ($\varepsilon'(\nu)$, Fig.3.1a) decreases with increasing concentration suggesting a reduction in the polarity of the media. On the other

hand, the dielectric loss ($\varepsilon''(\nu)$, Fig.3.1b), shows a solute specific increment in the lower part of the spectra and a decrement in the upper-frequency region caused by solvent specific contribution. Further analysis of the recorded spectra using eq. (3.2) yielded possible explanations for the underlying processes causing these changes in the complex permittivity, $\hat{\varepsilon}$.

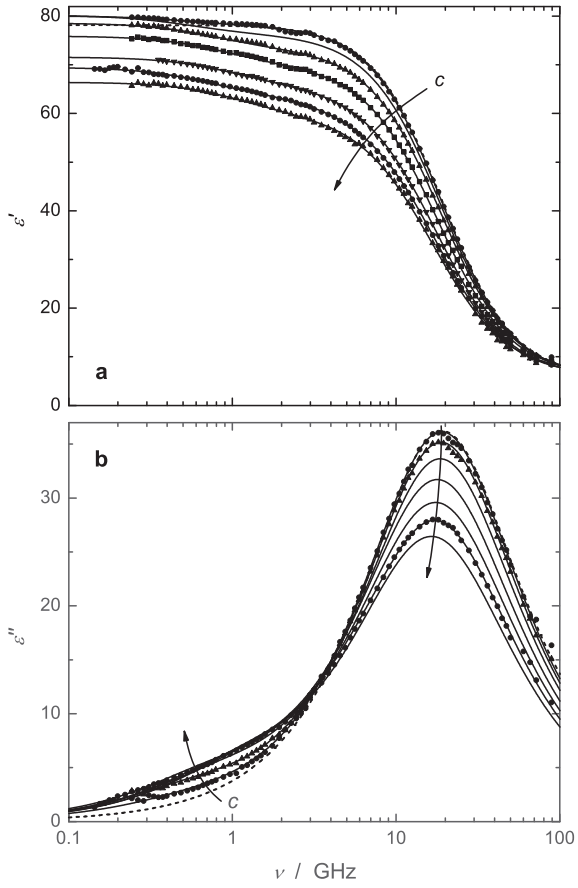

Figure 3.1: Spectra of (a) relative permittivity, $\varepsilon'(\nu)$, and (b) dielectric loss, $\varepsilon''(\nu)$, of aqueous solutions of TAM $\cdot$ $(HCl)_4$ at 298.15 K and concentrations $c/\mathrm{mol} \cdot \mathrm{L}^{-1} =$ 0.0101; 0.0296; 0.0569; 0.0937; 0.1346; 0.1734; and 0.2139 increasing in arrow direction. Symbols —partly omitted for clarity— show experimental data; lines represent fits with the 3D model.

3.3.1 Model Selection

Solutions of Na_4TES

Spectra of the DMSO solutions of Na_4TES, Figure A.1, were best described with a model consisting in the superposition of two Debye modes ($j = 1, 2$) for the lower frequency region and a Cole-Davidson mode ($j = 3$) for the dominant contribution at higher frequencies (Figure 3.2). This latter mode can be assigned to Bulk DMSO, as shown by previous studies of DMSO at 298.15 K using DRS[15,16].

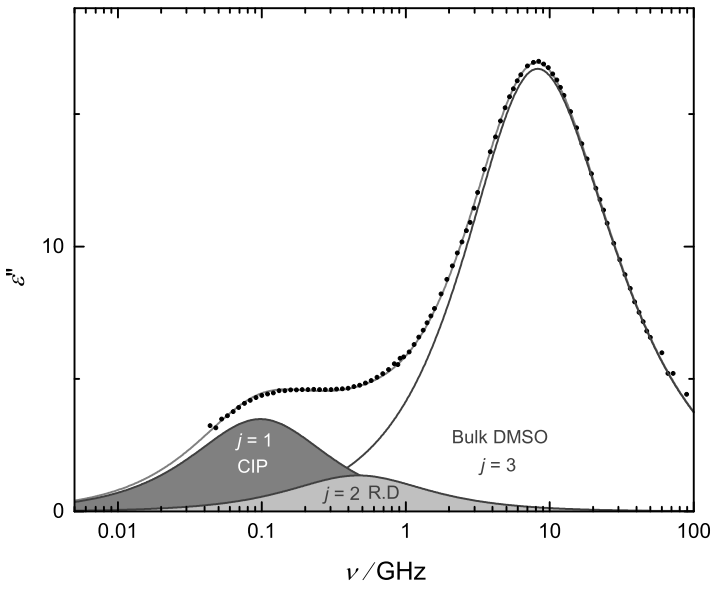

Figure 3.2: Dielectric loss spectrum, $\varepsilon''(\nu)$, for a solution of Na_4TES in DMSO with $c = 0.0724\ \mathrm{mol \cdot L^{-1}}$ at 298.15 K. Experimental data (points) where fitted with a 2D+CD Model (eq. 3.2) Designations CIP and R.D indicate contributions due to Contact ion pairs and rotational diffusion of TES^{4-}ion respectively (See text).

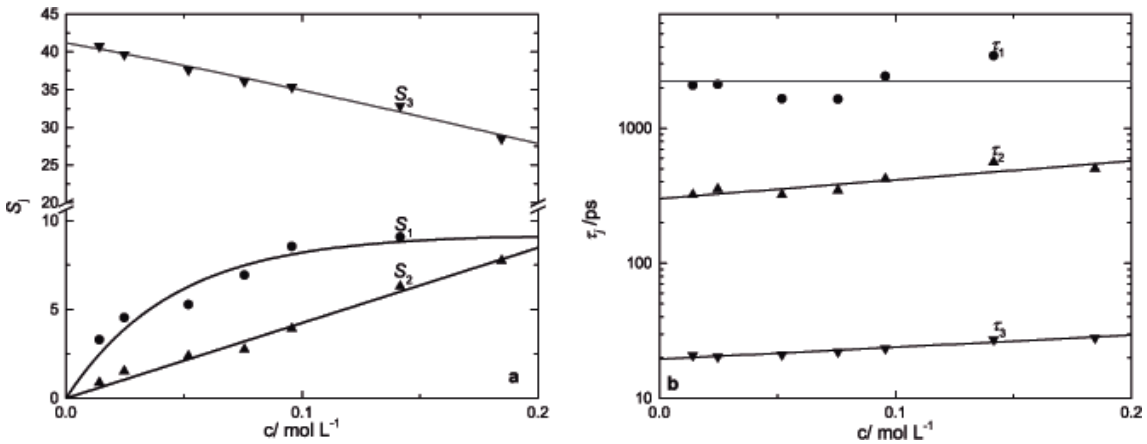

Figure 3.3: (a) Resolved amplitudes, S_j, and (b) relaxations times, τ_j, as function of Na_4TES concentration, c, in DMSO at 298.15 K. Lines are for eye guidance.

The low frequency, $j = 1$, and the intermediate mode, $j = 2$, can be assigned to a solute specific contribution. Particularly, $j = 2$ can be assigned to the rotational diffusion of the TES^{4-}anion. Analysis of the mode amplitudes ($S_2 = S_{TES^{4-}}$) as function of concentration, c (Figure 3.3a), shows a linear correlation that can be described by means of the generalized Cavell equation[17]:

$$c_j = \frac{\varepsilon + A_j(1-\varepsilon)}{\varepsilon} \frac{3k_B T \varepsilon_0}{N_A \cdot \mu_{\text{eff,j}}^2} S_j \tag{3.3}$$

which serves to determine the concentration of dipole moments, c_j, contributing to the dielectric relaxation with amplitude S_j using A_j, the cavity field factor, that depends on the size and shape of the dipole, and $\mu_{\text{eff,j}}$, the effective dipole moment, which accounts for the reaction field and possible dipole-dipole correlations[4,5]. The remaining factors are the Boltzmann constant, k_B, absolute temperature, T, and Avogadro Number, N_A. From the linear fit of the resolved $S_{TES^{4-}}$ with the solute concentration, c, $\mu_{\text{eff}} = 21.3$ D is obtained from the fitted slope, after assuming an spherical cavity shape ($A_j = 1/3$). This latter value, agrees well with the semi-empirical calculation (MOPAC2016 with RM1 hamiltonian[18]) of 20.9 D for the TES^{4-}anion in a dielectric continuum with dielectric permittivity of pure DMSO ($\varepsilon = 46.5$). Furthermore, calculation of the rotational diffusion time, τ_{rot}, using the Stokes-Einstein-Debye equation:

$$\tau_{\text{rot}} = \frac{3V_{\text{eff}}\eta}{k_B T} \tag{3.4}$$

where V_{eff} is the effective molecular volume and η is the macroscopic viscosity of the solvent, yielded the value of 560 ps, which agrees well with the resolved values of $\tau_2 = \tau_{TES^{4-}}$(Figure 3.3b) which are within the range $300 \leq \tau_3 \leq 560$ ps. The estimation of V_{eff} of the TES^{4-}ion was done using the Winmostar software[19]. Other approaches assuming *stick* or *slip* boundary conditions yielded larger rotational times.

In a similar way, the $j = 1$ mode can be assigned to the formation of contact ion-pairs (CIP). The mode position in the spectra[3] and the analysis of the relaxation time ($\tau_1 = \tau_{\text{CIP}}$) serves to do this assignment. The averaged $\tau_1 = \tau_{\text{CIP}}$ value(Figure 3.3b) is 2.22 ns and the calculated is 2.75 ns. In this case, the the rotational diffusion relaxation time for a contact ion-pair $[Na...TES]^{3-}$ in DMSO was not calculated directly from eq. (3.4) since the volume swept out by the rotation of the dipole of the CIP is closer to an oblate spheroid rather than an spherical. Thus, the estimation of the τ_{rot} was done with the following equation[20]:

$$\tau_{\text{rot}} = \frac{8\pi\eta a^3}{3k_B T} \cdot \frac{1-q^4}{\left(\frac{2-q^2}{\sqrt{q^2-1}}\right)\left(\arctan\sqrt{q^2-1}\right) - 1} \tag{3.5}$$

where the ratio q is defined as the ratio between the distances along the short axis, a, and the long axis, b of the oblate spheroid, thus $q = b/a > 1$ is always fulfilled. The distances a and b where calculated using the open-access software Avogadro (V 1.1.1)[21].

Figure A.2 shows the recorded spectra for the aqueous solutions of Na_4TES. As can be seen in Figure 3.4, description of the spectra is done with a model consisting

of three Debye modes (3D). However, its selection was not as straightforward as in the previous case for the DMSO solutions. According to the criteria by Stoppa et al[14], the best model, shown in Figure A.3, consist in the superposition of a broad Cole-Cole mode, $j = 1$, for the low frequency and a Debye mode, $j = 2$, for the higher frequencies (CC+D). In the latter case, the Debye mode can be straightforwardly attributed to the unperturbed solvent relaxation[3]; however, the broadness of the CC mode (Figure A.3) characterized by the rather large α values ($0.05 < \alpha < 0.45$, Table A.3), suggest the presence of more than one mode. For this reason, a "guided" fit was done by fixing the relaxation time of an intermediate Debye mode at 60 ps, since the results from the CC+D fit (Table A.3) suggest that at-large concentration the CC mode settles at approximately this value. Accordingly, this approach yielded a stable fit with a plausible physical interpretation of the resolved contributions; something that was not possible to achieve from a typical free fit with the same 3D model.

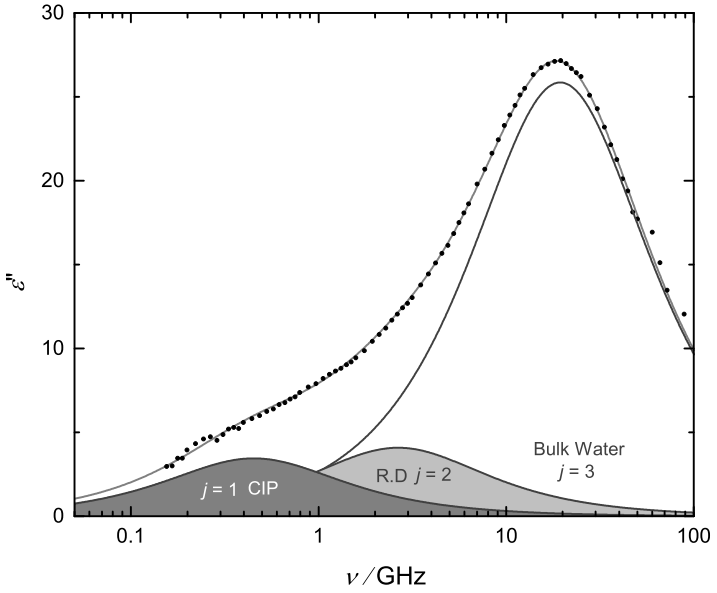

Figure 3.4: Dielectric loss spectrum, $\varepsilon''(\nu)$, for aqueous solutions of Na_4TES with $c = 0.1841\ \text{mol} \cdot \text{L}^{-1}$ at 298.15 K. Experimental data (points) where fitted with a 3D Model (eq. 3.2) Designations CIP and R.D indicate contributions due to Contact ion pairs and rotational diffusion of TES^{4-}ion respectively (See text).

Mode assignment for the Guided 3D fit was done in analogy with the previous assignment for the DMSO solutions. As mentioned before, from its position ($\sim$ 20 GHz), the dominant mode, $j = 3$, is immediately attributed to the unperturbed bulk water relaxation. Additionally, the decrease of S_3 showed in Figure 3.5a with concentration supports the assignment. In the case of $j = 1$ and $j = 2$, they were assigned once again to CIP formation and rotational diffusion of the TES^{4-}ion. This interpretation is supported with analysis of the intermediate mode amplitudes ($S_2 = S_{\text{TES}^{4-}}$, Figure 3.5a) with eq. (3.3), which gives $\mu_{\text{eff}} = 21.1$ D. This value is in agreement with the calculated (MOPAC2016/PM6) 20.0 D for the TES^{4-}ion in a dielectric continuum with static permittivity equal to the pure water at 298.15

K ($\varepsilon = 78.4$). Additionally, estimation of the relaxation time for the CIP using equation eq. (3.5) gives $\tau_{\text{rot}} = 463$ ps, that can be considered in agreement with the resolved $247 \leq \tau_1 = \tau_{\text{CIP}} \leq 352$ ps (Figure 3.5b) considering that the spectra was recorded in the range $0.2 \leq \nu/\text{GHz} \leq 89$. Lastly, the non-linear behavior of S_1, Figure 3.5a, suggest an equilibrium process which is consistent with the CIP formation.

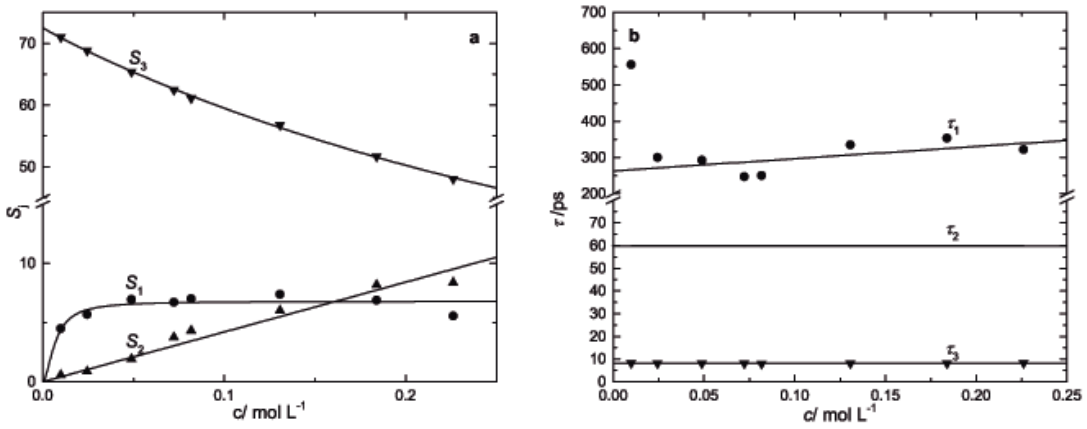

Figure 3.5: (a) Resolved amplitudes, S_j, and (b) relaxations times, τ_j, as function of Na_4TES concentration, c, in water at 298.15 K. Relaxation time of the $j = 2$ was fixed to $\tau_2 = 60$ ps during all fits. Lines are for eye guidance.

Solutions of TAM·(HCl)$_4$

Recorded spectra of aqueous solutions were already shown in Figure 3.1. Closer inspection of the spectra using eq.(3.2) reveals that they are best fitted by a superposition of three Debye-type relaxation processes (Fig. 3.6, see the Table A.4 for details). Figure 3.6 display a typical recorded dielectric loss, $\varepsilon''(\nu)$, spectrum of aqueous $\text{TAM} \cdot (\text{HCl})_4$ solution, where the $j = 1$ mode is assign to a solute contribution and the $j = 2, 3$ to solvent specific contributions. As mentioned before for the aqueous solutions of Na_4TES, the $j = 3$ contribution is associated with the cooperative relaxation of the hydrogen-bond network of essentially unperturbed solvent water[3]. On the contrary, the $j = 2$ can be attributed to retarded or "slow" water. It has been mentioned before that perturbed water, due to the presence of a solute, may display slower dynamics[22], leading to an independent contribution in the dielectric spectrum[3,5]. Regarding the $j = 1$ mode, this low-frequency mode exhibits a steeply increasing amplitude, S_1, which levels off at $c > 0.05\,\text{mol} \cdot \text{L}^{-1}$ (Fig. 3.7a), whereas its relaxation time first decreases before reaching a plateau value (Fig 3.7b). Such behavior is typical for ion-pair (IP) formation at a rate comparable to the rotational correlation time of the ion pair[3,23]. Further analysis (see section 3.3.3) will provide quantitative evidence of the ion-pair formation.

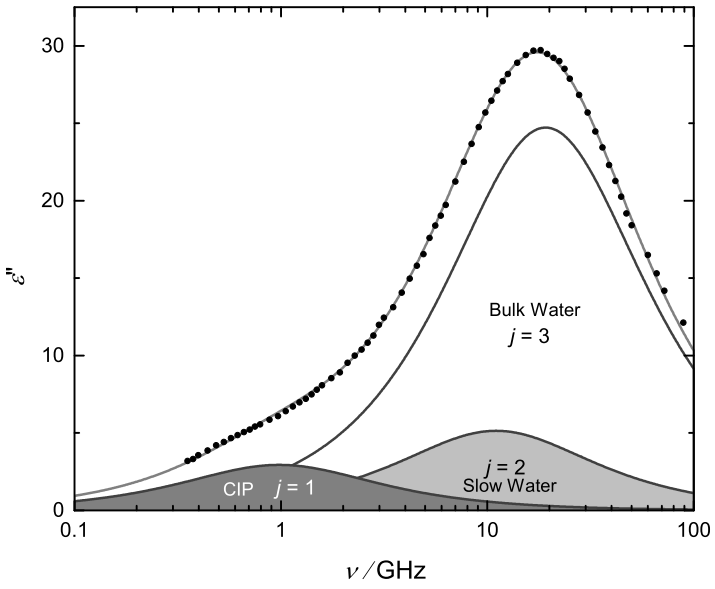

Figure 3.6: Dielectric loss spectrum, $\varepsilon''(\nu)$, for aqueous solution of TAM $\cdot$ $(HCl)_4$ with $c = 0.1233$ mol $\cdot$ L^{-1} at 298.15 K. Experimental data (points) where fitted with a 3D Model (eq. 3.2) Designations CIP indicate contribution due to Contact Ion Pairs (See text)

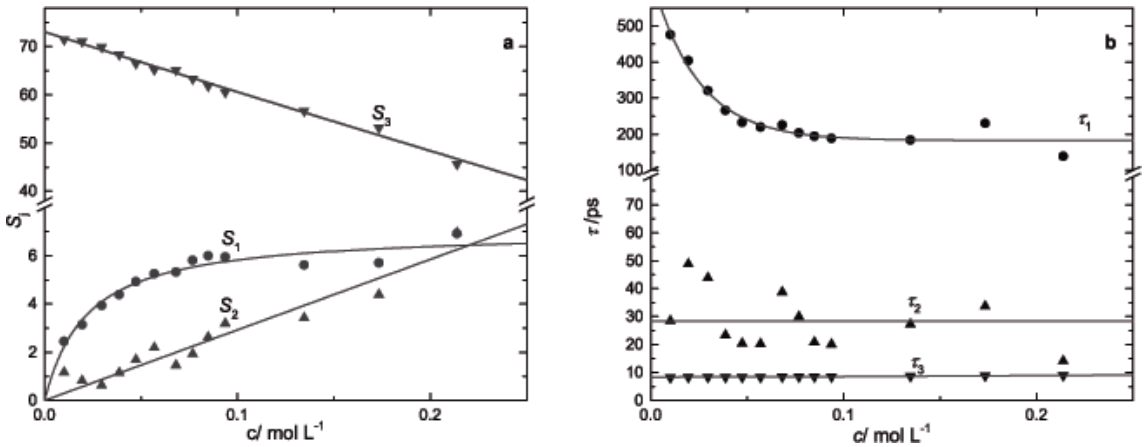

Figure 3.7: (a) Resolved amplitudes, S_j, and (b) relaxations times, τ_j, as function of TAM $\cdot$ $(HCl)_4$ concentration, c, in water at 298.15 K. Lines are for eye guidance.

Unfortunately, determination of the spectra for $TAM \cdot (HCl)_4$ in DMSO was limited due to its low solubility. Figure 3.8a shows a comparison of the recorded spectra at the maximum concentration (0.047 mol L^{-1}) of $TAM \cdot (HCl)_4$ in neat DMSO. As can be seen, a notable shift of the dominant peak is evident although at low frequency, were important phenomena is expected, only a small difference between the solution and the solvent exist. Different models according to equation (3.2) were tested, being a three Debye model the best one ($\chi^2 = 3.8\text{x}10^{-2}$). From the first and dominant mode (Figure 3.8b), $j = 1$ ($\tau_1 = 37.5$ ps, $S_1 = 45.04$) estimation of the dipole moment using equation (3.3), with the total solvent concentration, gives μ_{eff} =6.27 D, which is very close to the μ_{eff} =5.6 D, calculated using MOPAC2016 with the PM6 hamiltonian[18]. Assignment of the remaining $j = 2, 3$ modes is not simple. Figure 3.8b shows their positions and magnitudes ($\tau_2 = 10.3$ ps, $S_2 = 6.98$) and ($\tau_3 = 0.732$ ps, $S_3 = 2.63$). Considering the values from the relaxations times, assignment to solute specific contributions seems unrealistic, especially when the calculated rotational relaxation time of the free $TAM \cdot H^{4+}$ is at least 610 ns (depending on the conditions assumed for the V_{eff} eq. (3.4)). Consequently, these contributions might belong to the solvent.

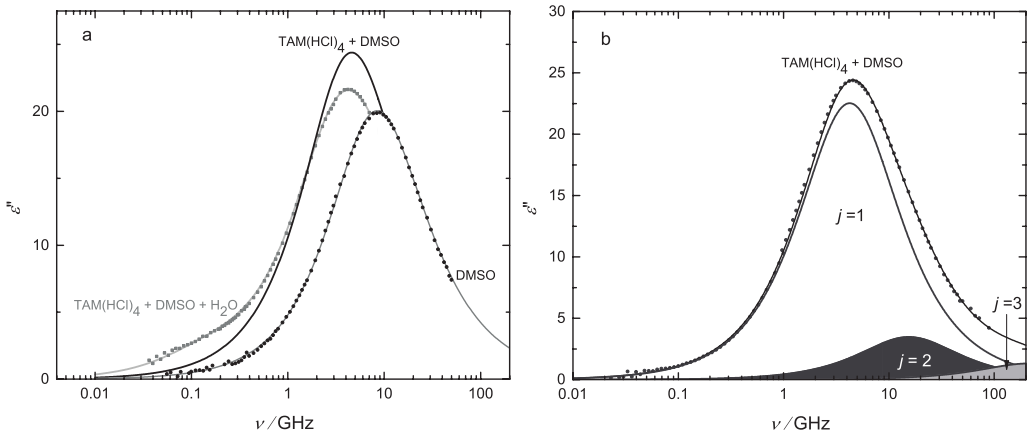

Figure 3.8: Panel a shows the dielectric loss spectrum of pure DMSO, $TAM \cdot (HCl)_4$ in DMSO at $c = 0.051$ mol $\cdot$ L^{-1} and $TAM \cdot (HCl)_4$ in DMSO-Water(10.9%) mixture at $c = 0.055$ mol $\cdot$ L^{-1}. Panel b shows the best fit of the $TAM \cdot (HCl)_4$-DMSO sample consisting in 3 Debye modes.

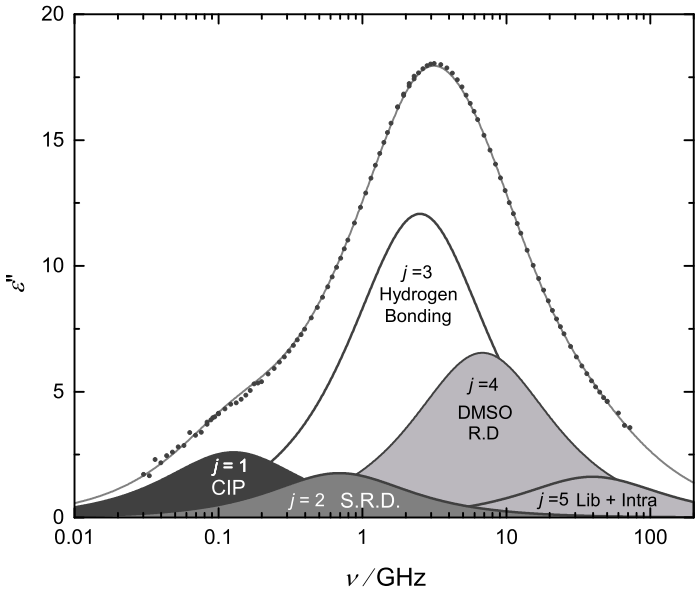

Figure 3.9: Dielectric loss spectrum, $\varepsilon''(\nu)$, for a solution of TAM $\cdot$ $(HCl)_4$ in DMSO-Water (10.9% w) with $c = 0.1727$ mol $\cdot$ L^{-1} at 298.15 K. Experimental data (points) where fitted with a 5D Model (eq. 3.2) Designations CIP and S.R.D indicate contributions due to Contact ion pairs and solute (TAM $\cdot$ H^{4+}) rotational diffusion respectively. Assingment of $j = 4$ and $j = 5$ is tentative (See text).

In order to study the interactions between TAM $\cdot$ $(HCl)_4$ and DMSO, solutions of TAM $\cdot$ $(HCl)_4$ in a mixture of (10.9% w H_2O)-DMSO as solvent were studied. This solvent mixture was chosen because it allowed concentrations comparable with the other studied systems. Figure A.4 shows the recorded spectra of TAM $\cdot$ $(HCl)_4$ in the mixture of DMSO-H_2O. As it can be seen in Figure 3.9, the selected model consists in five Debye modes (5D), where $j = 1$ and $j = 2$ can be attributed to solute specific modes while $j = 3, 4$ and 5 to the solvent. From the position in the spectra, the trend of S_1 with c (Figure 3.10a) and comparison with the previous systems, $j = 1$ can be attributed to CIP formation. Moreover, analysis of the resolved S_2 (Fig. 3.10a) using eq. (3.3) yield a $\mu_{\text{eff}} = 14.9$ D, which is consistent with the calculated 13.9 D using MOPAC/PM6[18] for a molecule of TAM $\cdot$ H^{4+} in a dielectric continuum with $\varepsilon = 54.07$. Thus, $j = 2$ is assigned to the rotational diffusion of the TAM $\cdot$ H^{4+} ion. On the other hand, analysis of the relaxations times for the CIP formation using eq.(3.5) gives a value of $\tau_{\text{rot(CIP)}} = 6.35$ ns and for the rotational diffusion of the TAM $\cdot$ H^{4+} ion using eq. (3.4), with different boundary conditions, gives τ_{rot}(RD,TAM $\cdot$ H^{4+})> 1.5 ns which are larger than the resolved ones (Figure 3.10c). According to these results, contributions arising from rotational diffusion of the species should not be observed, as in the case of the TAM $\cdot$ $(HCl)_4$-DMSO sample. Interestingly, the addition of water to the sample make possible to detect them as shown from the previous analysis of the modes amplitudes. Figure 3.10b shows the different resolved amplitudes for $j = 3, 4$ and 5 along with calculations of the expected amplitudes for the DMSO and Water according to the Cavell equation (eq. 3.3). Focusing at $c = 0$, it can be seen that the expected amplitude

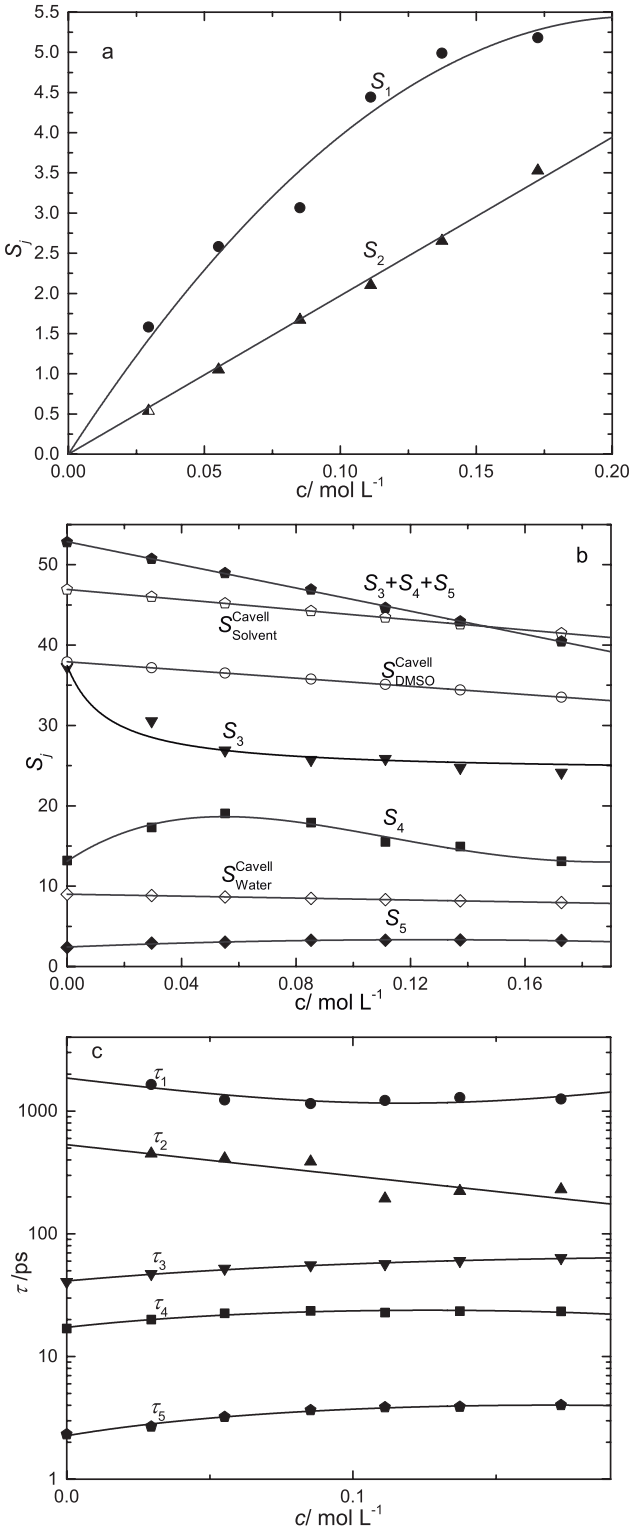

Figure 3.10: Fitted parameter for TAM $\cdot$ $(HCl)_4$ in DMSO-Water(10.9% w) at 298.15 K. Figure (a) shows resolved amplitudes, S_j, for the low frequency modes $j = 1 - 2$ and (b) Comparison of the solvent $j = 3 - 5$ mode amplitudes with calculated values (empty symbols) for the DMSO and Water using equation (3.3). The values of $S^{\text{Cavell}}_{\text{Solvent}}$ were calculated as $S^{\text{Cavell}}_{\text{DMSO}} + S^{\text{Cavell}}_{\text{Water}}$. Figure (c) shows relaxations times, τ_j, as function of TAM $\cdot$ $(HCl)_4$ concentration, c. Lines are for eye guidance.

for the solvent mixture, $S^{\text{Cavell}}_{\text{Solv}}$ is clearly less than the measured one ($S_3 + S_4 + S_5$). Considering the relationship S_j and μ_{eff}, stated by equation (3.3), this may be an indication of some parallel alignment of dipoles in the mixture. Such alignment seems to decrease with increasing solute concentration. Examination of the calculated DMSO amplitude, $S^{\text{Cavell}}_{\text{DMSO}}(0)$, shows good agreement with $S_3(0)$, which is consistent with the result from the TAM $\cdot$ $(\text{HCl})_4$ + DMSO sample. However, at higher concentrations $S^{\text{Cavell}}_{\text{DMSO}}$ is larger than S_3, indicating that a certain amount of DMSO is either interacting with water or solute molecules. Considering that at the ratio of the DMSO-Water mixture, hydrogen bonding between two DMSO molecules and water molecule exist with similar relaxation time [24] it could be considered that S_4 may include water and DMSO contributions, which seems to be supported from the fact that $S_4 > S^{\text{Cavell}}_{\text{Water}}$.

Regarding $j = 3 - 5$ modes in Figure 3.9, they are located in a region similar to the $j = 2, 3$ modes of the TAM $\cdot$ $(\text{HCl})_4$ + DMSO spectrum (Figure 3.8b). Previous studies of DMSO-Water mixtures as a function of composition using DRS [15,16,25,26] suggest that the recorded spectra for the neat DMSO and the mixtures can be described either using one Cole-Davidson mode or two Debye relaxations. Unfortunately, this ambiguity causes that assignment of modes $j = 3-5$ to be not definitive. In this study, the DMSO-H_2O mixture, without TAM $\cdot$ $(\text{HCl})_4$, was best described using a combination of three Debye modes ($\chi^2(3\text{D}) = 3.02$ x 10^{-2}) rather than a single Cole-Davidson ($\chi^2(\text{CD}) = 3.55$ x 10^{-2}). Inspection of the resolved parameters (table A.5 of the supporting information) suggests that other solvent contributions in the far infrared may exist since $\varepsilon_\infty \sim 4.5$ is rather large to the estimation of $1.1 n_D^2 = 2.4$, where n_D is the refractive index of the mixture taken from reference [27]. This latter claim is supported from a study of water dynamics in Water-DMSO mixtures using vibrational spectroscopy [24], which indicate that at water compositions below 50%, a hydrogen network mostly governed by DMSO-Water hydrogen bonding with a small contribution of water-water hydrogen bonding is responsible for the solvent structure. Interestingly, the orientational time for the water and DMSO show a similar value of 18 ps as determined by optical heterodyne detected optical Kerr effect (OHD-OKE). Considering that DRS detects first-order relaxation time, $\tau^{\text{or}(1)}$, it can be related with the values obtained from vibrational spectroscopy which are of second order, $\tau^{\text{or}(2)}$, by $\tau^{\text{or}(1)} = 3\tau^{\text{or}(2)}$ [26]. This relationship holds for neat DMSO [26], however for aqueous DMSO solutions the jump reorientation of DMSO and Water may caused that $\tau^{\text{or}(1)}/\tau^{\text{or}(2)} < 3$. Considering the data in reference [24] at $x_{\text{DMSO}} = 0.66$, $\tau^{\text{or}(1)}/\tau^{\text{or}(1)} \approx 2.3$ after taking $\tau^{\text{or}(1)} = \tau_3$. This might indicate that the $j = 3$ mode monitors the waiting time between the breakup of the associate DMSO-Water-DMSO and the formation of a new one. This assignment can be extended for the $j = 1$ mode of the system TAM $\cdot$ $(\text{HCl})_4$ + DMSO (Figure 3.8b), where hydrogen bonding between TAM $\cdot$ $(\text{HCl})_4$ and DMSO can be expected.

Calculation of τ_{rot} for a DMSO molecule using equation (3.4) under slip conditions ($V_{\text{eff}} = 7.58\text{Å}^3$ [26]) gives the value of $\tau_{\text{rot}} = 6.12$ ps in pure DMSO and $\tau_{\text{rot}} = 15.5$ ps in the DMSO-Water mixture. This may attribute that mode $j = 4$ in the DMSO + Water + TAM $\cdot$ $(\text{HCl})_4$ system and $j = 2$ in the DMSO + TAM $\cdot$ $(\text{HCl})_4$ can be attributed to free DMSO rotational diffusion. Finally, the high frequency mode, $j = 5$ in DMSO + Water + TAM $\cdot$ $(\text{HCl})_4$ and $j = 3$ in DMSO + TAM $\cdot$ $(\text{HCl})_4$ can be assigned to librations and intermolecular vibrations

from the terahertz region, as observed previously[24].

As mentioned before, an alternative interpretation might be constructed on the claims made in reference[25], which by using a two Debye mode description of the dielectric relaxation spectrum of pure DMSO they attribute the dominating relaxation at 19 ps to the waiting time for the break-up of non-polar DMSO dimers, whereas the fast mode close to 4 ps represents the rotational diffusion of free DMSO monomers. In this scenario, the $j = 3$ mode in Figure 3.9 could be assign to the waiting time between the breakup of a DMSO-Water-DMSO associate and the formation of a new one, $j = 4$ to the break-up of DMSO dimers and $j = 5$ to the rotational diffusion of free DMSO monomers.

3.3.2 Solvation

Solutions of Na_4TES

Analysis of the solvent amplitudes may yield information on the solvation of the ionic resorcin[4]arenes in solution. This is plausible by calculation of the DRS total solvation numbers, Z_t, which is defined as:

$$Z_\mathrm{t} = (c_\mathrm{solv} - c_\mathrm{b})/c \tag{3.6}$$

where c is the molar concentration of the sample. The quantity c_solv is calculated using the solution density, ρ/g cm^{-3}, sample molarity, c/ mol L^{-1} and molecular weights of the solute (g mol^{-1}), M_2, and the solvent, M_1:

$$c_\mathrm{solv} = \frac{1000\rho - cM_2}{M_1} \tag{3.7}$$

To determine solvation numbers of Na_4TES, calculation of c_b was done using the normalized version of eq.(3.3)[1]:

$$c_\mathrm{b} = \frac{\varepsilon(0)(\varepsilon(c) + A_i(1 - \varepsilon(c)))}{\varepsilon(c)(\varepsilon(0) + A_i(1 - \varepsilon(0)))} \cdot \frac{(1 - f_b(c)\alpha_i)^2}{(1 - f_b(0)\alpha_i)^2} \cdot \frac{c_\mathrm{solv}(0)}{S^\mathrm{eq}_\mathrm{slip}(0)} \cdot S^\mathrm{eq}_\mathrm{slip} \tag{3.8}$$

where α_i is the polarizability of water and $f_b(c)$ is the reaction field factor[28]:

$$f_b(c) = \frac{3}{4\pi\varepsilon_0 a_j b_j c_j} \cdot \frac{A_j(1 - A_j)(\varepsilon(c) - 1)}{\varepsilon(c) + (1 - \varepsilon)A_j} \tag{3.9}$$

which for a spherical particle, like water or DMSO, it is reduce to:

$$f_b(c) = \frac{1}{4\pi\varepsilon_0 r_j^3} \cdot \frac{2\varepsilon(c) - 2}{2\varepsilon(c) + 1} \tag{3.10}$$

where r_j is the solvent radius ($r_\mathrm{water} = 1.425$ Å[29] and $r_\mathrm{DMSO} = 3.03$ Å[26]).

Equation (3.8) demands the inclusion of the corrected mode amplitudes , $S^\mathrm{eq}_\mathrm{slip}$, rather than using immediately the resolved ones, S_3. Such correction is done with the following expression:

$$S^\mathrm{eq}_\mathrm{slip}(c) = S_3 + \varepsilon_\infty(c) - \varepsilon_\infty(0) + \Delta\varepsilon(c)_\mathrm{DD} \tag{3.11}$$

where the addition of $\varepsilon_\infty(c)$ and later subtraction of the solvent $\varepsilon_\infty(0)$ value, tries to correct for the contributions outside the studied frequency range. For example, for the aqueous solutions the fast H-bond flip of water[6] at ∼500 GHz (S_f, τ_f = 0.28 ps)[13] and thus outside the covered frequency range, could not be resolved but its presence was obvious from the large high-frequency permittivities of the present fits (Table A.2,A.4). Accordingly, its contribution to the total amplitude of bulk water, S_3, was consider by assuring that the total amplitude of bulk-like water, encompasses the small contribution, S_f, from the fast water mode centered at ∼ 500 GHz[13]. Thus, the expression $S_\mathrm{b}(c) = S_3(c)+\varepsilon_\infty(c)-\varepsilon_\infty(0)$, where $\varepsilon_\infty(0) = 3.52$ was determined from a pure-water spectrum up to 2 THz[5], approximately corrects for S_f. However, in the case of DMSO, no data covering the THz region is available. In this case, estimation of $\varepsilon_\infty(0)$ is done using the expression $1.1n_\mathrm{D}^2$, where n_D is the refractive index of the solvent; thus, for the DMSO the value of $\varepsilon_\infty(0) = 2.65$ was used.

Besides the contributions at higher frequencies, the last term in eq. (3.11) refers to the kinetic depolarization contribution, $\Delta\varepsilon_\mathrm{DD}$. In the case of Na_4TES solutions, the kinetic depolarization, was calculated using the equation proposed by Sega et al[30]:

$$\Delta\varepsilon_{DD} = \Delta\varepsilon_{HO} \cdot e^{(-\kappa_D \cdot R)} \cdot \frac{\kappa_D \cdot R + 2}{2} \tag{3.12}$$

where $\Delta\varepsilon_{HO}$ is the correction model proposed by Hubbard and Onsager[30]:

$$\Delta\varepsilon_{HO} = \xi \cdot \kappa(c) \tag{3.13}$$

with

$$\xi = p \cdot \frac{\varepsilon(0) - \varepsilon_\infty(0)}{\varepsilon(0)} \cdot \frac{\tau(0)}{\varepsilon_0} \tag{3.14}$$

which calculate the kinetic depolarization from the product between the sample electrical conductivity, $\kappa(c)$, and ξ which take into accounts the hydrodynamic parameter, p, that characterizes the translational motion of the ions with $p = 1$ for stick, $p = 2/3$ for slip and $p = 0$ for negligible boundary conditions. In this case slip conditions where assumed since they are generally considered to be the most physically realistic for the dielectric relaxation of solvated ions[3]. Additionally, in eq. (3.12) the product between the Debye length and the ionic size, $\kappa_D \cdot R$, can be calculated as:

$$\kappa_D \cdot R = 50.290 \cdot R_\mathrm{eff} \left(\frac{I}{\varepsilon T}\right)^{1/2} \tag{3.15}$$

where R_eff is the averaged effective radius (in Å) of the cation and anion. In the case of Na_4TES only the solvated sodium contribution was taken into account ($R_\mathrm{eff} = r_\mathrm{Na} + 2r_\mathrm{water} = 3.72$ Å or $R_\mathrm{eff} = r_\mathrm{Na} + 2r_\mathrm{DMSO} = 7.016$ Å), since the cation mobility is reduced due to the large size of the resorcin[4]arene.

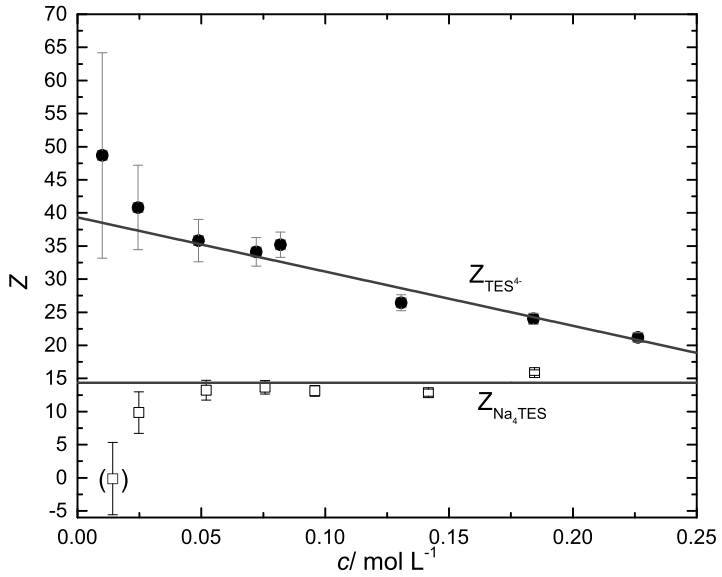

Figure 3.11: Total solvation numbers for the aqueous solutions of TES^{4-}in water, $Z_{TES^{4-}}$, and in DMSO solutions, Z_{Na_4TES}. Lines are averaged weighted fits.

In the case of electrolyte solutions, the total solvation numbers, Z_t, can be separated in ionic contributions. In the case of Na_4TES:

$$Z_t = Z_{TES^{4-}} + 4Z_{Na^+} \tag{3.16}$$

Figure 3.11 shows the solvation of TES^{4-} in water and of Na_4TES in DMSO. In the first case, by means of eq. (3.16) and the reported value of $(Z_{Na^+}) \approx (4.5 \pm 0.2)$ [31] the amount of water dipoles directly interacting with the TES^{4-}ion as function of the concentration is calculated. Unfortunately, the lack of knowledge of Z_{Na^+} in DMSO prevent the determination of $Z_{TES^{4-}}$ in this solvent. It can be seen that in aqueous solution, solvation of $TES^{4-}$is reduced while in DMSO is not only less, but also tends to be constant. Extrapolation to the limit when $c \to 0$ using an averaged weighted linear fit yield the value of $Z_{TES^{4-}} = (39.3 \pm 1.7)$ in water.

Solutions of TAM·(HCl)$_4$

For aqueous solutions, typically Z_t comprises all the water molecules involved in the solvation of the solute. In the case of $TAM \cdot (HCl)_4$, the amplitude of slow water, $S_2 = S_s$, directly yields the corresponding number, $Z_s = c_s/c$, of those hydrating water molecules that are retarded by a factor of $r = \tau_2/\tau_3 \approx 3$, whereas the possible difference, $Z_{ib} = Z_t - Z_s$, counts those solvent molecules which are apparently frozen (irrotationally bound, ib) on the timescale of the experiment. Although pretty noisy because of its small value, $S_2 = S_s$ increases linearly with c, whereas S_b decreases in the same way. Thus, the slope method of Ref. [32] could be applied for the evaluation of these amplitudes. This approach is based on the facts that amplitudes S_2 and S_b changed linearly with solute concentration, c, suggesting constant hydration numbers Z_t and Z_s in the covered range. Also ρ and κ were sufficiently

linear. This permitted the calculation of Z_t and Z_s from the slopes, $dS_2/dc = (29.3 \pm 1.4)\,M^{-1}$, $dS_b/dc = (-119 \pm 3)\,M^{-1}$, $d\rho/dc = (0.2435 \pm 0.0010)\,kg\,mol^{-1}$, and $d\kappa/dc = (17 \pm 2)\,S\,m^{-1}M^{-1}$, as described in detail in Ref.[32], yielding for the total hydration number:

$$Z_t = \lim_{c\to 0}\left(\frac{dc_w}{dc}\right) - \lim_{c\to 0}\left(\frac{dc_b^{eq}}{dc}\right) \tag{3.17}$$

where

$$\lim_{c\to 0}\left(\frac{dc_w}{dc}\right) = \left[\lim_{c\to 0}\left(\frac{d\rho}{dc}\right) - M\right]/M_s \tag{3.18}$$

with M and M_s as the molar masses of solute and solvent, and

$$\lim_{c\to 0}\left(\frac{dc_b^{eq}}{dc}\right) = \frac{c_w(0)}{S_b(0)} \times \left[\lim_{c\to 0}\left(\frac{dS_b}{dc}\right) + \xi \times \lim_{c\to 0}\left(\frac{d\kappa}{dc}\right)\right] \tag{3.19}$$

The second summand in Eq. (3.19), with

$$\xi = p \times \frac{\varepsilon(0) - \varepsilon_\infty(0)}{\varepsilon(0)} \times \frac{\tau(0)}{\varepsilon_0} \tag{3.20}$$

corrects for kinetic depolarization assuming slip boundary conditions ($p = 2/3$) for ion transport[33]. The corresponding slow-water hydration number is given by

$$Z_s^0 = \lim_{c\to 0}\left(\frac{dc_s}{dc}\right) = \frac{c_w(0)}{S_b(0)} \times \lim_{c\to 0}\left(\frac{dS_3}{dc}\right) \tag{3.21}$$

For the present TAM $\cdot$ $(HCl)_4$ solutions a total hydration number of $Z_t = 43 \pm 3$ was obtained, of which $Z_s = 21.6 \pm 1.0$ H_2O dipoles are moderately retarded and thus $Z_{ib} = 21 \pm 4$ apparently frozen. Since the hydration of the anion, Cl^-, is only weak, *i.e.* the dynamics of its hydration water similar to that of the bulk[3,34], the above hydration numbers can be entirely assigned to the TAM $\cdot$ H^{4+} cation. For the solutions of TAM $\cdot$ $(HCl)_4$ in DMSO and in the mixture of DMSO-Water, quantitative solvation analysis is not possible due to the uncertainty in the mode assignment.

3.3.3 Ionic interactions

From the ion-pair concentrations, c_{IP}, obtained from S_1 with the aid of eq.(3.3) association numbers

$$K_A = \frac{c_{IP}}{(4c - c_{IP})^2} \tag{3.22}$$

were then calculated under the assumption that each of the four well-separated groups of the receptor independently binds its counter ion. This assumption allows to treat the resorcin[4]arene as a pseudo-1:1 electrolyte and not as a 4:1 electrolyte as formally implied by the charge of the ions. In other words, each of the four groups on the resorcin[4]arene ions was treated as an independent binding site. This seems justified from their large mutual separation in the predominating all-*cis* crown conformation (see Chapter 2) and from the unrealistically large K_A°; for example, K_A°=(464 $\pm$50) M^{-1} obtained when treating TAM $\cdot$ $(HCl)_4$ as a 4:1 electrolyte in aqueous solution. Calculation of c_{IP} is done using eq. (3.3) with effective dipole

Table 3.1: Effective dipole moments, μ_{eff}, and thermodynamic association constants, K°_{A}, with their uncertainties, $u_{K^{\circ}_{\text{A}}}$, calculated from the fit using eq. (3.23).[a]

CIP	Solvent	μ^{b}_{eff}	K°_{A}	$u_{K^{\circ}_{\text{A}}}$
$[\text{TES}^{4-} \cdot \text{Na}^{+}]^{3-}$	DMSO	46.2	92.1	30.3
$[\text{TES}^{4-} \cdot \text{Na}^{+}]^{3-}$	Water	46.3	85.1	41.2
$[\text{TAMH}^{4+} \cdot \text{Cl}^{-}]^{3+}$	DMSO-Water	53.6	2.8	0.6
$[\text{TAMH}^{4+} \cdot \text{Cl}^{-}]^{3+}$	Water	59.7	7.5	0.7

[a] Units: μ_{eff} in D; K°_{A} in M^{-1}. [b] Calculated using MOPAC[18](See text).

moments, μ_{eff}, calculated with MOPAC[18](Table 3.1) and cavity-field factor $A_j = 1/3$.

Figure 3.12a shows a typical extrapolation of K_{a} to vanishing (nominal) ionic strength, $I = 4c$, with the extended Guggenheim-type equation[35]

$$\log K_{\text{A}} = \log K^{\circ}_{\text{A}} - \frac{2A_{\text{DH}}|z_{+}z_{-}|\sqrt{I}}{1 + R_{ij}B_{\text{DH}}\sqrt{I}} + C \cdot I + D \cdot I^{3/2} \tag{3.23}$$

Such extrapolation yields the standard-state association constants, K°_{A} (M^{-1}), which are summarized with their uncertainties in the table 3.1. In eq. (3.23) $A_{\text{DH}} = 1.82481 \cdot 10^{6} \times (\varepsilon T)^{-3/2}$ (in units $\text{M}^{-1/2}$) is the Debye-Hückel constant, $B_{\text{DH}} = 502.90 \times (\varepsilon T)^{-1/2}$ (in $\text{M}^{-1/2}\text{nm}^{-1/2}$) and R_{ij} (in nm) the charge distance; C (M^{-1}) and D ($\text{M}^{-3/2}$) are empirical parameters. During the fit the values of $A_{\text{DH}} = 0.51093\ \text{M}^{-1}$ and $R_{\text{ij}}B_{\text{DH}} = 1$ were used as suitable assumptions for aqueous systems at 298.15 K[35]. For the solutions in DMSO, R_{ij} was calculated as the averaged radius between the -SO_3^{-} and the Na^{+} as well as the averaged between the $\text{-N(CH}_3\text{)H}^{+}$ and Cl^{-}. The radii of the residues was obtained from the its volume calculated using Winmostar[19].

The relaxation time of $j = 1$ for the aqueous solutions of $\text{TAM} \cdot (\text{HCl})_4$, τ_1 (Fig.3.7b), exhibits a rapid initial decrease before reaching a plateau value of ∼180 ps at $c > 0.07$ M. Such behavior suggests for low c a contribution from the kinetics of ion-pair formation to τ_1 in addition to dipole rotation, characterized by τ_{rot}[23]. For labile ion pairs the characteristic times of ion-pair formation and decay are comparable to their rotational correlation time, τ_{rot}, giving rise to a chemical relaxation rate, τ_{ch}^{-1}, which contributes to the observed ion-pair relaxation time, $\tau_{\text{IP}} = \tau_1$, as:

$$\tau_{\text{IP}}^{-1} = \tau_{\text{rot}}^{-1} + \tau_{\text{ch}}^{-1} = \tau_{\text{rot}}^{-1} + k_{21} + k_{12}(c^{\text{f}}_{+} + c^{\text{f}}_{-}) \tag{3.24}$$

where k_{12} and k_{21} are the rate constants of formation and decay respectively; c^{f}_{+} and c^{f}_{-} are the concentrations of free cations and anions respectively[23]. Treating $\text{TAM} \cdot (\text{HCl})_4$ as a pseudo-1:1 electrolyte, as indicated above, the total concentration of free ions is calculated as $c_{\text{free}} = c^{\text{f}}_{+} + c^{\text{f}}_{-} = 8c - 2c_{\text{IP}}$, with ion-pair concentrations calculated from the solute amplitude, S_1, as discussed above. Figure 3.12b shows τ_{IP}^{-1} as a function of c_{free}. The linear part, at $c < 0.6\,\text{mol} \cdot \text{L}^{-1}$, can be described by an intercept of $\tau_{\text{rot}}^{-1} + k_{21} = (1.59 \pm 0.12)\,\text{ns}^{-1}$ and a slope of $k_{12} = (7.4 \pm 0.4)\,\text{ns}^{-1}\text{M}^{-1}$. Consequently, from the intercept and $\tau_{\text{rot}} = 2.51$ ns (obtained using equation (3.5))

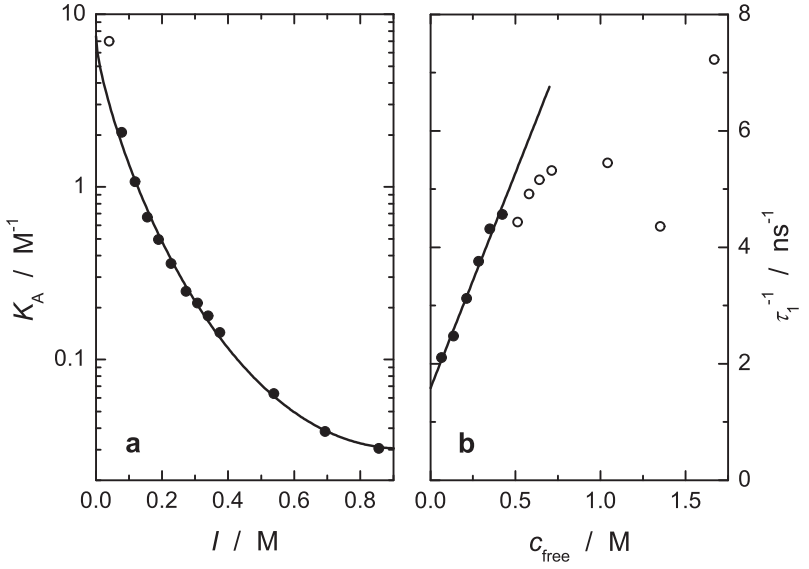

Figure 3.12: (a) Association numbers, K_A (symbols), of aqueous solutions of $TAM \cdot (HCl)_4$ at 298.15 K as a function of ionic strength, I, and associated Guggenheim fit (Eq. (3.23), line). (b) Corresponding ion-pair relaxation rates, τ_1^{-1} (symbols), as a function of total free-ion concentration, c_{free}, and their fit with Eq. (3.24) (line). Open symbols were not used in the fits.

is evaluated with a decay-rate constant of $k_{21} = 1.18\,ns^{-1}$. This corresponds to an ion-pair lifetime of $\tau_l = \ln 2/k_{21} \approx 600\,ps$. The slope gave the formation-rate constant of $k_{12} = (7.4 \pm 0.4)\,M^{-1}ns^{-1}$. Thus, from the concentration dependence of the solute relaxation time at $c < 0.07\,mol \cdot L^{-1}$ a standard-state association constant of $K_A^\circ = k_{12}/k_{21} = (6.3 \pm 1.0)\,M^{-1}$ is obtained. This is in good agreement with the value derived from S_1, $(7.5 \pm 0.7)\,M^{-1}$ (see Table 3.1) and thus lends credit to the assumption that aqueous $TAM \cdot (HCl)_4$ solutions can be treated as a pseudo-1:1 electrolyte.

3.4 Discussion

According to the calculated Z_i values, solvation of ionic resorcin[4]arenes is strongly affected by the nature of the ionic moiety. Analysis and comparison of the DRS spectra and their corresponding resolved modes revealed that for Na_4TES only irrotationally bound water was detected, with a value close to the $TAM \cdot H^{4+}$ total hydration number, ($Z_t(TAM \cdot H^{4+}) \approx 43$ and $Z_t(TES^{4-}) \approx 39$). Moreover, in the latter case the total amount of hydrating water can be separated in ~ 22 water molecules, which exhibit retarded dynamics, and ~ 21 frozen or irrotationally bound. Unfortunately, DRS cannot tell where the Z_{ib} and Z_{slow} are located in the solvation shell. However, $TAM \cdot H^{4+}$, with its $Z_{slow} \approx 22$, shares four phenyl groups with the hydrophobic tetraphenylborate and the tetraphenylphosphonium ions, where $Z_t = Z_{slow} \approx 25$[36]; accordingly, it can be tentatively assigned the detected slow water to solvent molecules surrounding the hydrophobic part of $TAM \cdot H^{4+}$. This would then formally leave $\sim$5 frozen H_2O molecules for each -$N(CH_3)_2H^+$ residue. However, at least for the NH_4^+ ion it is known from MD simulations[37] and spectroscopic studies[38] that hydration water is not strongly bound. Obviously, cooperative

effects arising from the particular crown-shaped structure of $TAM \cdot H^{4+}$ must operate to explain the presence of $Z_{ib} \approx 21$ frozen water molecules. Consequently, from this analysis and the fact that for aqueous solutions moderate retardation arises from solute-solvent interactions being somewhat larger than water-water interaction (hydrophilic hydration) but also from the excluded-volume effect exerted by hydrophobic solutes[6], it may be said that for $TAM \cdot H^{4+}$ solvation is governed by both mechanisms. Following the same reasoning for the TES^{4-}should lead to a similar interpretation, but the fact that no slow water was detected is an indication that the sulfonate moiety affects directly the solvation pattern. In fact, Okouchi et al[39] by determining ^{17}O-NMR spin-lattice relaxation times of aqueous solutions of *n*-alkylsulfonate and arylsulfonic anions evidence that the -SO_3^- group, due to its strong "structure breaking" nature, affects even more the dynamics of water molecules involved in hydrophobic hydration[39]. Moreover, they also show that the structure breaking effect decreases in the order -SO_3^- >-NH_3^+ >-OH>-NH_2[39] which may serve as an indication on the strength of solute-solvent interaction.

In the case of Na_4TES in DMSO solutions, the previous discussion cannot be fully extended because Z_t of the sodium ion is not known. Even so, comparison of Z_{Na_4TES} in DMSO with $Z_{TES^{4-}}$ in water clearly shows that solvation of the $TES^{4-}$is lower in DMSO, with an rapidly increasing value that reaches $Z_{Na_4TES} \approx 11$(Figure 3.11). Additionally, estimations of solvation numbers, n_s, from electrostriction and entropy of immobilization[8] suggest that Na^+ in DMSO has a $n_s = 0-2.7$, while recent MD simulations suggest that Na^+ at 298 K has a coordination number (CN) in DMSO of 5-6[40]. Although DRS ionic solvation numbers are not strictly equal to n_s or CN, for example the latter strongly depend on the nature of the ion[1], assuming the CN value as an upper limit for $Z_t(Na^+,DMSO)$, something that seems reasonable for a monovalent ion[1], allows to narrow Z_{ib} for the TES^{4-}in DMSO, namely $Z_{TES^{4-}}(DMSO)$, to the range $5 \leq Z_{TES^{4-}}(DMSO) \leq 11$ solvent molecules immobilized probably by either hydrogen bonding with the eight -OH groups attached to the phenyl rings or donor-acceptor interaction with the -SO_3^- moiety. Moreover, as seen it in the case of aqueous solutions, DMSO solutions of ions exhibit solvation mechanisms, i.e. "solvophobic" and "solvophilic" solvation, where the former solvation is characteristic for large organic ions, like tetraphenylborate or tetralkylammonium ions, while solvophilic solvation is mainly displayed by inorganic ions that interact directly with the solvent[41]. Thus, by considering the $Z_t(Na_4TES)$ it can be considered that in contrast to aqueous solutions, solvophobic solvation prevail.

Analysis of Gibbs energy of solvation[42] suggest that DMSO is a better-suited solvent for cations rather than for anions. Despite that, solutions of $TAM \cdot (HCl)_4$ in DMSO could not be studied in a concentration range comparable with the one explored with the Na_4TES solutions in DMSO. Nonetheless, it is worthy to point out that addition of $TAM \cdot (HCl)_4$ to DMSO in a concentration of approximately 0.05 mol kg^{-1} increased the $\varepsilon'(\nu)$ from 46.5 to approximately 57 and shifted the total dielectric loss from $\sim$ 9 GHz to 4.5 GHz as shown in Figure 3.8a, while for a similar concentration of Na_4TES the static permittivity increment was not that high, $\varepsilon'(\nu) = 49.3$ and the shifting is negligible. This effect seems to be correlated with the observation from MD simulations where positively charged ions showed a larger orienting influence on the solvent than anions and neutral molecules re-

spectively[41]. Furthermore, analysis of the spectra from the TAM · $(HCl)_4$-DMSO sample and TAM · $(HCl)_4$-DMSO-Water samples indicate that the shift of the dominant contribution can be attributed to a retardation of DMSO dynamics. In analogy to the TAM · $(HCl)_4$-Water system, this retardation might indicate that a solvophobic mechanism is responsible for the TAM · $(HCl)_4$ solvation in DMSO. Interestingly, in both solvents evidence of solvent retardation was only found for TAM · $(HCl)_4$. Thus, considering that the calculated volume of TES^{4-} is less than the calculated volume of TAM · H^{4+} , it can be an indication that volume exclusion effect may be also an important contribution, in addition to the difference in ionic moieties, to the difference in solvation patterns between ionic resorcin[4]arenes.

Among different techniques, DRS has become prominent for studying ion association[8]. However, estimation of association constants from the DRS spectra are usually larger than the obtained by other methods due to the always present contribution arising from the ion-cloud relaxation[31]; thus, DRS calculated K_A° values should be considered only as an upper limit. With this in mind, it can be considered that the formation of $[TAMH^{4+} \cdot Cl^-]^{3+}$ in any of the studied media is weak. However, the K_A° values suggest that association in water is larger than in the DMSO-Water mixture, despite the fact that this medium has a lower $\varepsilon'(\nu)$.

Additionally, only for aqueous solutions of TAM · $(HCl)_4$ was possible to obtain information of the kinetics of the ion-pair formation process, yielding the very fast rate constants, $k_{12} = (7.4 \pm 0.4)\,M^{-1}ns^{-1}$ and $k_{21} = 1.18\,ns^{-1}$. Neglecting possible steric constraints, the corresponding rate constants for diffusion-controlled ion-pair formation, k_{12}^D, and decay, k_{21}^D, can be estimated as

$$k_{12}^D = \frac{N_A z_+ z_- e_0^2}{\varepsilon_0 \varepsilon k_B T} \times \frac{D_+ + D_-}{\exp\left[\frac{z_+ z_- e_0^2}{4\pi\varepsilon_0 \varepsilon k_B T d}\right] - 1} \tag{3.25}$$

and

$$k_{21}^D = \frac{3 z_+ z_- e_0^2}{4\pi\varepsilon_0 \varepsilon k_B T d^3} \times \frac{D_+ + D_-}{1 - \exp\left[\frac{-z_+ z_- e_0^2}{4\pi\varepsilon_0 \varepsilon k_B T d}\right]} \tag{3.26}$$

where D_+ and D_- are the diffusion coefficients of TAM · H^{4+} and Cl^-, $z_+ = 1$ and $z_- = -1$ the charge numbers of the interacting ionic sites approaching to the distance, d[43]. For the large cation $D_+ \approx 0$ was assumed, D_- was taken as $2.032 \times 10^{-9}\,m^2s^{-1}$[8], and $d = 460\,pm$ approximated as the sum of the radii of Cl^- and the tetramethylammonium ion given in Ref.[8]. This yielded $k_{12}^D = 8.7\,ns^{-1}M^{-1}$ and $k_{21}^D = 12\,ns^{-1}$. In particular, ion-pair formation is close to the diffusion-controlled limit, $k_{12}^D \approx 8.7\,ns^{-1}M^{-1}$. This means that the dehydration of $–CH_2NH(CH_3)_2^+$ and Cl^- must occur at least as fast, which in line with existing information on the hydration of cloride[3,34] and ammonium[37,38] ions. On the other hand, the decay rate constant of the ion pair is an order of magnitude smaller than expected for a diffusion-controlled reaction, $k_{21}^D = 12\,ns^{-1}$.

Lastly, association between the $TES^{4-}$and the Na^+ (Table 3.1) yielded larger values than $[TAMH^{4+} \cdot Cl^-]^{3+}$ although with larger uncertainty. However, as shown in the mode assignment section, estimation of relaxation times supports the presence of $[TES^{4-} \cdot Na^+]^{3-}$. Interestingly, the magnitudes of K_A° are similar in both solvents

and comparable with association constants of moderate associated multivalent ions like Eu^{3+} and La^{3+} [44]. Considering that the strength of ion association depends on the charge and the relative permittivity of the solvent [45], can be considered that K_A° may be reflecting more than the simple formation of the CIP.

3.5 Conclusions

Solvation and ion interactions of the two ionic resorcin[4]arenes $TAM \cdot (HCl)_4$ and Na_4TES in two polar solvents were studied by means of dielectric relaxation spectrospcopy in the frequency range $0.02 \leq \nu/GHz \leq 89$ at 298.15 K. Analysis of the DRS solvation numbers indicate that both resorcin[4]arenes ions have a close total hydration number, but $TAM \cdot H^{4+}$ displayed a hydration shell with both retarded and frozen water molecules while for TES^{4-} only irrotationally bound water molecules were detected. This finding led to the proposition that hydration of TES^{4-} is dominated by the hydrophilic mechanism while for the $TAM \cdot H^{4+}$ both hydrophilic and hydrophobic mechanism operate. A similar analysis showed that in DMSO the TES^{4-} solvation is mainly governed by solvophovicity. Interactions between $TAM \cdot (HCl)_4$ and DMSO are harder to quantify since the presence of the solute causes an increment in the solvent amplitude and relaxation time which translates in changes in the effective dipole moment and solvents dynamics, reflecting the large "effort" of the solvent to solubilize $TAM \cdot (HCl)_4$. Addition of water to the mixture enhances the $TAM \cdot (HCl)_4$ solubility as well as their dynamics, which can be related to the presence of a hydrogen bond network form between 2 DMSO molecules with 1 Water molecule.

Unfortunately, the conflicting view of the liquid DMSO prevents to conclude on the molecular origin of the detected relaxation modes. Consequently, solvation of $TAM \cdot H^{4+}$ in the mixture is certainly complicated. Nonetheless, addition of water into the sample enhance solvation and accelerate the dynamics of the rotational diffusion of the ion associate and free $TAM \cdot H^{4+}$, which according to the Stokes-Einstein-Debye equation (eq. 3.4) should be observed at lower frequencies than the covered in this study.

Analysis of ionic interactions between the resorcin[4]arenes and their counter ions showed that the assumption of pseudo 1:1 electrolytes give a reasonable interpretation of the obtained results. Accordingly, $TAM \cdot (HCl)_4$ forms labile contact ion-pairs which are slightly stronger in water than in DMSO. Meanwhile, ion association between TES^{4-} and Na^+ seems to be similar in water and DMSO and from the magnitude further processes might be expected; however, such interpretation should be taken carefully since estimated values of K_A° have a rather large uncertainty.

Bibliography

[1] Buchner, R. *Pure and Applied Chemistry* **2008**, *80*, 1239–1252.

[2] Kremer, F., Schoenhals, A., Eds. *Broadband Dielectric Spectroscopy*; Springer Berlin Heidelberg: Berlin, Heidelberg, 2003.

[3] Buchner, R.; Hefter, G. *Physical Chemistry Chemical Physics* **2009**, *11*, 8984.

[4] Akilan, C.; Rohman, N.; Hefter, G.; Buchner, R. *ChemPhysChem* **2006**, *7*, 2319–2330.

[5] Eiberweiser, A.; Nazet, A.; Hefter, G.; Buchner, R. *Journal Physical Chemistry B* **2015**, *119*, 5270–5281.

[6] Laage, D.; Stirnemann, G.; Sterpone, F.; Rey, R.; Hynes, J. T. *Annual Review of Physical Chemistry* **2011**, *62*, 395–416.

[7] Barthel, J.; Krienke, H.; Kunz, W. *Physical chemistry of electrolyte solutions: modern aspects*; Springer Science & Business Media, 1998; Vol. 5.

[8] Marcus, Y. *Ions in Solution and their Solvation*; John Wiley & Sons, 2015.

[9] Sonnleitner, T.; Turton, D. A.; Waselikowski, S.; Hunger, J.; Stoppa, A.; Walther, M.; Wynne, K.; Buchner, R. *Journal of Molecular Liquids* **2014**, *192*, 19–25.

[10] Barthel, J.; Buchner, R.; Eberspächer, P.-N.; Münsterer, M.; Stauber, J.; Wurm, B. *Journal of Molecular Liquids* **1998**, *78*, 83–109.

[11] Böttcher, C. F. J.; Bordewijk, P. *Theory of Electric Polarization, Vol. 2*; Elsevier: Amsterdam, 1978.

[12] Shaukat, S.; Buchner, R. *Journal of Chemical and Engineering Data* **2011**, *56*, 4944–4949.

[13] Fukasawa, T.; Sato, T.; Watanabe, J.; Hama, Y.; Kunz, W.; Buchner, R. *Physical Review Letters* **2005**, *95*, 197802.

[14] Stoppa, A.; Nazet, A.; Buchner, R.; Thoman, A.; Walther, M. *Journal of Molecular Liquids* **2015**, *212*, 963–968.

[15] Kaatze, U.; Pottel, R.; Schäfer, M. *The Journal of Physical Chemistry* **1989**, *93*, 5623–5627.

[16] Lu, Z.; Manias, E.; Macdonald, D. D.; Lanagan, M. *The Journal of Physical Chemistry A* **2009**, *113*, 12207–12214.

[17] Cavell, E.; Knight, P.; Sheikh, M. *Transactions of the Faraday Society* **1971**, *67*, 2225–2233.

[18] Stewart, J. J. *Journal of computer-aided molecular design* **1990**, *4*, 1–103.

[19] Senda, N. *Idemitsu Tech. Rep.* **2006**, *49*, 106–111.

[20] Raicu, V.; Feldman, Y. *Dielectric relaxation in biological systems: Physical principles, methods, and applications*; Oxford University Press, USA, 2015.

[21] Hanwell, M. D.; Curtis, D. E.; Lonie, D. C.; Vandermeersch, T.; Zurek, E.; Hutchison, G. R. *Journal of cheminformatics* **2012**, *4*, 17.

[22] Laage, D.; Stirnemann, G.; Hynes, J. T. *The Journal of Physical Chemistry B* **2009**, *113*, 2428–2435.

[23] Buchner, R.; Barthel, J. *Journal of molecular liquids* **1995**, *63*, 55–75.

[24] Wong, D. B.; Sokolowsky, K. P.; El-Barghouthi, M. I.; Fenn, E. E.; Giammanco, C. H.; Sturlaugson, A. L.; Fayer, M. D. *The Journal of Physical Chemistry B* **2012**, *116*, 5479–5490.

[25] Shikata, T.; Sugimoto, N. *Physical Chemistry Chemical Physics* **2011**, *13*, 16542–16547.

[26] Nazet, A. Dynamic and Ion-Association of Ethylammonium Nitrate and Ethanolammnium Nitrate in Polar Solvents. M.Sc. Thesis, Universitët Regensburg, 2013.

[27] LeBel, R.; Goring, D. *Journal of Chemical and Engineering Data* **1962**, *7*, 100–101.

[28] Boettcher, C. J. F. C. J. F.; van. Belle, O. C.; Bordewijk, P. P.; Rip, A. *Theory of electric polarization*; Elsevier Scientific Pub. Co, 1973.

[29] Marcus, Y. *Chemical Reviews* **1988**, *88*, 1475–1498.

[30] Sega, M.; Kantorovich, S.; Arnold, A. *Physical Chemistry Chemical Physics* **2015**, *17*, 130–133.

[31] Eiberweiser, A.; Buchner, R. *Journal of Molecular Liquids* **2012**, *176*, 52–59.

[32] Friesen, S.; Buchecker, T.; Cognigni, A.; Bica, K.; Buchner, R. *Langmuir* **2017**, *33*, 9844–9856.

[33] Hubbard, J. B.; Colonomos, P.; Wolynes, P. G. *The Journal of Chemical Physics* **1979**, *71*, 2652–2661.

[34] Annapureddy, H. V. R.; Dang, L. X. *Journal of Physical Chemistry B* **2014**, *118*, 8917–8927.

[35] Zemaitis, J. F.; Clark, D. M.; Rafal, M.; Scrivner, N. C. *Handbook of Aqueous Electrolyte Thermodynamics: Theory & Application*; Wiley-AIChE: New York, 1986.

[36] Wachter, W.; Buchner, R.; Hefter, G. T. *The Journal of Physical Chemistry B* **2006**, *110*, 5147–5154.

[37] Intharathep, P.; Tongraar, A.; Sagarik, K. *Journal of Computational Chemistry* **2005**, *26*, 1329–1338.

[38] Ekimova, M.; Quevedo, W.; Szyc, Ł.; Iannuzzi, M.; Wernet, P.; Odelius, M.; Nibbering, E. T. J. *J. Am. Chem. Soc.* **2017**, *139*, 12773–12783.

[39] Okouchi, S.; Thanatuksorn, P.; Ikeda, S.; Uedaira, H. *Journal of Solution Chemistry* **2011**, *40*, 775–785.

[40] Kerisit, S.; Vijayakumar, M.; Han, K. S.; Mueller, K. T. *The Journal of chemical physics* **2015**, *142*, 224502.

[41] Kalugin, O. N.; Adya, A. K.; Volobuev, M. N.; Kolesnik, Y. V. *Physical Chemistry Chemical Physics* **2003**, *5*, 1536–1546.

[42] Pliego Jr, J. R.; Riveros, J. M. *Physical Chemistry Chemical Physics* **2002**, *4*, 1622–1627.

[43] Strehlow, H. *Rapid reactions in solution*; VCH: Weinheim, Germany, 1992.

[44] Friesen, S.; Krickl, S.; Luger, M.; Nazet, A.; Hefter, G.; Buchner, R. *Physical Chemistry Chemical Physics* **2018**,

[45] Marcus, Y.; Hefter, G. *Chemical reviews* **2006**, *106*, 4585–4621.

Chapter 4

Temperature Effect on the Solvation of Two Ionic Resorcin[4]arenes from Volumetric and Acoustic Properties in Polar Media

4.1 Introduction

Solvation has been traditionally studied by a combination of techniques[1,2], being analysis of thermodynamic properties one of the most common. Among them, partial or apparent molar volumes and isentropic compressibilities are two quantities, derived from the solution density and speed of sound, able to provide an overview of the interactions between solute and solvent. This information is obtained after an appropriate analysis of the derived quantities as a function of concentration and temperature. Consequently, determination of these properties for solutions of supramolecular receptors is desirable in the study of their interaction with the surrounding medium. However, such studies are limited in number to a few receptors like Cyclodextrins[3,4], Crown Ethers[5,6] and Resorcin[4]arenes[7].

Considering the previous results from the DRS studies at 298.15 K (see chapter 3), in the present chapter the standard molar volumes and isentropic compressibilities of two ionic *C*-methylresorcin[4]arenes, namely Na_4TES and $TAM \cdot (HCl)_4$, were studied in Water and Dimethylsulfoxide (DMSO) as function of concentration and temperature. This was done by measuring the density and speed of sound of the corresponding aqueous and DMSO solutions of each ionic *C*-methylresorcin[4]arene in a concentration range where solute-solute interactions are minimal and in a temperature range where changes in solvent-solvent interactions are appreciable due to the proximity to the fusion temperatures of the solvents.

4.2 Experimental

4.2.1 Materials and chemicals

Synthesis of Na_4TES and $TAM \cdot (HCl)_4$ was done as described in Chapter 2 following already reported procedures [8,9,10]. After synthesis, these compounds were purified by recrystallization using water-ethanol mixtures. Characterization was done using ^{1}H-NMR, and TG analysis. The signal pattern of the ^{1}H-NMR in deuterated water and in deuterated DMSO suggest an averaged crown conformation (see chapter 2). Analysis of the TG thermogram suggest a mass lost coherent with the presence of hydrates: $TAM \cdot (HCl)_4 \cdot 2H_2O$ and $Na_4TES \cdot 3H_2O$. Chromatographic purity was assessed using HPLC-DAD, obtaining values better than 99% (Table 6.1). High purity water (Type 1, Millipore MilliQ, US) was degassed prior its use with a conductivity $< 2\mu$S cm^{-1}. The used DMSO was from Alfa-Aesar (US, > 0.99 by mass fraction) and used without further purification. Pure solvent was stored with 3 Å molecular sieve.

Table 4.1: Chemicals specifications for the solutes used in this work.

Solute	Source	Purification Method	Mass Fraction Purity	Method
$TAM \cdot (HCl)_4$	Synthesis	Recrystallization	>0.99	HPLC-DAD
Na_4TES	Synthesis	Recrystallization	>0.99	HPLC-DAD
DMSO	Alfa Aesar, US		>0.99	
Water	Milli-Q, Millipore			

4.2.2 Samples preparation

Solutions of $TAM \cdot (HCl)_4$ and Na_4TES were prepared by mass using an analytical balance with a sensibility of $1 \cdot 10^{-5}$ g in the range of interest. Hydration waters were taken into account for the calculation of the molality, m (mol·kg^{-1}), of the solutions. In the case of the DMSO solutions, hydrations water introduces 0.25% of humidity into the DMSO, which was treated as an impurity. Aqueous solutions were prepared in the range of $0.0045 < m/\text{mol·kg}^{-1} < 0.1$ and solutions in DMSO in the range of $0.005 < m/\text{mol·kg}^{-1} < 0.045$.

4.2.3 Density and Speed of Sound measurements

The density and speed of sound of the solutions of Na_4TES and $TAM \cdot (HCl)_4$ in water or DMSO, were determined simultaneously using a DSA 5000 M (Anton Paar, Austria) density and speed of sound meter, with a temperature control of ± 0.001 K. All the measurements were carried out at the local atmospheric pressure (0.0474 MPa). Calibration of the instrument was done using dry air and high purity water at 20, 40 and 60 °C. Calibration was checked by measuring water at the working temperatures and contrasting against literature values [11,12] yielding an experimental uncertainty in the density of $1 \cdot 10^{-5}$ g·cm^{-3} and 0.5 m·s^{-1} in speed of sound.

4.3 Results and Discussion

4.3.1 Standard molar Volumes

From the measured solution densities, ρ, tables B.1-B.3 in the supporting information, the apparent molal volumes, V_ϕ, of the solutions of TAM $\cdot$ $(HCl)_4$ and Na_4TES were calculated using the equation:

$$V_\phi = \frac{M_2}{\rho} - \frac{1000(\rho - \rho_0)}{m\rho\rho_0} \tag{4.1}$$

where M_2 is the respective *C*-methylresorcin[4]arene molar mass (Na_4TES: 1008.9 g·mol^{-1}, TAM $\cdot$ $(HCl)_4$: 918.8 g·mol^{-1}), m is the molal concentration and ρ_0 is the density of the pure solvent.

Figure B.1 shows the calculated V_ϕ (tables B.1-B.3) as a function of the molal concentration m at different temperatures. For all cases, V_ϕ values increase with concentration and temperature, being larger in aqueous solutions than in DMSO solutions. For the aqueous solutions, the dependence of V_ϕ with m, Figure B.1a, is described using the Redlich-Rosenfeld-Meyer model[13]:

$$V_\phi = V_2^o + S_V m^{1/2} + B_V m + C_V m^{3/2} \tag{4.2}$$

where $V_2^o (= V_\phi^\infty)$ is the standard (infinite dilution) partial molar volume of the solute in solution, and parameters B_V and C_V are empirical. The term S_V corresponds to the Debye-Hückel limiting slope, modified for unsymmetrical electrolytes, which is calculated as[14]:

$$S_V = kw^{1.5} \tag{4.3}$$

where $w = 0.5\Sigma n_i z_i^2$ with n_i representing the number of ions with charge z_i in one molecule of electrolyte. Parameter k depends on the temperature and solvent properties[14] like isothermal compressibility, κ_T, static permittivity, ε and its change with pressure, $(\partial \ln\varepsilon/\partial P)_T$. For the aqueous solutions, the values of k were taken from Ref.[15]. However, for the DMSO solutions $(\partial \ln\varepsilon/\partial P)_T$ is only available at 298.15 K[16], restricting the calculation of k, and S_V, at other temperatures. Consequently, analysis of V_ϕ with molality in DMSO was done using a Masson type equation:

$$V_\phi = V_2^o + S_V^* m^{1/2} \tag{4.4}$$

where S_V^* is a fitting parameter. Inclusion of further terms in eq.(4.4) did not improve the obtained results. Resulting parameters from the fits using eq.(4.2) are shown in Table 4.2 and the results from the fits using eq.(4.4) are shown in Table 4.3.

Table 4.2: Standard molar volumes, V_2^o, Debye-Hückel slope, S_V [a], and parameters B_V and C_V with their uncertainties, u, in brackets for the aqueous solutions of TAM · $(HCl)_4$and Na_4TES.[b]

Solute	T	$V_2^o(\pm u_{V_2^o})$	S_V	$B_V(\pm u_{B_V})$	$C_V(\pm u_{C_V})$
TAM · $(HCl)_4$	278.15	667.3(±0.7)	49.733	-118(±37)	158(±102)
	283.15	670.0(±0.6)	51.924	-94(±35)	68(±99)
	288.15	673.5(±0.5)	54.233	-144(±26)	189(±72)
	293.15	676.1(±0.5)	56.674	-151(±26)	184(±72)
	298.15	678.4(±0.3)	59.270	-156(±17)	179(±47)
	303.15	681.3(±0.2)	62.031	-231(±15)	402(±50)
	308.15	683.6(±0.2)	64.975	-294(±12)	624(±33)
Na_4TES	278.15	524.0(±0.4)	49.733	-173(±18)	238(±48)
	283.15	530.5(±0.2)	51.924	-201(±9)	271(±25)
	288.15	535.8(±0.1)	54.233	-221(±6)	297(±17)
	293.15	541.2(±0.1)	56.674	-265(±7)	378(±18)
	298.15	545.7(±0.2)	59.270	-293(±9)	418(±24)
	303.15	549.9(±0.2)	62.031	-331(±12)	489(±30)
	308.15	552.3(±0.2)	64.975	-323(±10)	469(±27)

[a] Calculated as described in Ref.[14] using the data of Ref.[15]. [b] Units: T in K; V_2^o in $cm^3 \cdot mol^{-1}$; S_V in $cm^3 \cdot kg^{1/2} \cdot mol^{-3/2}$; B_V in $cm^3 \cdot kg \cdot mol^{-2}$; C_V in $cm^3 \cdot kg^{3/2} \cdot mol^{-5/2}$. Pressure atmospheric, $p = 0.07466$ MPa. Standard uncertainties, u, are $u(T) = 0.005$ K; $u(p) = 1$ kPa.

Table 4.3: Standard partial molar volumes, V_2^o, and the parameter S_V^* for the solutions in DMSO of TAM · $(HCl)_4$ and Na_4TES.[a]

Solute	T	$V_2^o(\pm u_{V_2^o})$	$S_V^*(\pm u_{S_V^*})$
TAM · $(HCl)_4$	293.15	659.5(±0.5)	55.4(±2.4)
	298.15	659.9(±0.3)	56.4(±1.8)
	303.15	660.0(±0.4)	58.5(±1.9)
	308.15	660.2(±0.2)	59.9(±0.8)
Na_4TES	293.15	614.6(±0.5)	93.9(±2.8)
	298.15	615.6(±0.4)	82.4(±2.4)
	303.15	614.9(±0.7)	89.6(±3.9)
	308.15	614.6(±0.5)	93.9(±2.8)

[a] Units: T in K; V_2^o in $cm^3 \cdot mol^{-1}$; S_V^* in $cm^3 \cdot kg^{1/2} \cdot mol^{-3/2}$. Pressure atmospheric, $p = 0.07466$ MPa. Standard uncertainties, u, are $u(T) = 0.005$ K; $u(p) = 1$ kPa.

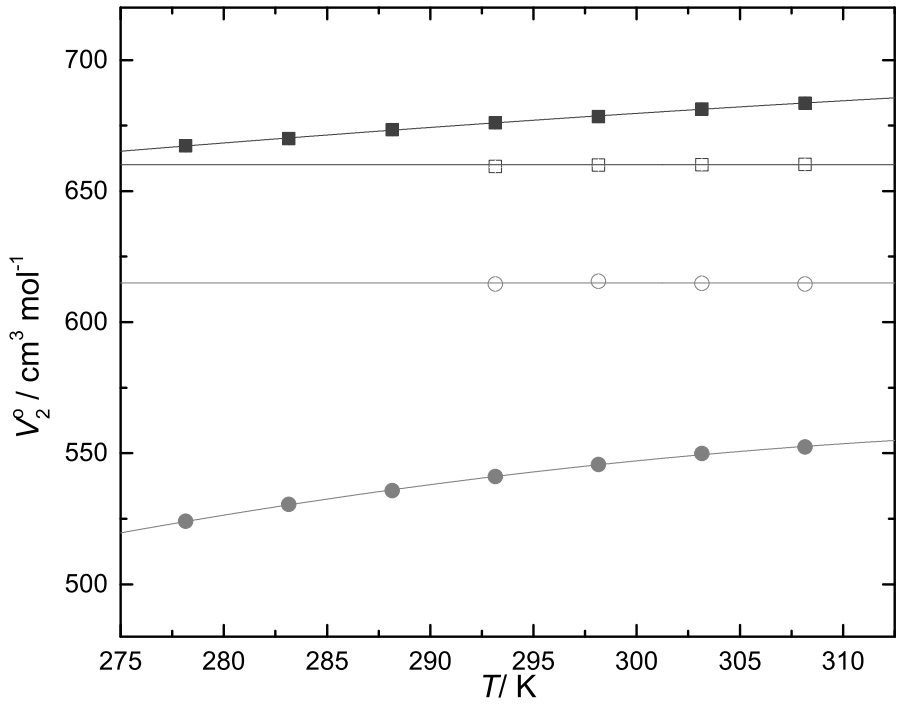

Figure 4.1: Standard partial molar volume, V_2^o, of (●) Na_4TES and (■) $TAM \cdot (HCl)_4$ as a function of temperature in water (filled symbols) and DMSO (empty symbols). Lines are for the eye guidance.

Figure 4.1 shows the values of V_2^o for the *C*-methylresorcin[4]arenes in water and DMSO at different temperatures. There it can be seen that the V_2^o for the aqueous solutions (filled symbols) increases with temperature, whereas V_2^o in DMSO solutions the increment is smaller. In the same way, differences of V_2^o between *C*-methylresorcin[4]arenes are larger in water than in DMSO.

The V_2^o of electrolytes are usually separated in ionic contributions which reflect the ion-solvent interactions[13]. Thus, in the case of ionic resorcin[4]arenes the V_2^o can be split into additive contributions of the constituents ions:

$$V_2^o = V^o(\mathrm{R[4]A}^{4z}) + 4V^o(X^{-z}) \tag{4.5}$$

where $V^o(\mathrm{R[4]A}^{4z})$ represents the ionic partial molar volume of the solute: $V^\circ(\mathrm{TES}^{4-})$ for $\mathrm{TES}^{4-}$and $V^\circ(\mathrm{TAM \cdot H}^{4+})$ for $\mathrm{TAM \cdot H}^{4+}$. Accordingly, $V^o(X^{-z})$ represent the counter ion molar volume. Table 4.4 contains the calculated values of $V^o(\mathrm{R[4]A}^{4z})$. In the case of $V^o(\mathrm{TES}^{4-})$, the reported values of $V^o(\mathrm{Na}^+)$ in Ref.[7] where used, while for $V^o(\mathrm{TAM \cdot H}^{4+}$) in aqueous solutions the values of $V^o(\mathrm{Cl}^-)$ at different temperatures were calculated using the following additive expression:

$$V^o(\mathrm{Cl}^-) = V^o(\mathrm{HCl}) - V^o(\mathrm{H}^+) \tag{4.6}$$

where $V^o(\mathrm{HCl})$ and $V^o(\mathrm{H}^+)$ at different temperatures are calculated from the fol-

lowing polynomials[14,17]:

$$V^o(\mathrm{HCl})/\mathrm{cm}^3\cdot\mathrm{mol}^{-1} = 16.22 + 0.108(T/\mathrm{K} - 273.15) \\ -1.99\cdot10^{-3}(T/\mathrm{K} - 273.15)^2 \\ +9.7\cdot10^{-6}(T/\mathrm{K} - 273.15)^3 \tag{4.7}$$

$$V^o(\mathrm{H}^+)/\mathrm{cm}^3\cdot\mathrm{mol}^{-1} = -5.1 - 0.008(T/^\circ\mathrm{C}) - 1.7\cdot10^{-4}(T/^\circ\mathrm{C})^2 \tag{4.8}$$

unfortunately, eqs.(4.7) and (4.8) are only useful for the estimation of the ionic contribution of the Cl^- in aqueous solutions. For the solutions in DMSO, only the value at 298.15 K was found[18].

Table 4.4: Intrinsic volume of the *C*-methylresorcin[4]arene, V_{int}, ionic molar volume of the *C*-methylresorcin[4]arene, $V^o(\mathrm{R[4]A}^{4z})$, ionic molar volume of the *C*-methylresorcin[4]arene counter ion, $V^o(X^{-z})$, and the interaction volume, $\Delta V_{\mathrm{inter}}$, as function of temperature, T.[a]

Solvent	Solute	V_{int}	T	$V^o(X^{-z})$	$V^o(\mathrm{R[4]A}^{4z})$	$\Delta V_{\mathrm{inter}}$
Water	$\mathrm{TAM}\cdot(\mathrm{HCl})_4$	447.5	278.15	21.9[b]	579.9	132.4
			283.15	22.3[b]	580.9	133.4
			288.15	22.6[b]	582.9	135.4
			293.15	22.9[b]	584.3	136.8
			298.15	23.1[b]	585.9	138.4
			303.15	23.3[b]	588.2	140.7
			308.15	23.4[b]	590.1	142.6
	$\mathrm{Na_4TES}$	417.4	278.15	-7.8[c]	555.2	137.8
			283.15	-7.4[c]	560.1	142.7
			288.15	-7.0[c]	563.8	146.4
			293.15	-6.7[c]	568.0	150.6
			298.15	-6.5[c]	571.6	154.2
			303.15	-6.4[c]	575.5	158.1
			308.15	-6.3[c]	577.5	160.1
DMSO	$\mathrm{TAM}\cdot(\mathrm{HCl})_4$	447.5	293.15	-	623.4[e]	175.9[e]
			298.15	9[d]	623.9	176.4
			303.15	-	624.0[e]	176.5[e]
			308.15	-	624.2[e]	176.7[e]
	$\mathrm{Na_4TES}$	417.4	293.15	5.2[c]	593.8	176.4
			298.15	5.0[c]	595.6	178.2
			303.15	4.8[c]	595.7	178.3
			308.15	4.6[c]	596.2	178.8

[a] Units: T in K; V_{int}, $V^o(X^{-z})$, $V^o(\mathrm{R[4]A}^{4z})$ and $\Delta V_{\mathrm{inter}}$ in $\mathrm{cm}^3\ \mathrm{mol}^{-1}$. [b] This values where calculated using eqs. (4.7,4.8). [c] From reference[7] and references therein. [d] Reference[18]. [e] Estimation based on the assumption of constant $V^\circ(\mathrm{Cl}^-)$(see text).

Figure 4.2 shows the calculated $V^o(\mathrm{R[4]A}^{4z})$ as a function of temperature. The change of $V^o(\mathrm{R[4]A}^{4z})$ with temperature is represented by the ionic molar expansibility, $E^o(\mathrm{R[4]A}^{4z}) = (\partial V^o(\mathrm{R[4]A}^{4z})/\partial T)_P$, and it is calculated after a weighted fit

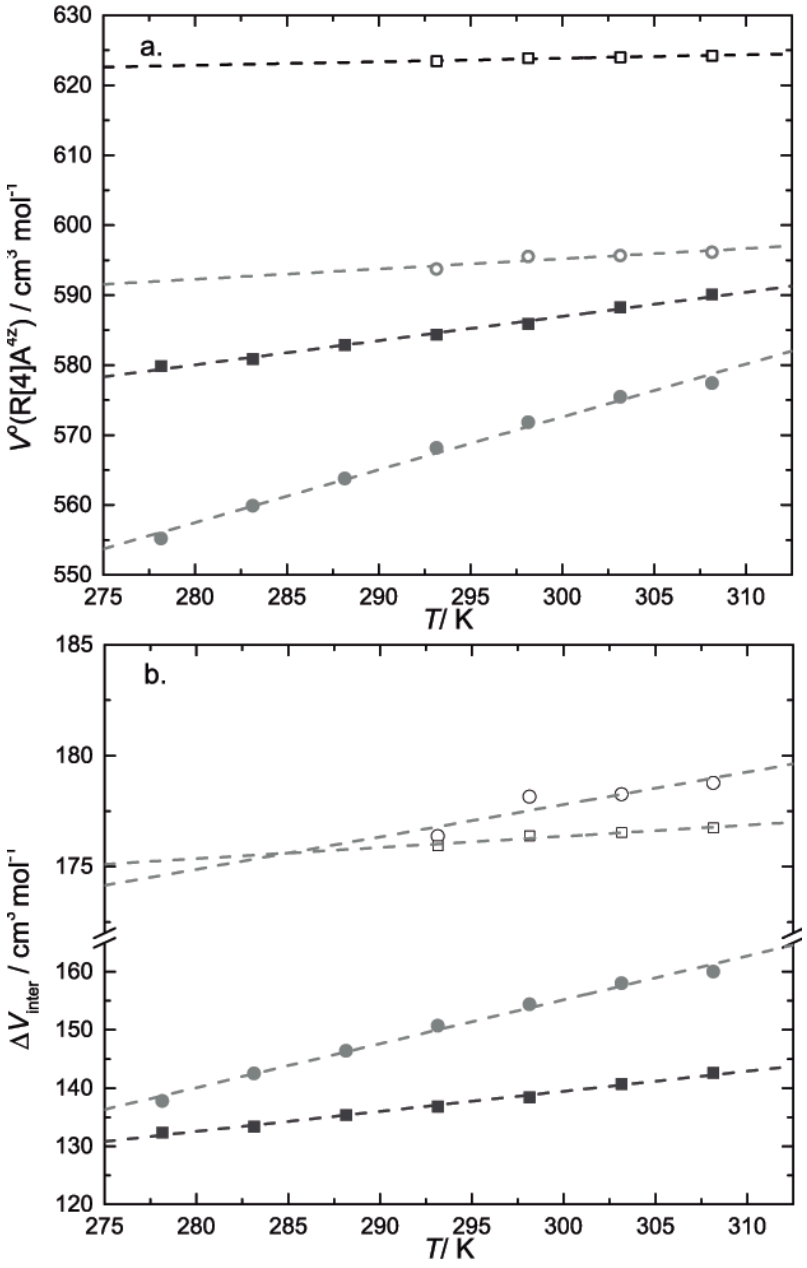

Figure 4.2: (a.) Ionic partial molar volumes, $V^o(\mathrm{R[4]A}^{4z})$, and (b.) interaction volume, $\Delta V_{\mathrm{inter}}$, as function of temperature for the aqueous solutions of (•) TES^{4-}, (■) $\mathrm{TAM \cdot H}^{4+}$ and DMSO solutions (empty symbols). Dashed lines in (a.) are the fits using equation 4.9. Lines in (b.) are for the eye guidance.

to the following equation:

$$V^o(\mathrm{R[4]A}^{4z}) = E^o(\mathrm{R[4]A}^{4z}) \cdot T + b \tag{4.9}$$

where b is an empirical parameter. The calculated $E^o(\mathrm{R[4]A}^{4z})$ showed no dependency with temperature in the studied experimental conditions and resulted in a larger value for TES^{4-} with respect to $\mathrm{TAM \cdot H}^{4+}$ in aqueous solutions ($E^o(\mathrm{TES}^{4-}) = 0.75 \pm 0.03$ cm^3 mol^{-1} K^{-1}; $E^o(\mathrm{TAM \cdot H}^{4+}) = 0.35 \pm 0.01$ cm^3 mol^{-1} K^{-1}). Positive values of the molar expansibility have been correlated with a weakening of the solute-solvent interactions and solvent-solvent interactions promoted by ther-

mal motion[7]. Consequently, the obtained values may indicate that the temperature changes have a rather larger influence on the interactions between TES^{4-} and surrounding water, respect to the interactions between water and $TAM \cdot H^{4+}$. Additionally, the value of $E^o(TES^{4-}) = 0.15 \pm 0.05$ for TES^{4-} in DMSO shows that the dependence with temperature is larger in water than with DMSO. Derivation of $E^o(TAM \cdot H^{4+})$ in DMSO is not possible since only at 298.15 K $V^o(TAM \cdot H^{4+})$ is known. Nonetheless, considering that the V_2^o of $TAM \cdot (HCl)_4$ hardly change with temperature (see Figure 4.1 and Table 4.3), seems reasonable to assume a constant value of $V^o(Cl^- = 9)$ cm^3 mol^{-1} for the purpose of the ongoing analysis. As a result, $E^o(TAM \cdot H^{4+}) = 0.005 \pm 0.009$ cm^3 mol^{-1} K^{-1} in DMSO is obtained, reflecting again that temperature effect is stronger in water than in DMSO having a larger effect in TES^{4-} than in $TAM \cdot H^{4+}$. All the parameters derived from the fits using eq. (4.9) are shown in table B.4 of the supporting information.

Figure 4.2a shows that for aqueous solutions (filled symbols) $V^o(TAM \cdot H^{4+})$ is always larger than $V^o(TES^{4-})$ at all temperatures. After assuming again constant $V^o(Cl^-)$, the same can be stated for solutions in DMSO (Table 4.4). These results come from the fact that the $TAM \cdot H^{4+}$ structure has larger intrinsic volume, V_{int}, than the TES^{4-}. Estimation of the van der Waals volume of the ions using the Winmostar software[19], after a semi-empirical optimization using MOPAC2016[20] with the PM7 hamiltonian, yielded the values $V_{int}(TES^{4-}) = 417.4$ cm^3 mol^{-1} and $V_{int}(TAM \cdot H^{4+}) = 447.5$ cm^3 mol^{-1}.

Typically, the ionic partial molar volumes can be further separated into four different contributions[13]:

$$V^o(R[4]A^{4z}) = V_{int} + V_{ele} + V_{cov} + V_{str} \tag{4.10}$$

where V_{int} represent the intrinsic volume of the ion (which can be estimated as the van der Waals volume); V_{ele}, the electrostriction contribution, which represents the change in volume that arise from the compression of the surrounding solvent shell caused by the electric field exerted by the ion; V_{cov}, which reflects the contribution from all the short range interactions such as donor-acceptor and hydrogen bonding between the ion and the solvent; and V_{str}, which contains the changes to the solvent structure caused by the interaction with the ions, but excluding electrostriction[13]. Unfortunately, not all these contributions to $V^o(R[4]A^{4z})$ are simple to calculate. Thus, it is convenient to group all the contribution on the right hand side of eq.(4.10), except V_{int}, into one contribution that contains all the effects that arise from the interactions between resorcin[4]arenes ions and the solvent: the interaction volume contribution, $\Delta V_{inter} = V_{ele} + V_{cov} + V_{str}$. Values of ΔV_{inter}, calculated from the difference between $V^o(R[4]A^{4z})$ and V_{int}, are summarized in Table 4.4 and are showed as function of temperature in Figure 4.2b.

Surprisingly, and contrary to what it was seen in the trends of $V^o(R[4]A^{4z})$ with temperature (Fig.4.2a), where $V^o(TAM \cdot (HCl)_4)$ is larger than $V^o(Na_4TES)$, the data in Figure 4.2b shows that $\Delta V_{inter}(TES^{4-})$ is larger than $\Delta V_{inter}(TAM \cdot H^{4+})$, although with a contrary temperature effect. In the case of $V^o(R[4]A^{4z})$,(Fig.4.2a) the difference between them in the same solvent is reduced upon a temperature increment, being more evident for aqueous solutions (filled symbols) and corroborated by the calculated expansibilities. In DMSO solutions the temperature effect is not evident, but present from the calculated $E^o(R[4]A^{4z})$. On the contrary, the difference in ΔV_{inter} (Fig.4.2b) is larger upon increasing temperature. Additionally,

when the temperature is close to the fusion point of the solvent, both ionic resorcin[4]arenes have very similar ΔV_{inter} values (Table 4.4). Moreover, comparison of ΔV_{inter} values in DMSO at 293.15 K with the reported one by Sanabria et al[7] in the same solvent of 178.7 cm^3 mol $^{-1}$ for the tetrasulfonated resorcin[4]arene with *C*-butyl chains(Bu-TES^{4-}) shows an interesting coincidence. However, in the case of aqueous solutions, the resorcin[4]arenes studied here have a lower ΔV_{inter} than the Bu-TES^{4-}, which is 189.2 cm^3 mol $^{-1}$[7].

One useful quantity that represents the differences in ion-solvent interactions in the two studied solvents is the ionic transfer volume, $\Delta_t V^o$[13,18]. This quantity is defined as the difference between $V^o(\text{R[4]A}^{4z})$ of the same ion in different solvents:

$$\Delta_t V^o(\text{R[4]A}^{4z}, \text{DMSO} \rightarrow \text{Water}) = V^o(\text{R[4]A}^{4z})_{\text{Water}} - V^o(\text{R[4]A}^{4z})_{\text{DMSO}} \quad (4.11)$$

Comparison of eq.(4.11) with eq.(4.10) revealed that the purpose of the former equation is to compare ΔV_{inter} in different solvents by canceling V_{int}. Calculated values of $\Delta_t V^o$ are shown in Table 4.5. As it can be seen there, in all cases negative $\Delta_t V^o$ values were obtained, indicating a volume contraction during the transference process from DMSO to water. Such contraction can be explained in an increment of magnitude of solute-solvent interactions as expected from the change of dielectric constant along with donor-acceptor capacity of the medium (solvophilic solvation) and increment of the free space around the solute (solvophobic solvation).

Comparison of $\Delta_t V^o(\text{TES}^{4-})$ with the values of Bu-TES^{4-} at the same temperature, $10.6 \leq \Delta_t V^o/\text{cm}^3 \cdot \text{mol}^{-1} \leq 26.1$[7], shows that they have different signs. This might be an evidence of a possible effect on the solute-solvent interactions related to the lower rim chain length (methine substituent) on the strength of solute-solvent interactions.

Table 4.5: Ionic transfer volume from water to DMSO, $\Delta_t V^o(\text{Water} \rightarrow \text{DMSO})$, of TES^{4-}as function of temperature, T, and TAM $\cdot$ H^{4+} at 298.15 K.[a]

Solute	T	$\Delta_t V^o$(DMSO → Water)
TES^{4-}	293.15	-25.6
	298.15	-23.7
	303.15	-20.2
	308.15	-18.7
TAM $\cdot$ H^{4+}	293.15	-39.1[b]
	298.15	-38.0
	303.15	-35.8[b]
	308.15	-34.1[b]

[a] Units: T in K; $\Delta_t V^o$ in cm^3 mol^{-1}.[b] Estimations based on the assumption of constant $V^\circ(\text{Cl}^-)$(see text).

4.3.2 Standard partial molar isentropic compressibilities

The standard (infinite dilution) molar isentropic compressibilities, $\kappa^o_{s,\phi}$, were calculated following the procedure proposed by Garnsey et al[21]:

$$\kappa^o_{s,\phi} = \kappa_{s,o}\left[2V^o_2 - \frac{M_2}{\rho_o} - \frac{2000F}{v_o}\right] \tag{4.12}$$

where $\kappa_{s,o}$ is the isentropic compressibility of the pure solvent and is calculated using the Newton-Laplace equation with the pure solvent values of ρ_0 and v_0 reported in table B.8:

$$\kappa_{s,0} = \frac{1}{v_0^2\rho_0} \tag{4.13}$$

The parameter F is the slope of the dependence of the difference in speed of sound, v (Tables B.5-B.7) between the solution and the solvent, $\Delta v = v - v_0$, with the concentration of the solute, c, in mol·L^{-1}:

$$\Delta v = Fc \tag{4.14}$$

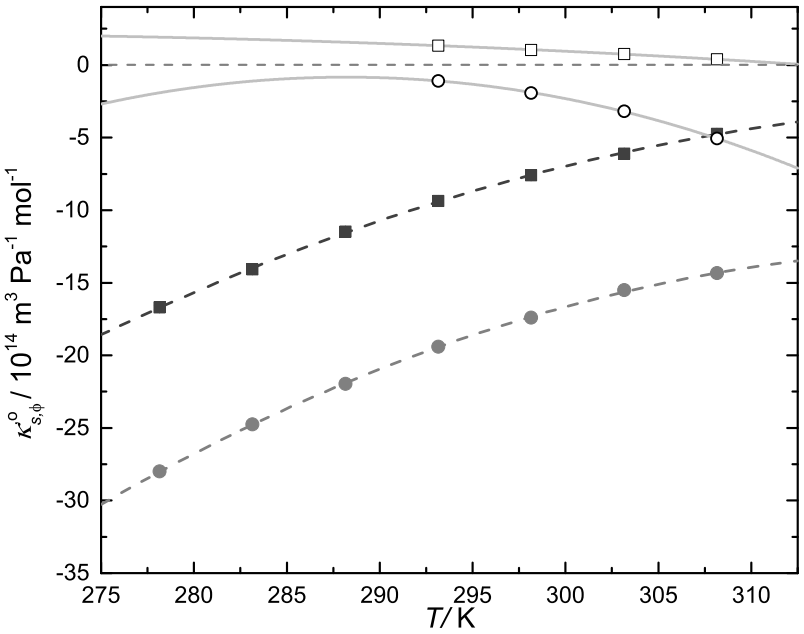

Figure 4.3: Partial molar isentropic compressibility, $\kappa^o_{s,\phi}$, of (●) Na_4TES and (■) $TAM\cdot(HCl)_4$ in aqueous solutions and (□) $TAM\cdot(HCl)_4$ and (○) Na_4TES in solutions of DMSO at different temperatures. Lines are for the eye guidance.

The obtained values of F and $\kappa^o_{s,\phi}$ at different temperatures are shown in Table 4.6 for the aqueous and DMSO solutions. Figure 4.3 depicts the dependence of $\kappa^o_{s,\phi}$ with temperature. For the aqueous solutions (filled symbols), increasing the temperature causes an increment of $\kappa^o_{s,\phi}$, while for the DMSO solutions the effect is

Table 4.6: Calculated parameter F from eq. (4.14) and standard partial molar isentropic compressibility, $\kappa^o_{s,\phi}$, from eq. (4.12), and Solvation number, n, and parameter b_n from eq. (4.16) with their uncertainties in brackets for the solutions of $TAM \cdot (HCl)_4$ and Na_4TES in water and DMSO at different temperatures.[a]

Solvent	Solute	T	$F(\pm u_F)$	$10^{14}\kappa^o_{s,\phi}(\pm u_{\kappa^o_{s,\phi}})$	$n^\infty(\pm u_{n^\infty})$	b_n
DMSO	$TAM \cdot (HCl)_4$	293.15	277.4(±2.1)	1.3(±0.1)	8.0(± 0.2)	-19.(± 5.)
		298.15	277.7(±2.1)	1.0(±0.1)	8.0(± 0.2)	-20.(± 5.)
		303.15	277.1(±1.9)	0.8(±0.1)	8.1(± 0.2)	-19.(± 6.)
		308.15	277.7(±1.9)	0.4(±0.1)	8.2(± 0.2)	-20.(± 6.)
	Na_4TES	293.15	255.4(±1.3)	-1.1(±0.1)	9.1(± 0.1)	-18.(± 2.)
		298.15	265.3(±1.3)	-1.9(±0.1)	9.3(± 0.1)	-17.(± 3.)
		303.15	279.0(±1.4)	-3.2(±0.1)	9.5(± 0.1)	-13.(± 3.)
		308.15	302.3(±1.6)	-5.1(±0.1)	9.8(± 0.1)	-9.(± 3.)
Water	$TAM \cdot (HCl)_4$	278.15	475.2(±1.4)	-16.7(±0.2)	50.8(± 0.3)	-65.(± 5.)
		283.15	453.1(±1.0)	-14.1(±0.1)	48.5(± 0.2)	-64.(± 3.)
		288.15	428.0(±1.0)	-11.5(±0.1)	45.9(± 0.2)	-58.(± 3.)
		293.15	405.5(±1.3)	-9.4(±0.1)	43.7(± 0.3)	-54.(± 4.)
		298.15	385.3(±1.3)	-7.6(±0.1)	42.0(± 0.3)	-54.(± 4.)
		303.15	368.0(±1.3)	-6.1(±0.1)	40.5(± 0.2)	-54.(± 4.)
		308.15	350.3(±1.2)	-4.7(±0.1)	38.7(± 0.3)	-54.(± 4.)
	Na_4TES	278.15	434.9(±3.2)	-28.0(±0.3)	60.9(± 0.7)	-76.(± 9.)
		283.15	413.3(±3.1)	-24.8(±0.2)	58.5(± 0.7)	-73.(± 9.)
		288.15	391.4(±2.9)	-22.0(±0.2)	56.2(± 0.6)	-70.(± 8.)
		293.15	369.0(±2.4)	-19.4(±0.2)	53.6(± 0.5)	-62.(± 7.)
		298.15	350.4(±1.8)	-17.4(±0.1)	52.0(± 0.3)	-63.(± 4.)
		303.15	330.7(±2.2)	-15.5(±0.2)	49.9(± 0.5)	-56.(± 6.)
		308.15	318.3(±0.9)	-14.3(±0.1)	48.4(± 0.2)	-51.(± 2.)

[a] Units: T in K; F in L mol^{-1}; $\kappa^o_{s,\phi}$ in m^3 Pa^{-1} mol^{-1} and n^∞ is dimensionless. Pressure atmospheric, $p = 0.07466$ MPa. Standard uncertainties, u, are $u(T) = 0.005$ K; $u(p) = 1$ kPa.

opposite. However, for every system, except the $TAM \cdot (HCl)_4$ in DMSO, $\kappa^o_{s,\phi}$ has negative values. Since this quantity reflects the difference in isentropic compressibility between the solution and the solvent, negative values of $\kappa^o_{s,\phi}$ can be related with a structuring effect: enhancement of the solution structure due to the presence of the solute. Such effect, in the case of aqueous solutions, is reduced by the increment of temperature, whereas for the solutions in DMSO is improved. Another aspect that is worthy to mention is that in both solvents, $\kappa^o_{s,\phi}$ of Na_4TES are always more negative than the ones calculated for $TAM \cdot (HCl)_4$.

4.3.3 Solvation numbers

In order to analyze resorcin[4]arene-solvent interactions, calculation of the solvation numbers, n_s, from the isentropic compressibility is useful. Pasynski[22] proposed a model based on the assumption that the change of the solution compressibility is proportional to the number of solvent molecules involved in the solvation shell of

the electrolyte:

$$n_s = \frac{n_1}{n_2}\left(1 - \frac{\kappa_s}{\kappa_{s,0}}\right) \tag{4.15}$$

where n_1 and n_2 are the amount of moles of solvent and solute, respectively, and κ_s and $\kappa_{s,0}$ the isentropic compressibility of the solution and the solvent, respectively, which are calculated using eq.(4.13)(Table B.5-B7). Afterwards, the calculated n_s values (Table B.5-B.7), where analyzed as a function of concentration m, using an averaged weighted fit to the equation:

$$n_s = n_s^{\infty} + b_n m \tag{4.16}$$

where n_s^{∞} is the solvation number at infinite dilution and b_n is an empirical parameter. The obtained values are included in Table 4.6 with their corresponding uncertainties.

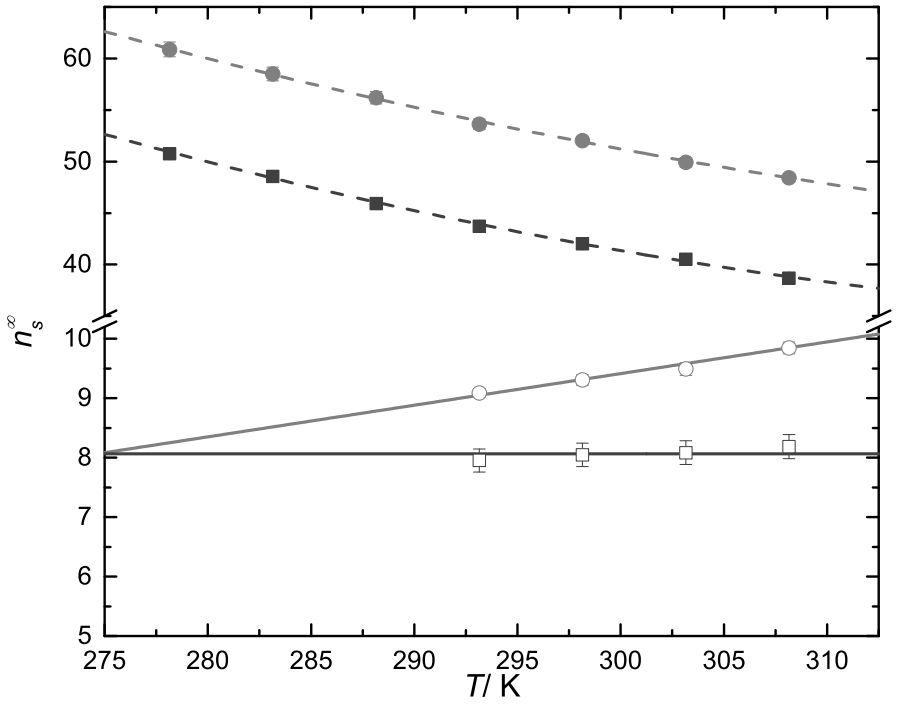

Figure 4.4: Solvation numbers at infinite solution, n^{∞}, of (•) Na_4TES and (■) $TAM \cdot (HCl)_4$ in aqueous solutions and (□) $TAM \cdot (HCl)_4$ and (○) Na_4TES in DMSO at different temperatures. Lines are for the eye guidance.

Figure 4.4 shows the trends of n_s^{∞} with temperature. For aqueous solutions (filled symbols), the increment of temperature promotes desolvation. Interestingly, n_s^{∞} of Na_4TES is always larger than the values for $TAM \cdot (HCl)_4$ with a constant difference within the studied temperature range of $\Delta n_s^{\infty} = n_s^{\infty}(Na_4TES) - n_s^{\infty}(TAM \cdot (HCl)_4) \approx 10$. Although this difference could arise from counter ion

hydration, an estimation of this contribution at 298.15 K assuming ionic additivity, $n_s^\infty = n_s^\infty(\mathrm{R[4]A}^{4z}) + 4n_s^\infty(X^{-z})$, with $n_s^\infty(\mathrm{Na}^+{=}4)$ and $n_s^\infty(\mathrm{Cl}^-{=}3.1)$[23], indicate that $n_s^\infty(\mathrm{TES}^{4-}) = 36.0$ is larger than $n_s^\infty(\mathrm{TAM \cdot H}^{4+}) = 29.6$ by ∼6 water molecules. Considering that the analysis of the molar volumes and isentropic compressibilities suggest a larger hydrophilic hydration of TES^{4-} due the large $\Delta V_{\mathrm{inter}}$ and more negative $\kappa_{s,\phi}^o$ than $\mathrm{TAM \cdot H}^{4+}$, the calculated solvation numbers can be interpreted as an indication of larger hydrophilicity. A similar conclusion was drawn from DRS data (see chapter 3) despite DRS total ionic solvation numbers ($Z_t(\mathrm{R[4]A}^{4z})$ in aqueous solutions at 298.15 K, showed an opposite result: $\mathrm{TAM \cdot H}^{4+}$ has a total ionic solvation number, ($Z_t(\mathrm{TAM \cdot H}^{4+}) \approx 43$), slightly larger than TES^{4-} ($Z_t(\mathrm{TES}^{4-}) \approx 39$). The reason for this difference is the fact that solvation numbers, n_s^∞ and Z_t, are not directly comparable. For example, while for TES^{4-} $n_s^\infty \approx Z_t$ for $\mathrm{TAM \cdot H}^{4+}$ $n_s^\infty < Z_t$. Thus, they coincide in the idea that each quantity represents the extend of solvent molecules affected by the presence of a solute, yet that does not necessarily imply they are probing exactly the same solvent molecules.

Although the Pasynski method has been mostly used in aqueous solutions, it has been shown that it can be used in nonaqueous media[22] as well. Figure 4.4 shows n_s^∞ in DMSO solutions are significantly lower than in aqueous solutions, thus it can be expected that solvation shells around ionic resorcin[4]arenes are not as crowded as in aqueous solutions. Furthermore, the solvation in $\mathrm{Na_4TES}$ barely increases with temperature while for $\mathrm{TAM \cdot (HCl)_4}$ seems to remain constant. This weak temperature dependence was also found for $\Delta V_{\mathrm{inter}}$ and $\kappa_{s,\phi}^o$ where negligible changes take place.

Comparison of n_s^∞ with the reported values for the Bu-$\mathrm{Na_4TES}$[7] showed than in aqueous solutions at $T < 288.15$ K, n_s^∞(Bu-$\mathrm{Na_4TES}$) is greater than n_s^∞($\mathrm{Na_4TES}$), but at temperatures above they show similar values. The same comparison in DMSO solutions shows values of n_s^∞(Bu-$\mathrm{Na_4TES}$) are very close to the values obtained in this work, lying in between $8.6 < n_s^\infty(\text{Bu-}\mathrm{Na_4TES}) < 9.4$[7]. These results complement the observations from $\Delta V_{\mathrm{inter}}$ values, which showed that in aqueous solutions the length of the chain in the lower rim of the resorcin[4]arene structure seems to affect solute-solvent interactions especially at low temperatures. On the contrary, the structural effects on the solvation of ionic resorcin[4]arenes in DMSO are larger with increasing temperatures.

4.4 Conclusions

Standard molar volumes and compressibilities were determined in water and DMSO as a function of temperature from measurements of solutions density and speed of sound. Analysis of standard molar volumes revealed that they are dominated by the intrinsic volume of the resorcin[4]arene ions, but when subtracted the intrinsic contribution, the resulting $\Delta V_{\mathrm{inter}}$ indicate that TES^{4-} has larger interaction contribution than $\mathrm{TAM \cdot H}^{4+}$. These results suggest that despite being water and DMSO polar solvents, clear differences on the solute-solvent interaction exist. In DMSO changes are very similar despite the solute structure differences, while in water solute structure seems to be highly relevant. This observation is also supported from the analysis of solutions $\Delta V_{\mathrm{inter}}$, $\kappa_{s,\phi}^o$ and compressibility-derived solvation numbers, n_s^∞, where their magnitudes suggest larger solute-solvent interactions in water than

in DMSO.

Determination of transfer volumes, V_t^o, from DMSO to water suggests a contraction, which can be explained by an enhancement of the solute-solvent interactions. Additionally, the increment on temperature reduces the contraction suggesting a weakening of solute-solvent interactions. This latter observation is coherent with the reduction of n_s^∞ with temperature. On the other hand, standard partial molar compressibilities suggest an enhancement of solvent structure in the case of aqueous solutions, being larger in solutions of Na_4TES, but reduced by temperature increment. In DMSO solutions of Na_4TES, calculated $\kappa_{s,\phi}^o$ values indicate that they are more "structured" than $TAM \cdot (HCl)_4$ solutions; however, an increment in temperature slightly enhance the solvent structure. Calculation of solvation numbers from isentropic compressibilities showed that TES^{4-} might be more solvated than $TAM \cdot H^{4+}$ in both solvents, but solvation in water being larger than in DMSO.

Generally, the temperature effect in water is different from the solutions in DMSO. For aqueous solutions, raising the temperature cause an increment in all the determines quantities except for the solvation numbers. In the case of DMSO solutions, temperature doesn't affect as much within the studied range. This is illustrated by the magnitude of molar expansibilities, $E^o(R[4]A^{4z})$, which suggest that in aqueous solutions, solvent-TES^{4-} interactions are more temperature sensitive than solvent-$TAM \cdot H^{4+}$, while in DMSO solutions the temperature effect is observed in a lesser extent. Additionally, the increment of ΔV_{inter} with temperature while solvation numbers tend to decrease in aqueous solutions and to remain constant in DMSO, might suggest that an increment on the contribution from the free space around the resorcin[4]arene structure is taking place in water and in a lesser extent in DMSO. Thus, these results might suggest that in DMSO solute-solvent interactions seem to be not the predominant force driving solvation as it seems to be the case for aqueous solutions.

Bibliography

[1] Marcus, Y. *Ions in Solution and their Solvation*; John Wiley & Sons, 2015.

[2] Ohtaki, H. *Monatshefte für Chemie/Chemical Monthly* **2001**, *132*, 1237–1268.

[3] Miyajima, K.; Sawada, M.; Nakagaki, M. *Bulletin of the Chemical Society of Japan* **1983**, *56*, 3556–3560.

[4] Spildo, K.; Høiland, H. *Journal of solution chemistry* **2002**, *31*, 149–164.

[5] Cibulka, I.; Alexiou, C. *The Journal of Chemical Thermodynamics* **2010**, *42*, 274–285.

[6] Patil, K.; Pawar, R.; Gokavi, G. *Journal of Molecular Liquids* **1998**, *75*, 143–148.

[7] Español, E. S.; Villamil, M. M.; Esteso, M. A.; Vargas, E. F. *Journal of Molecular Liquids* **2018**, *249*, 868–876.

[8] Morozova, Y. E.; Shalaeva, Y. V.; Makarova, N. A.; Syakaev, V. V.; Kazakova, E. K.; Konovalov, A. I. *Russ. Chem. Bull.* **2009**, *58*, 95–100.

[9] Kazakova, E. K.; Makarova, N. A.; Ziganshina, A. U.; Muslinkina, L. A.; Muslinkin, A. A.; Habicher, W. D. *Tetrahedron Letters* **2000**, *41*, 10111–10115.

[10] Matsushita, Y.; Matsui, T. *Tetrahedron letters* **1993**, *34*, 7433–7436.

[11] Kell, G. *Journal of Chemical and Engineering data* **1967**, *12*, 66–69.

[12] Del Grosso, V.; Mader, C. *The Journal of the Acoustical Society of America* **1972**, *52*, 1442–1446.

[13] Hefter, G. *Volume Properties*; 2014; pp 493–511.

[14] Millero, F. J. *Chemical Reviews* **1971**, *71*, 147–176.

[15] Ananthaswamy, J.; Atkinson, G. *Journal of Chemical and Engineering Data* **1984**, *29*, 81–87.

[16] Warmińska, D.; Grzybkowski, W. *The Journal of Chemical Thermodynamics* **2010**, *42*, 1451–1457.

[17] Hedwig, G. R.; Hakin, A. W. *Physical Chemistry Chemical Physics* **2004**, *6*, 4690–4700.

[18] Marcus, Y.; Hefter, G. *Chemical Reviews* **2004**, *104*, 3405–3452.

[19] Senda, N. *Idemitsu Tech. Rep.* **2006**, *49*, 106–111.

[20] J.P. Stewart, J. **2016**, *Stewart Computational Chemistry*.

[21] Garnsey, R.; Boe, y. R.; Mahoney, R.; Litovitz, T. *The Journal of Chemical Physics* **1969**, *50*, 5222–5228.

[22] Burakowski, A.; Glinski, J. *Chemical Reviews* **2011**, *112*, 2059–2081.

[23] Burakowski, A.; Gliński, J. *Chemical Physics Letters* **2009**, *468*, 184–187.

Chapter 5

Electric Molar Conductivity of Two Ionic Resorcin[4]arenes

5.1 Introduction

Ion association and ion-solvent interactions are two important factors to be considered in the development of ionic receptors for supramolecular chemistry in polar solvents. For this purpose, electrical molar conductivity, Λ, is a convenient technique since it serves to determine whether the actual concentration of ions in solution is equal to the expected stoichiometric concentration. Electrical conductivity results from imposing an alternating external electric field ($\sim$1 kHz) to an electrolyte solution[1]. It has the advantage of being precisely measured even for dilute solutions[1,2]. Moreover, according to the law of independent migration of ions[3], Λ at infinite dilution, Λ_j^{∞}, can be directly separate into ionic contributions, λ_j, allowing the assessment of individual ion-solvents interactions. Such contributions can be determined experimentally for individual ions using the electrolyte conductivities and transference numbers[1,2].

Considering that the movement of ions in an electric field is expressed by their mobilities, it can be showed that at infinite dilution mobilities are directly proportional to the limiting ionic molar conductivities, λ_j^{∞} [1,3]. Additionally, the mobility of an ion also depends on its size and on the viscosity of the solvent[1]. Thus, from the ionic conductivities the size of the ions might be calculated provided the medium viscosity. Such relationship allowed to show that smaller ions have large mobilities. Interestingly, comparison with crystallographic data showed that ions in solutions show a different size. This difference has been attributed to ion-solvent interactions. For example, hydrodynamic radius, an estimation of the size of an ion in aqueous solutions, decrease as the ionic radius increases in the series of the alkali metal cations and the halide anions for any solvent[1]. This behavior has been correlated to the stronger solvation of the smaller ions, manifested by larger solvation numbers which in turn provides larger hydrodynamic volumes leading to slower mobilities[1].

On the other hand, ion–ion interactions cause the conductivities of electrolytes to decrease as the concentration increase. According to ion-association theories[1,2], conductivity reduction is explained by formation of ion pairs, which are form due to the coulombic attraction between oppositely charged ions. Considering that the distance between ions determines in a large extent the strength of the electrostatic interaction, it should be expected that upon concentration increment ion proxim-

ity will be promoted and, consequently, ion association. Nonetheless, not all the concentrate electrolyte solution shows ion association. Two other factors important in the formation of ion aggregates is the solvent permittivity and the charge of the participating ions.

An appropriate theoretical expression is required for the extrapolation that takes into account the indirect ion–ion and ion–solvent effects. For this purpose different expressions for the determination of limiting electrolyte conductivity and association constants exist[(2)]. Some of the most important differences between models are the range of applicability and the theoretical treatment of ion cloud relaxations and electrophoretic effects. Additionally most of the approaches are mostly suitable for symmetrical electrolytes.

Most of the electrolytic molar conductivity studies have been done in aqueous solutions using monovalent ions[(1)]. Studies including ionic resorcin[4]arenes have been limited to the determination of electrolytic conductivity (κ) in order to assess possible aggregates formation[(4)]. In this chapter the results from the determination of electrolytic molar conductivities as function temperature for aqueous and DMSO solutions of Na_4TES and $TAM \cdot (HCl)_4$ are presented.

5.2 Experimental

5.2.1 Sample Preparation

Synthesis and purification of Na_4TES and $TAM \cdot (HCl)_4$ were done as mentioned in chapter 2. Chromatographic purity was assessed using HPLC-DAD, obtaining values better than 99% (Table 6.1). High purity water (Type 1, Millipore MilliQ, US) was degassed prior its use with a conductivity $< 2\mu S\ cm^{-1}$. The used DMSO was from Alfa Aesar (US, > 0.99 by mass fraction) and used without further purification, it was stored with 3 Å molecular sieve.

Table 5.1: Chemicals specification

Solute	Source	Purification Method	Mass Fraction Purity	Method
$TAM \cdot (HCl)_4$	Synthesis	Recrystallization	>0.99	HPLC-DAD
Na_4TES	Synthesis	Recrystallization	>0.99	HPLC-DAD
DMSO	Alfa Aesar, US		>0.99	
Water	Milli-Q, Millipore			

Stock Solutions of $TAM \cdot (HCl)_4$ and Na_4TES were prepared by mass using an analytical balance with a sensibility of $1{\cdot}10^{-5}$ g. Hydration waters were taken into account for the calculation of the molality, m ($mol{\cdot}kg^{-1}$), of the solutions. In the case of the DMSO solutions, hydrations water introduces 0.25% of humidity into the DMSO, which was treated as an impurity.

5.2.2 Electrical molar conductivity

The electrical molar conductivity of the solutions, $\Lambda\,/\,cm^2 \cdot mol^{-1}$, was determined using two three-electrode cells[(5)] modified for low volumes ($\sim 150\,mL$). The cells were immersed in a thermostat (Lauda Proline RP 3530) controlling temperature

better to ±0.01 K. The resistance of solutions were measured as a function of temperature using a high-precision LCR Bridge (HAMEG 8118) controlled by a desktop computer and a custom made switch board. Prior to any measurement, the LCR bridge was calibrated to eliminate lead resistance. The cell constants, K_{cell}, were determined according to the procedure reported by Shreiner and Pratt[6]. The electrical conductivity, κ, of the studied solutions was determined according to the following procedure: first a known quantity of approximately 150.0 g of solvent was transferred into the cell under an inert atmosphere of $N_{2(g)}$. The cell was then immersed into the thermostat and the solvent resistance, $R_s(\nu)$, measured as a function of frequency in the range of $0.1 \leq \nu/\text{kHz} \leq 10$. Then known masses of stock solution (~ 0.15 mol kg^{-1}) of the target solute were subsequently added using a gas-tight syringe and —after stirring and sufficient time for equilibration— the solution resistance, $R(\nu)$, was determined.

To eliminate electrode polarization effects, solutions and solvent resistance, $R(\nu)$ and $R_s(\nu)$ respectively, were extrapolated to "infinite" frequency, R_∞, using a non-linear regression of the function:

$$R(\nu) = R_\infty + \frac{A}{\nu^b} \tag{5.1}$$

where A and b ($0.5 \leq b \leq 1$) are fitting parameters with no physical meaning[7]. For aqueous solutions the electrical conductivity of the solution calculated as:

$$\kappa = K_{\text{cell}} \times (1/R_\infty - 1/R_{\infty,\text{s}}) \tag{5.2}$$

which is used to calculate the corresponding molar conductivity,

$$\Lambda = 1000\kappa/c \tag{5.3}$$

Occasionally, dilute solutions (or pure solvents) with large resistance, eq. (5.1) may yield a negative R_∞. In these cases, the approximation $R_\infty \approx R(\nu = 10 \text{ kHz})$ was done, which seems to be reasonable according to what it is observed for solutions with large electrolyte concentration.

Molar concentration, $c/\text{mol} \cdot \text{L}^{-1}$, was calculated from the molal concentration, $m/\text{mol kg}^{-1}$, and solution densities, ρ, determined in a previous study (Chapter 4). Repeatability of κ was always better than 0.03 % and Λ better than 0.2 %. Calculated values of Λ as a function of m are shown in Tables C.1-C.X of the Supporting Information.

5.3 Data analysis

5.3.1 Molar electrical conductivities

The ionic resorcin[4]arenes studied here are unsymmetrical electrolytes: Na_4TES 1:4 and TAM $\cdot$ $(HCl)_4$ 4:1. The electrical molar conductivity of unsymmetrical electrolytes can be modeled using the Quint-Viallard model (Q-V)[8], which extend the idea behind the independent ionic migration law stated by Kohlrausch as function of concentration using the following set of equations[9]:

$$\Lambda = \sum_{j=1}^{h} \frac{c_j |z_j| \lambda_j}{c} \tag{5.4a}$$

$$\lambda_j = \lambda_j^{\infty} - S_j (I)^{1/2} + E_j I \ln I + J_{1,j} I - J_{2,j} I^{3/2} \tag{5.4b}$$

$$I = \frac{\alpha}{2} \sum_j z_j^2 c_j \tag{5.4c}$$

where in eq. (5.4a) c_j represents the concentration of species j with charge $|z_j|$ with respect to the total concentration, c. The ionic molar conductivity, λ_j, is calculated with eq. (5.4b) where the parameters $S_j, E_j, J_{1,j}$ and $J_{2,j}$ are complex quantities, presented in reference [9], which depends on λ_j, distances parameter a_j, and solvent viscosity and static permittivity, η and ε respectively. Originally, Q-V equations did not consider ion association. As a result, this problem is addressed [10] by coupling equations (5.4a-c) with a chemical equilibrium approach via the dissociation degree, α, which modifies the total ionic strength, I, as shown in equation (5.4c). Estimation of α is thus calculated from the ion association equilibrium:

$$K_{\mathrm{A}} = \frac{(1-\alpha)}{\nu_+ \nu_- c \alpha^2} F_\gamma \tag{5.5}$$

where ν_j is the stoichiometric coefficients and F_γ is the quotient of the activity coefficients γ_j [10], which are approximated in dilute solutions by the Debye-Hückel equation:

$$\log(\gamma_j) = \frac{z_j^2 A \sqrt{I}}{1 + a_j B \sqrt{I}} \tag{5.6a}$$

$$A = 1.825 \times 10^6 (\varepsilon T)^{3/2} \qquad B = 50.29 \times 10^8 (\varepsilon T)^{1/2} \tag{5.6b}$$

Validation of this approach combining Q-V model with chemical equilibrium was done by comparison with the results calculated using the low-chemical concentration model (lcCM) for the Formic acid [9], which was built upon the idea of ion association instead of amended to it, but is limited to symmetrical electrolytes solutions only.

As mentioned in Chapter 3, treating ionic resorcin[4]arenes solutes as pseudo 1:1 electrolytes simplify data treatment with reasonable results. Therefore, conductivity data was also analyzed using the low-concentration chemical model (lcCM) [2], which takes the form of the following set of equations:

$$\frac{\Lambda}{\alpha} = \Lambda^{\infty} - S(\alpha c)^{1/2} + E \alpha c \ln(\alpha c) + J_1 \alpha c + J_2 (\alpha c)^{3/2} \tag{5.7}$$

$$K_A^{\circ} = \frac{1-\alpha}{c \alpha^2 y_{\pm}'^2} = 4\pi N_A q \alpha c \int_a^R r^2 \exp\left(\frac{2q}{r} - \frac{W_{\pm}^*}{1 + k_B R}\right) \tag{5.8}$$

$$y_{\pm}' = \exp\left(\frac{-\kappa_D q}{1 + \kappa_D R_{ij}}\right) \tag{5.9}$$

$$\kappa_D^2 = 16\pi N_A q \alpha c, \; q = \frac{e^2}{8\pi \varepsilon \varepsilon_0 k_B T} \tag{5.10}$$

here Λ^∞ corresponds to the molar conductivity of the solute at infinite dilution, $(1-\alpha)$ is the fraction of oppositely charged ions acting as ion pairs at salt concentration c, and K_A° is the ion association equilibrium constant. The meaning of the symbols and explicit expressions for the parameters S, E, J_1 and J_2 of eq. (5.7) can be found in reference[2]. Here it may suffice to say that the limiting slope, S, and E are defined in terms of the density, viscosity and static permittivity of the solvent only, contrary to the analogous Q-V parameters that also depend on the ionic conductivities. The coefficients J_1 and J_2 are functions of the distance parameter R_{ij}. In the application of the lcCM not always a four parameter fit is required. Generally a three parameter fit is enough, where J_2 is generally treated as an adjustable quantity together with Λ^∞ and K_A° and J_1 is calculated assuming $R(J_1) = R_{ij}$. In this case, the associated distance, $R_{ij}(J_2)$, is used as a compatibility control of the fit. Nonetheless, two parameters fit (Λ^∞, K_A°) and even one parameter fit (Λ^∞) are plausible[2].

The lcCM model counts two oppositely charged ions as an ion pair if their mutual separation distance, r, is within the limits $a \leq r \leq R_{ij}$. The distance of closest approach of anion and cation, $a = a_+ + a_-$, is typically calculated from the radii of the cation, a_+, and anion, a_-. For the resorcin[4]arenes, the a_j value was calculated for the ionic residue, namely -SO_3^- for the Na_4TES and -$N(CH_3)_2H^+$ for TAM $\cdot$ $(HCl)_4$. The upper integration limit, R_{ij}, is the distance up to which oppositely charged ions can approach as independently-moving particles in the solution. Extensive investigations by Barthel et al.[2] revealed that the upper limit of association can be taken as $R_{ij} = a + ns$ where s is the length of an orientated solvent molecule and n is an integer number. In this study $s = 0.280$ nm was used for water[2] and $s = 0.640$ nm for DMSO[11].

5.4 Results

Analysis of the obtained Λ for aqueous solutions was done using Q-V model (eqs. 5.4-5.6) and lcCM equations according to the pseudo 1:1 approximation (eqs. 5.7-5.10). Within this latter approach, concentration of electrolytes c was taken as four times the analytical concentration, $c = 4c_{\text{calc}}$.

Within Table 5.2 are summarized the calculated values using Q-V model, while Table 5.3 contains lcCM results. The fit using Q-V equations was done as suggested by Apelblat[10] and lcCM according to Barthel recommendations[2]. Comparison of the obtained Λ^∞ from the two models varies $\sim 3\%$ for Na_4TES while $\sim 6\%$ for TAM $\cdot$ $(HCl)_4$. Comparison of K_A° values, show that Q-V yields larger values and possibly unrealistic association constants. On the other hand, comparison of the lcCM K_A° value for aqueous TAM $\cdot$ $(HCl)_4$ at 298.15 K (K_A°=6.4 M^{-1}) with the value obtained from DRS experiments ($K_A^\circ(S_1)$= 7.5 M^{-1}, $K_A^\circ(\tau_1)$= 6.3 M^{-1}) at 298.15 K (See Chapter 3) shows good agreement; giving consistency to the pseudo 1:1 electrolyte approach. In the case of aqueous solutions of Na_4TES (K_A°=33 M^{-1})and DMSO solutions (K_A°=52. M^{-1}) agreement with the DRS values in water (K_A°=85.$\pm$ 41.M^{-1}) and DMSO (K_A°=92. $\pm$ 30.M^{-1}) is also found; considering the large uncertainty and limitations of DRS to precisely determine association constants[12]. Additionally, Q-V equations may have another limitation in DMSO solutions since they require the ionic molar conductivities of Na^+ and Cl^- to do the fit. Unfortunately, these values are known with precision at 298.15 K only[11,1]. As a consequence, analysis using lcCM model was used for the analysis of Λ.

Table 5.2: Limiting molar conductivities, Λ^∞, association constants, K_A°, and distance parameters, a_j, calculated from the fits of Λ using Quint-Viallard model (eqs. 5.4-5.6) as function of temperature.[a]

Solute	T	a_j	Λ^∞	K_A°
$TAM \cdot (HCl)_4$	278.15	0.209	421.5	0.01
	283.15	0.211	475.9	141.7
	288.15	0.212	532.5	263.5
	293.15	0.214	589.6	417.1
	298.15	0.211	651.9	504.3
	303.15	0.212	715.3	496.3
	308.15	0.198	802.1	1.0
Na_4TES	278.15	0.276	306.9	709.0
	283.15	0.275	354.7	816.4
	288.15	0.282	406.7	757.1
	293.15	0.285	459.9	808.2
	298.15	0.287	515.8	872.6
	303.15	0.290	573.3	952.5
	308.15	0.291	633.0	1039.4

[a] Units: a_j in nm; Λ^∞ in $S \cdot cm \cdot mol^{-1}$; K_A° in M^{-1}; T in K.

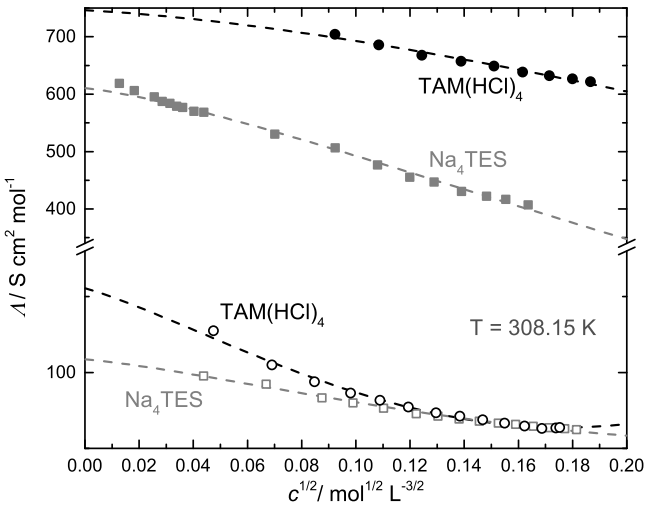

Figure 5.1: Electrical molar conductivities, Λ, of aqueous solutions (filled symbols) and solutions in DMSO (empty symbols) of Na_4TES (squares) and $TAM \cdot (HCl)_4$ (circles) at T=308.15 K

As an example, Figure 5.1 shows the results of the fits at a temperature of 308.15 K. During the fitting procedure different conditions were evaluated by changing the values of a and R_{ij} as well as the number of fitting parameters: Λ^∞, J_1, J_2 and K_A°. Consequently, it was found that the change of Λ with c was best described using two

Table 5.3: Upper distance of association, R_{ij}, distance of closest approach, a, limiting electrolyte conductivities, Λ^{∞}, and association constants, K_{A}°, of Na_4TES and $\mathrm{TAM}\cdot(\mathrm{HCl})_4$ in water and DMSO as function of temperature, T obtained from the fit using lcCM model (eqs.5.7-5.10). Parameter uncertainties are showing brackets.[a]

Solute	a	Solvent	R_{ij}	T	Λ^{∞}	K_{A}°
$\mathrm{TAM}\cdot(\mathrm{HCl})_4$	0.412	DMSO	1.692	293.15	114.(±5.)	130(±24.)
				298.15	127.(±6.)	134(±24.)
				303.15	141.(±7.)	139(±25.)
				308.15	156.(±7.)	144(±25.)
		Water	0.972	278.15	393.(±3.)	5.8(±0.5)
				283.15	447.(±3.)	5.9(±0.5)
				288.15	503.(±4.)	6.1(±0.5)
				293.15	561.(±4.)	6.2(±0.6)
				298.15	622.(±4.)	6.4(±0.5)
				303.15	682.(±5.)	6.5(±0.6)
				308.15	746.(±6.)	6.6(±0.6)
Na_4TES	0.329	DMSO	0.969	293.15	80.2(±0.9)	52.(±3.)
				298.15	89.(±1.)	52.(±3.)
				303.15	99.(±1.)	52.(±3.)
				308.15	109.(±1.)	52.(±3.)
		Water	0.609	278.15	296.7(±0.8)	33.5(±0.8)
				283.15	342.9(±0.8)	32.2(±0.6)
				288.15	393.(±1.)	32.7(±0.9)
				293.15	444.(±2.)	32.6(±0.9)
				298.15	498.(±2.)	33.(±1.)
				303.15	553.(±2.)	32.3(±0.9)
				308.15	611.(±2.)	32.(±1.)

[a] Units: a and R_{ij} in nm; Λ^{∞} in S cm mol^{-1}; K_{A}° in M^{-1}; T in K.

parameters fit adjusting the quantities $\Lambda^{\infty}$and K_{A}°. Lower limit a was assumed as the charge separation in a contact ion pair (CIP) and that of solvent-shared ion pair (SIP, $n = 1$ for Na_4TES and $n = 2$ for $\mathrm{TAM}\cdot(\mathrm{HCl})_4$) taken as R_{ij}. The assumption of CIP as the lower limit is based on the results of the previous dielectric relaxation study (See Chapter 3).

5.4.1 Association constants

As seen in table 5.3, obtained association constants, K_{A}°, and their uncertainties show no change with temperature in any of the studied systems at the experimental conditions. Moreover, the quantities at 298.15 K compares well with the results obtained from DRS(see Chapter 3), supporting the pseudo 1:1 electrolyte assumption. Additionally, K_{A}° values for the same solute are larger in DMSO, as expected from the lower static permittivity with respect to water within the studied temperature range. Interestingly, in aqueous solutions of Na_4TES seems to be more association with respect to the solutions with $\mathrm{TAM}\cdot(\mathrm{HCl})_4$, yet the opposite is found for the

DMSO solutions. This finding is correlated with the fact that DMSO is not as good solvent for Cl^- as it is for Na^+, as indicated by the rather low Gutmann acceptor number o DMSO.

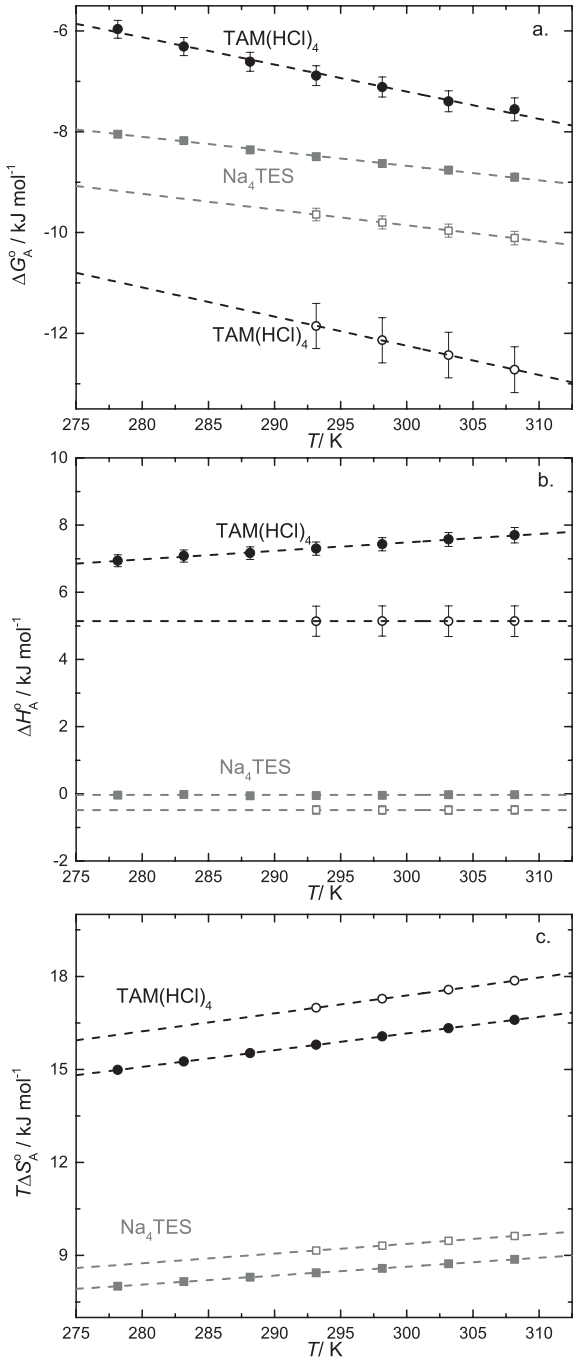

Figure 5.2: Thermodynamics of ion association (a) Gibbs free energy of association, ΔG^o_{A} (b) Enthalpy of ion association, ΔH^o_{A} and (c) Entropy of ion association, $T\Delta S^o_{\mathrm{A}}$ of aqueous solutions (filled symbols) and solutions in DMSO (empty symbols) of Na_4TES(squares) and $TAM \cdot (HCl)_4$(circles) as function of Temperature, T.

The thermodynamics of ion association can be determined with the calculation of the standard free energy of ion association, ΔG^o_{A}:

$$\Delta G^o_{\mathrm{A}} = -RT \ln K^o_{\mathrm{A}} \tag{5.11}$$

Table 5.4: Thermodynamic quantities for the ion association process of the ionic *C*-methylresorcin[4]arene in Water and DMSO at 298.15 K.[a]

Solute	Solvent	ΔG^o_A	ΔH^o_A	ΔS^o_A
Na_4TES	Water	-8.63	-0.04	28.8
Na_4TES	DMSO	-9.80	-0.48	31.3
$TAM \cdot (HCl)_4$	Water	-7.11	7.43	48.8
$TAM \cdot (HCl)_4$	DMSO	-12.14	5.14	58.0

[a] Units: ΔG^o_A and ΔH^o_A in kJ·mol^{-1}; ΔS^o_A in J·(mol K)$^{-1}$

In the same way, the change in enthalpy, ΔH^o_A, and entropy, ΔS^o_A, of the association process can be calculated as:

$$\Delta S^o_A = -(d\Delta G^o_A/dT) \tag{5.12a}$$

$$\Delta H^o_A = \Delta G^o_A + T\Delta S^o_A \tag{5.12b}$$

Since K_a has no change with temperature, the trends in Figure 5.2 of ΔG^o_A and $T\Delta S^o_A$ is solely caused due to the Temperature change, indicating that thermodynamic quantities are also temperature independent. Values at 298.15 are presented in Table 5.4, showing that in all cases association is entropy driven.

Figure 5.2 shows the calculated thermodynamic quantities as function of temperature. It is interesting to notice that ion association in solutions containing Na_4TES show a very similar thermodynamic profile, which seems to be mostly entropically driven (Table 5.4, Fig.5.2c). On the contrary, solvent nature seems to be more dramatic for $TAM \cdot (HCl)_4$ since stronger association is found in DMSO (Table 5.3), due to the poor solvation of Cl^-, and larger change of entropy (Table 5.4, Fig.5.2c) which goes along with a lower enthalpy change when compared with aqueous solutions (Table 5.4, Fig.5.2b).

5.4.2 Limiting Electrolyte conductivities

Figure 5.3 shows the obtained Λ^∞ as a function of temperature in water(Fig. 5.3a) and DMSO(Fig. 5.3b). It can be seen that in both systems the Λ^∞ seems to increase linearly, with $TAM \cdot (HCl)_4$ being always larger than Na_4TES.

The dependence of Λ^∞ with temperature permits to calculate the Eyring activation enthalpy of charge transport, $\Delta H^\ddagger$, which is describe as follows[11,13]

$$\ln(\Lambda^\infty) + \frac{2}{3}\ln(\rho_0) = -\frac{\Delta H^\ddagger}{RT} + B \tag{5.13}$$

where ρ_0 represents the solvent density and B is a non-dimensional constant. Obtained values are compiled in Table 5.5 and plots of the fits showed in Figure 5.4. From the calculated slope, it can be seen that for aqueous solutions $\Delta H^\ddagger$ values are close to the activation enthalpy of viscous flow for pure water (16 kJ mol^{-1} [14]) while DMSO solutions solutions have a larger $\Delta H^\ddagger$ than the pure solvent (11.8 kJ mol^{-1} [11]).

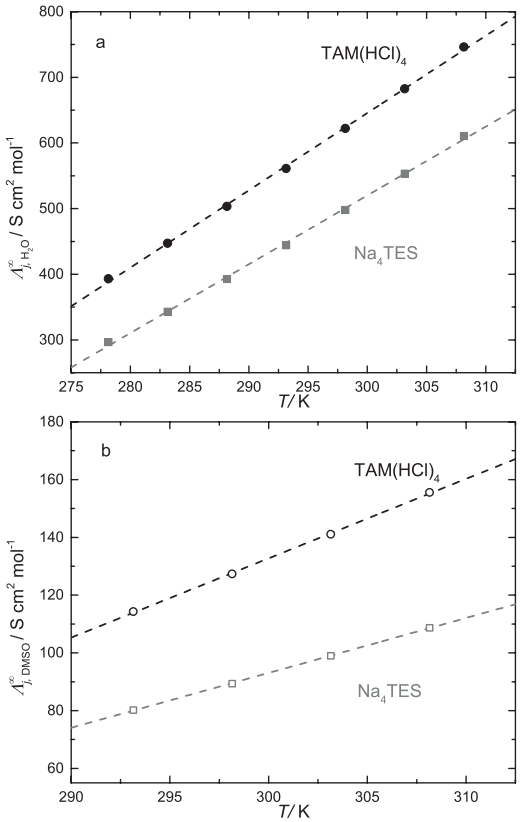

Figure 5.3: Limiting molar conductivities, Λ^{∞}, for the solutions of Na_4TES (squares) and $TAM \cdot (HCl)_4$ (circles) in water (filled symbols) and DMSO (empty symbols) as function of temperature, T. Lines represents linear fits.

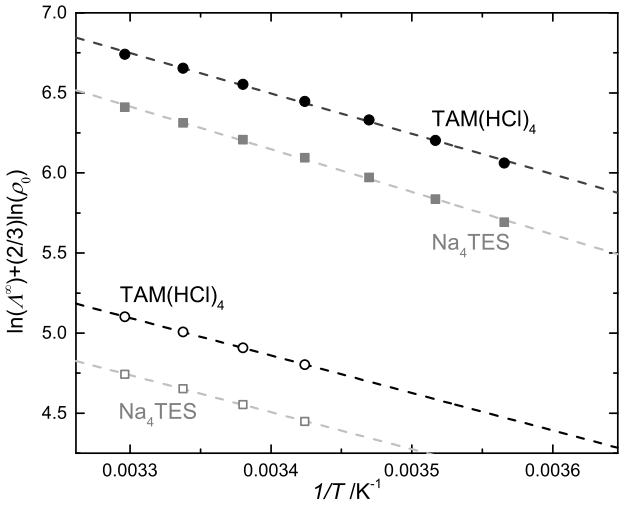

Figure 5.4: Eyring plot for the limiting ionic conductivities(see eq.5.13), Λ^{∞}, of aqueous solutions (filled symbols) and solutions in DMSO (empty symbols) of Na_4TES (squares) and $TAM \cdot (HCl)_4$ (circles) as function of the reciprocal of the Temperature. From the slope $\Delta H^{\ddagger}$ is calculated (see text).

Table 5.5: Calculated fit parameters from equation (5.13) with their uncertainties calculated from the limiting conductivities of Na_4TES and $TAM \cdot (HCl)_4$ in water and DMSO.[a]

Solute	Solvent	$-\frac{\Delta H^\ddagger}{R}$	B	$\Delta H^\ddagger$
	DMSO			11.8 [11]
	Water			16. [14]
Na_4TES	DMSO	-1778.(±23.)	10.52(±0.07)	14.8(±0.2)
	Water	-2049.(±38.)	13.1(±0.1)	17.0(±0.3)
$TAM \cdot (HCl)_4$	DMSO	-1801.(±11.)	10.95(±0.04)	15.0(±0.1)
	Water	-1940.(±42.)	13.1(±0.1)	16.1(±0.3)

[a] Units: $\frac{\Delta H^\ddagger}{R}$ in K; $\Delta H^\ddagger$ in kJ mol^{-1}; B is non-dimensional.

5.4.3 Limiting Ion Conductivities

According to Kohlrausch law of independent ion migration, ionic molar conductivities of the resorcin[4]arenes, λ^∞(R[4]A), can be calculated as:

$$\Lambda^\infty = \lambda^\infty(\text{R[4]A}) + 4\lambda^\infty(\text{X}) \tag{5.14}$$

where λ^∞(X) is the counter ion ionic conductivity. In the case of aqueous solutions, the values of $\lambda^\infty(Na^+)$ and $\lambda^\infty(Cl^-)$ were taken from Ref. [13]. In the case of solutions in DMSO, experimental values of $\lambda^\infty(Na^+)$ and $\lambda^\infty(Cl^-)$ only at 298.15 K are known [1,11]. Nonetheless, reference [15] provides values of $\lambda^\infty(Na^+)$ in DMSO at different temperatures that allow interpolation. In the same way, reference [16] give tentative values of $\lambda^\infty(Cl^-)$, however these data has not been verified independently, indicating that any interpretation should be taken with care. Calculated values are presented in Table 5.6.

Table 5.6: Limiting ionic conductivities, Λ^{∞}, for the ionic C-methylresorci[4]arenes, R[4]A, and their counter ions, X, as function of temperature, T, in water and DMSO.

Solute	Solvent	T	λ^{∞}(X)	λ^{∞}(R[4]A)
TAM · $(HCl)_4$	DMSO	293.15	22.7[b]	23.7
		298.15	24.1[b]	30.9
		303.15	25.6[b]	38.5
		308.15	27.3[b]	46.5
	Water	278.15	47.4[c]	203.3
		283.15	54.2[c]	230.3
		288.15	61.3[c]	258.0
		293.15	68.7[c]	286.3
		298.15	76.3[c]	316.9
		303.15	84.1[c]	345.8
		308.15	92.2[c]	377.5
Na_4TES	DMSO	293.15	12.5[d]	30.0
		298.15	14.2[d]	32.6
		303.15	15.9[d]	35.5
		308.15	17.5[d]	38.6
	Water	278.15	30.3[c]	175.5
		283.15	34.9[c]	203.3
		288.15	39.8[c]	233.7
		293.15	44.9[c]	264.6
		298.15	50.2[c]	297.0
		303.15	55.8[c]	330.1
		308.15	61.6[c]	364.2

[a] Units: λ^{∞} in S cm^2 mol^{-1};T in K.[b] Interpolated using data in Ref.[16]. [c] Taken from Ref.[13].[d] Interpolated using data in Ref.[15].

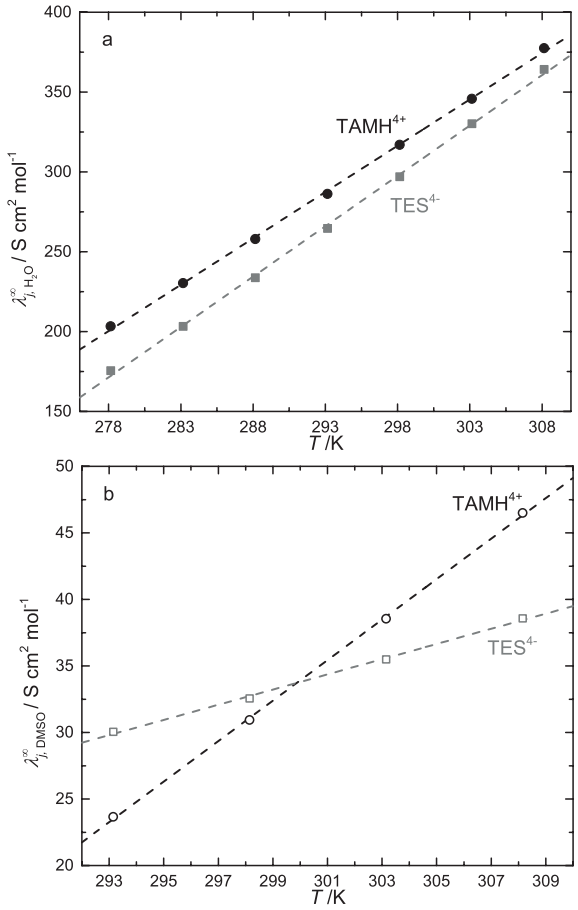

Figure 5.5: Ionic molar conductivities of aqueous solutions (filled symbols) and solutions in DMSO (empty symbols) of Na_4TES (squares) and $TAM \cdot (HCl)_4$ (circles) as function of Temperature, T. Dashed lines represents linear fits.

Figure 5.5 shows the calculated ionic molar conductivities of TES^{4-} and $TAM \cdot H^{4+}$ ions. In the case of aqueous solutions (Fig.5.5a), the $TAM \cdot H^{4+}$ shows a larger λ_j^{∞} than TES^{4-}, indicating that $TAM \cdot H^{4+}$ has a larger mobility. However, and contrary to what it is suggested in Figure 5.3a, increasing the temperature tends to reduce the difference. In DMSO solutions at temperatures below $\sim$ 300 K TES^{4-} has a larger mobility; however, at higher temperatures $TAM \cdot H^{4+}$ has a larger mobility.

From the values of the ionic molar conductivity the hydrodynamic Stokes radius, r_{St}, is calculated:

$$r_{\mathrm{St}} = \frac{|z|F^2}{6\pi N_A \eta_o \lambda_j^{\infty}} \tag{5.15}$$

where F is the Faraday constant. Table 5.7 shows the calculated r_{St} as function of temperature for both resorcin[4]arenes in water and DMSO. Considering that the geometric radii (see Chapter 4), r_{vdW}, of TES^{4-} and $TAM \cdot H^{4+}$ are 0.549 nm and 0.562 nm, respectively, it is worthy to point out that in aqueous solutions the r_{St} is lower than r_{vdW} while for solutions in DMSO the values are closer. Moreover, the temperature seems to affect in a larger extend the r_{St} of $TAM \cdot H^{4+}$ in DMSO than the other systems where the change seems to be negligible.

Table 5.7: Stokes radii, r_{St}, calculated using eq. (5.15) ionic resorcin[4]arenes for the solutions of $TAM \cdot H^{4+}$ (r_{vdW} =0.562 nm) and TES^{4-} (r_{vdW} =0.549 nm) in Water and DMSO as function of temperature, T.[a]

T	$TAM \cdot H^{4+}$		TES^{4-}	
	DMSO	Water	DMSO	Water
278.15		0.106		0.123
283.15		0.109		0.123
288.15		0.112		0.123
293.15	0.627	0.114	0.494	0.124
298.15	0.532	0.116	0.505	0.124
303.15	0.470	0.119	0.511	0.125
308.15	0.427	0.121	0.515	0.125

[a] Units: T in K; r_{St} in nm.

5.5 Discussion

Analysis of the conductivity data of the two ionic resorcin[4]arenes using the Quint-Viallard and low chemical concentration model provided evidence of ion association. In the case of the model based on the Quint-Viallard amended with a chemical equilibrium of ion association in most cases $K_{\mathrm{A}}^{\circ} > 141$ M^{-1} were obtained. According to Bjerrum's theory of ion association [2], mostly the dielectric medium and ionic charge determine ion association. Particularly, it is expected that in solvents with a static permittivity lower than $\varepsilon = 40$ all electrolytes solutions form at least ion pairs [2]. Thus, in solvents with high static permittivity like water, association constants will

depend mainly on the charge of the ions, having larger association constants symmetrical high charged ions. As an example, in water $Mg(SO_4)$, a 2:2 electrolyte, has a $K_A^\circ = 163\ M^{-1}$ whereas a 3:3 electrolyte like $LaFe(CN_6)$ has an association constant of about 5500 M^{-1} [17]. Then it could be expected that the reason why large association constants values obtained from the Q-V model arise from the assumption that resorcin[4]arenes are represented by a sphere with a large charge ($|z| = 4$). Nonetheless, considering structural aspects, this assumption seems to be limited since the total charge in the resorcin[4]arene is split and localized as single charges ($|z| = 1$) in well separated ionic moieties on the upper rim of the resorcin[4]arene structure. Additionally, the resolved distance of closest approach, a_j, for the Q-V model (Table 5.2) in all cases is smaller than the distance parameter suggested by Kielland in water for the counter-ion, which is 0.450 nm for Na^+ and 0.300 nm for Cl^- [18]. With this in mind, seems reasonable to consider the resorcin[4]arenes salts as pseudo 1:1 electrolyte. Analysis of the electrolytic molar conductivity using the lcCM yield lower K_A° and similar values of Λ^∞ when comparing with the Q-V results. Additionally, the agreement with the DRS calculated association constants lends consistency to this approach.

From the results using the lcCM equations, it was determined that ion association in aqueous solutions of $TAM \cdot (HCl)_4$ is lower than Na_4TES solutions. Comparison with the tetraehtylammonium chloride at 298.15 K, which has a K_A°=2.5 M^{-1} [19] indicate that the obtained value of 6.4 M^{-1} seems reasonable considering the resemblance of the ionic moiety in $TAM \cdot H^{4+}$ and the tetraethylammonium ion. On the other hand, aqueous solutions of Na_4TES exhibit a considerably large K_A° values. Typically, aqueous solutions of Alkali metal salts are considered to be the prototype of complete dissociation [2]; thus, the values of $\sim$30 M^{-1} can be considered surprisingly high. A plausible explanation might be in terms of counter ion condensation as proposed by Manning [20], which state that if the distance between two neighboring groups is larger than the Bjerrum distance ($q =\sim 7$Å for water at 298.15, see eq. 5.10) ion condensation will take place [20]. In this case, an ion triple formation of the form -SO_3^-...Na^+...-SO_3^- might be the most likely configuration, showed in Figure 5.6. In that case, the distance between the two neighboring -SO_3^- groups involved in the ion pairing is about 4 Å (determined using Avogadro [21]) which is lower than the Bjerrum distance.

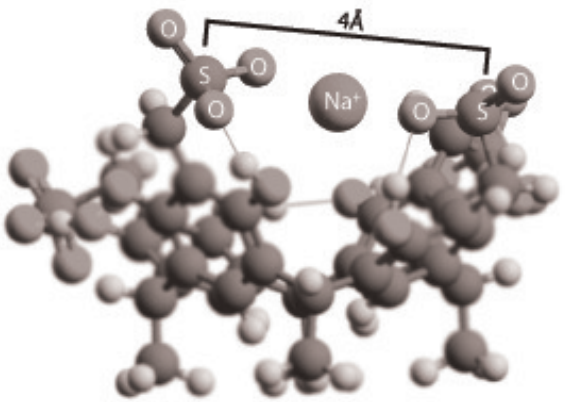

Figure 5.6: Representation of the possible ion triple formed between sodium ion, Na^+, and two sulphonate groups, -SO_3^-, in the upper rim of TES^{4-}.

Association constants in DMSO are larger than in aqueous solutions as expected from the lower static permittivity. Surprisingly, the resolved K_A° for the DMSO solutions of $TAM \cdot (HCl)_4$ are larger in two orders of magnitude than in aqueous solutions. This drastic change can be attributed to solvation effects[22]. For example, the low Gutmann acceptor number suggest that DMSO poorly solvates Cl^-, promoting association. Unfortunately association data from DRS is not available due to the low solubility of $TAM \cdot (HCl)_4$ in DMSO. Nonetheless, the low solubility can be correlated with the large degree of ion association, which seems to be disrupted when water is added since the K_A° value in solutions of $TAM \cdot (HCl)_4$ in the DMSO-Water(10.9 % w) mixture is about 3 M^{-1} (see Chapter 3). This change may suggest that the counter ion solvation plays an important role, since solute-solvent interactions of Cl^- are larger in water than in DMSO.

Analysis of the thermodynamic associations quantities, showed that ion association in all the studied systems is entropy driven considering that ΔH_A^o is positive or very close to zero (see Table 5.4). Positive ΔS_A^o has been correlated with solvent release during the ion association process and changes in the degrees of freedom of the ions[22]. According to this, could be that the association of the resorcin[4]arenes with their counter ions is favored from the change in translational and rotational degrees of freedom along with a loss in the electrostatic entropy and the desolvation entropy[22].

Analysis of limiting conductivities as function of temperature, in the framework of Eyring theory, yielded for aqueous solutions the change in activation enthalpy, $\Delta H^\ddagger$, very similar values to the activation enthalpy of viscous flow and for DMSO larger values(see Table 5.5). This indicates that charge transport in these solutions requires ion desolvation and rearrangement of solvent molecules in the vicinity of the ion to some extent[11]. In order to estimate the ionic contribution, limiting ionic conductivities were calculated. Using Λ^∞ values obtained from lcCM approach the resorcin[4]arenes ionic conductivity was calculated according to equation (5.14). Comparison of the ionic conductivity of TES^{4-} in DMSO with the ionic conductivity of methylsulfonate ($CH_3SO_3^-$) ion in DMSO at 298.15 K it can be seen that

$\lambda^{\infty}(TES^{4-})$=90 S cm^2 mol^{-1} < $4\lambda^{\infty}(CH_3SO_3^-)$=141.5 S cm^2 mol^{-1}, reflecting the decrease in mobility due the attachment to the large resorcin[4]arene structure.

Stokes radii reflect the effect of solvation[1]. The calculated radii are summarizes in Table 5.7 indicate that in solution TES^{4-} and $TAM \cdot H^{4+}$ seems to have a smaller size, especially in water. This observation can be correlated with the fact that resorcin[4]arenes ions moves without a tight solvation shell. Interestingly, the determined r_{St} seems to have a weak dependence with temperature, except for the $TAM \cdot H^{4+}$ in DMSO. Close inspection of the data for limiting ionic conductivity of Cl^- in DMSO with temperature[16] includes data for temperatures below the freezing point of the solvent. As a result, the trend with temperature of $\lambda(Cl^-)$ might be systematically affected, biasing further quantities derived from their values.

5.6 Conclusions

Electrical molar conductivities of resorcin[4]arenes Na_4TES and $TAM \cdot (HCl)_4$ in water and DMSO were determined as a function of concentration and temperature. Analysis of the measured values showed a better consistency treating the resorcin[4]arene ions as pseudo 1:1 electrolyte instead of a 4:1 electrolyte, yielding values for ion association constants in good agreement with previous DRS studies(see chapter 3). Ion association resulted to be stronger in DMSO solutions than in aqueous medium as expected from the dielectric constants. In aqueous solutions of Na_4TES association values are considerably large and very close to the association constants in DMSO. On the contrary, association in $TAM \cdot (HCl)_4$ solutions showed a large difference in both media, suggesting solvation effects.

Analysis of the limiting conductivities, Λ^{∞}, with temperature indicated that charge transport is promoted with increasing temperature, an the process is governed by the properties of the medium. Analysis of the ionic limiting molar conductivities, λ^{∞}, indicate that in water TES^{4-} and $TAM \cdot H^{4+}$ have a very close mobility, being larger for $TAM \cdot H^{4+}$ within the studied temperature range. In DMSO differences are larger, but they rapidly become similar at $\sim$ 300 K. Below this temperature TES^{4-} has a larger mobility and above $TAM \cdot H^{4+}$ is larger. Calculation of stokes radii indicate that in aqueous solutions, TES^{4-} and $TAM \cdot H^{4+}$ have a smaller size than the expected from the van der Waals radius, suggesting that ions move with a loose solvation shell. Interestingly, $TAM \cdot H^{4+}$ showed smaller Stokes radii than TES^{4-}, despite having a larger van der Waals radius. This results is in agreement with the previous solvation studies that suggest that TES^{4-} ion is more solvate than $TAM \cdot H^{4+}$ (see Chapters 3 and 4). Temperature dependence of the Stokes radii is similar for all the systems except for $TAM \cdot H^{4+}$ in DMSO. However, $TAM \cdot H^{4+}$ limiting conductivity values and further derived quantities need to be taken with care since they are based on values of $\lambda^{\infty}(Cl^-)$ in DMSO with arguably quality.

Bibliography

[1] Marcus, Y. *Ions in Solution and their Solvation*; John Wiley & Sons, 2015.

[2] Barthel, J.; Krienke, H.; Kunz, W. *Physical chemistry of electrolyte solutions: modern aspects*; Springer Science & Business Media, 1998; Vol. 5.

[3] Robinson, R. A.; Stokes, R. H. *Electrolyte solutions*; Courier Corporation, 2002.

[4] Amirov, R.; Nugaeva, Z.; Mustafina, A.; Fedorenko, S.; Morozov, V.; Kazakova, E. K.; Habicher, W.; Konovalov, A. *Colloids and Surfaces A: Physicochemical and Engineering Aspects* **2004**, *240*, 35–43.

[5] Barthel, J.; Wachter, R.; Gores, H.-J. *Modern Aspects of Electrochemistry*; Springer US: Boston, MA, 1979; pp 1–79.

[6] Shreiner, R. H.; Pratt, K. W. *NIST Special Publication* **2004**, *260*, 142.

[7] Hoover, T. B. *J. Phys. Chem.* **1970**, *74*, 2667–2673.

[8] Quint, J.; Viallard, A. *Journal of Solution Chemistry* **1978**, *7*, 533–548.

[9] Apelblat, A.; Neuder, R.; Barthel, J. *Chemistry data series. 12, Electrolyte data collection: 4c. Electrolyte conductivities, ionic conductivities and dissociation constants of aqueous solutions of organic dibasic and tribasic acids: tables, diagrams, correlations, and literature survey*; Dechema, 2006.

[10] Apelblat, A. *Journal of solution chemistry* **2011**, *40*, 1234.

[11] Bešter-Rogač, M.; Hunger, J.; Stoppa, A.; Buchner, R. *Journal of Chemical & Engineering Data* **2009**, *55*, 1799–1803.

[12] Eiberweiser, A.; Buchner, R. *J. Mol. Liq.* **2012**, *176*, 52–59.

[13] Bešter-Rogač, M.; Neueder, R.; Barthel, J. *Journal of solution chemistry* **1999**, *28*, 1071–1086.

[14] Buchner, R.; Hölzl, C.; Stauber, J.; Barthel, J. *Phys. Chem. Chem. Phys.* **2002**, *4*, 2169–2179.

[15] Yao, N.-P.; Bennion, D. *Journal of The Electrochemical Society* **1971**, *118*, 1097–1106.

[16] Ergin, S. P. *Ionics* **2014**, *20*, 1463–1470.

[17] Dunsmore, H. S.; James, J. *Journal of the Chemical Society (Resumed)* **1951**, 2925–2930.

[18] Kielland, J. *Journal of the American Chemical Society* **1937**, *59*, 1675–1678.

[19] Tissier, M.; Douhéret, G. *Journal of Solution Chemistry* **1978**, *7*, 87–98.

[20] Manning, G. S. *The journal of chemical Physics* **1969**, *51*, 924–933.

[21] Hanwell, M. D.; Curtis, D. E.; Lonie, D. C.; Vandermeersch, T.; Zurek, E.; Hutchison, G. R. *Journal of cheminformatics* **2012**, *4*, 17.

[22] Marcus, Y.; Hefter, G. *Chemical reviews* **2006**, *106*, 4585–4621.

Chapter 6

Solvation and Ionic Association of Resorcin[4]arenes in polar media

6.1 Introduction

To achieve association in polar media, supramolecular receptors makes use of electrostatic interactions. Some examples include encapsulation using ionic Calixarenes[1,2], anion recognition with Bis(Cyclopeptides)[3], and ionic Resorcin[4]arenes[4,5]. However, assuring the shape and binding sites is not enough to achieved association. In this scenarios solvation plays an important role. This is illustrated by the determination of the association between Pyrene and a macrobicyclic receptor in different solvents[6], were the association constant value (affinity) is correlated with increasing medium polarity. Thus, to design a receptor it is important to considered the medium where the binding process will take place[7].

Study of noncovalent complexes requires to consider the solvation of the host, guest, and host-guest complex[8]. Despite of this, traditionally the design of supramolecular architectures has been mainly done considering only the structural features of the receptor and guest molecules. This lead to the development of structures limited to organic non-polar media, where the used intermolecular interactions are easily to manipulate and solvation is not difficult to overcome. On the contrary, in polar media and specially in water, implementation of supramolecular chemistry solutions has found more difficulties.

Currently solvation effects in supramolecular chemistry are known but are still limited to relationships with polarity of the medium[9,10]. Further attempts to understand other phenomenons like preferential solvation has been done but with limitations[3]. A good strategy to study the relation of solvation and supramolecular affinity is by measuring association constants in different media. For this purpose isothermal titration calorimetry (ITC) results in a convenient tool[11,10]. This technique measures the amount of heat liberated after addition of aliquots of the guest to the host (or vice versa)[11,10], resulting in binding isotherms which provide the association constants, K_{ass}, stoichiometry, and enthalpy change of the process, ΔH^o. Alternatively, dilutions experiments using ITC also serve to study other phenomena as association in solution[12]. The complete energetic profile comprising Gibbs Free energy, ΔG^o, and entropy change, ΔS^o, of the process is accessible from the data of a single experiment by means of thermodynamic relationships. Unfortunately,

due to the nature of the observables measured in a ITC experiment, information at the molecular level is not directly accessible. For this reason, complementary spectroscopic techniques are useful.

Considering the previous results of the study of $TAM \cdot (HCl)_4$ in DMSO-water mixture (see Chapter 3) and previously reported results[4], in this chapter studies of the formation of the capsule resembling associate[4] $[TES^{4-} \cdot (TAM \cdot H^{4+})]$ in DMSO-water mixtures using ITC at 298.15 K are presented. Additionally, studies in the presence of Cadmium and Choline ions were also included. The results were assessed considering the findings presented in previous chapters, giving a possible explanation of why encapsulation of a guest using ionic resorcin[4]arenes has not been yet possible.

6.2 Experimental

6.2.1 Sample Preparation

Ionic c-methylresorcin[4]arenes Na_4TES and $TAM \cdot (HCl)_4$ were synthesize and purified as reported in Chapter 2. Purity of the samples was assessed using quantitative ^{1}H-NMR (qNMR)[13] using Maleic Acid (0.99,Sigma-Aldrich) as internal reference. Obtained purities were better than 99% (Table 6.1). High purity water (Type 1, Millipore MilliQ, US) was degassed prior its use with a conductivity $< 2\mu S\ cm^{-1}$. The used DMSO was from Alfa Aesar (US, > 0.99 by mass fraction) and used without further purification. Pure DMSO was stored with 3 Å molecular sieve. Solvent mixtures were prepared by mass combining the appropriate amount of water and DMSO to reach a final mass of 200 g. For the experiments in the presence of Cadmium and Choline ions, Cadmium Perchlorate hexahydrate (CAS 10326-28-0, 0.99, Alfa-Aesar) and Choline Chloride (CAS 67-48-1, 0.99, Sigma-Aldrich) were used without further purification.

Table 6.1: Chemicals specification

Solute	Source	Purification Method	Mass Fraction Purity	Method
$TAM \cdot (HCl)_4$	Synthesis	Recrystallization	>0.99	qNMR
Na_4TES	Synthesis	Recrystallization	>0.99	qNMR
$Cd(ClO_4)_2{\cdot}6H_2O$	Alfa-Aesar		>0.99	
Choline Chloride	Sigma-Aldrich		>0.99	
DMSO	Alfa Aesar, US		>0.99	
Water	Milli-Q, Millipore			

6.2.2 Isothermal Titration Calorimetry

Experiments were carried out using a Low Volume (170 μL) NanoITC (TA Instruments, USA) using a 50 μL chemical resistance syringe. Prior the study, instrument calibration was checked by acid-base titration of hydrochloric acid (HCl) and potassium bicarbonate ($KHCO_3$) and cleanliness was check with Water-Water titration.

Dilution Experiments

Samples for dilutions experiments were prepared by mass using an Ohaus analytical balance with a sensibility of $1{\cdot}10^{-5}$ g in the range of interest. Dilutions were carried out by additions of 2.5 μL of a resorcin[4]arene solution ($\sim$ 11.5 mM) into an initial solvent mixture sample of 300 μL in the cell. Constant stirring rate of 250 RPM was applied and injections were done every 300 s. The reference cell was fill with 350 μL of solvent mixture. Solutions densities were determine using an Anton Paar DSA 5000 M and used to calculate samples molar concentrations.

Interaction experiments

Injections of 2.5 μL of $\sim$ 11.5 mM solution of Na_4TES into a solution $\sim$ 2.5 mM of $TAM \cdot (HCl)_4$ with an initial volume of 300 μL were carried out. Constant stirring rate of 250 RPM was applied and injections were done every 300 s. Experiments including Cadmium ion were carried out by preparing a solution of $TAM \cdot (HCl)_4$ ($\sim$ 2 mM) and Cadmium perchlorate ($\sim$ 7 mM) or Cadmium perchlorate alone ($\sim$ 7 mM, corrected for hydration water molecules). A similar procedure was done using Choline Chloride ($\sim$ 8 mM).

Data Analysis

Obtained isotherms were analyzed via the evaluation of different equilibrium models, which where implemented using the online data analysis tool AFFINImeter (`www.affinimeter.com`). During the fits, the association constant, K_A, and enthalpy change, ΔH^o, were used as fitting parameters. Considering the quality of the data and nature of the system correction for dilution heats and baseline shift were applied during the fit.

6.3 Results

6.3.1 Dilution experiments

Dilution experiments of $TAM \cdot (HCl)_4$ and Na_4TES in six different mass fractions of DMSO-Water mixtures $0.5 \leq w_{\mathrm{DMSO}} \leq 1$, were recorded at 298.15 K. Figure D.1(Appendix D) shows the different patterns of the recorded heat rate as function of time. In case of Na_4TES dilutions(Fig.D.1a) is important to point out that all samples containing water are exothermic. On the contrary, $TAM \cdot (HCl)_4$ dilutions (Fig.D.1b) all samples showed a similar pattern, where the first injections are endothermic and then a switch to exothermic is observed. After signal integration, Na_4TES heats suggest that simple dilution is taken place (Figure 6.1a) while for $TAM \cdot (HCl)_4$ data (Figure 6.1b) a better description was obtained considering the dimer dissociation model[14]:

$$\mathrm{TAMH}^{4+} + \mathrm{TAMH}^{4+} \overset{K_{\mathrm{dim,TAM}}}{\rightleftharpoons} (\mathrm{TAMH}^{4+})_2 \tag{6.1}$$

The dimer dissociation constants, $K_{\mathrm{dim,TAM}}$, along with their thermodynamic quantities ($\Delta G^{\circ}_{\mathrm{dim,TAM}}, \Delta H^{\circ}_{\mathrm{dim,TAM}}$ and $\Delta S^{\circ}_{\mathrm{dim,TAM}}$) are presented in Table 6.2 as function of DMSO mass fraction. There it can be seen that resolved association

constants are within the lower limit for the ITC technique[10] and thus it can be consider as weak association. Determined $\Delta H^{\circ}_{\mathrm{dim,TAM}}$ have negative values with rather high uncertainty. Neither $K_{\mathrm{dim,TAM}}$ nor $\Delta H^{\circ}_{\mathrm{dim,TAM}}$ present a systematic trend with solvent composition. Derived thermodynamic quantities, showed in Table 6.2, were obtained from by using the Gibbs-Helmholtz relation:

$$\Delta G^{o}_{\mathrm{i}} = -RT \ln K^{o}_{\mathrm{i}} \tag{6.2a}$$

$$\Delta G^{o}_{\mathrm{i}} = \Delta H^{o}_{\mathrm{i}} - T\Delta S^{o}_{\mathrm{i}} \tag{6.2b}$$

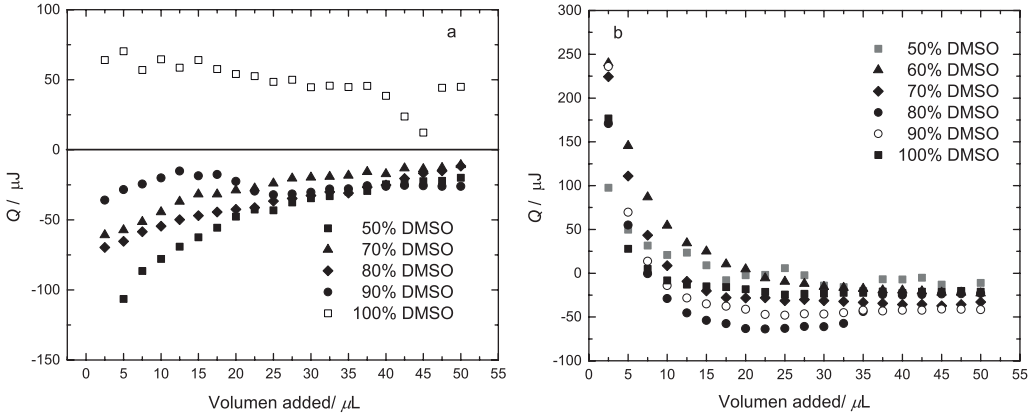

Figure 6.1: Enthalpograms for the dilution titration of $\sim$ 11.5 mM (a) Na_4TES and (b) $TAM \cdot (HCl)_4$ solutions in different mixtures of DMSO-Water at 298.15 K.

Table 6.2: Association constant, $K_{\mathrm{dim,TAM}}$, and Standard Enthalpy Change, $\Delta H^{\circ}_{\mathrm{dim,TAM}}$, for dimer dissociation model of $TAM \cdot (HCl)_4$ in DMSO-Water mixtures at 298.15 K. Derived thermodynamic quantities calculated using eq. (6.2) as function of DMSO mass content, w_{DMSO}.[a]

w_{DMSO}	$\log K_{\mathrm{dim,TAM}}$	$\Delta H^{\circ}_{\mathrm{dim,TAM}}$	$\Delta G^{\circ}_{\mathrm{dim,TAM}}$	$T\Delta S^{\circ}_{\mathrm{dim,TAM}}$
0.50	3.0(±0.1)	-141.(±3.)	-7.5	134.2
0.60	3.2(±0.6)	-327.(±19.)	-7.9	319.5
0.70	3.38(±0.04)	-132.(±16.)	-8.4	123.6
0.80	3.45(±0.04)	-469.(±107.)	-8.6	460.2
0.90	3.5(±0.3)	-194.(±31.)	-8.8	185.6
1.00	3.6(±0.2)	-201.(±18.)	-9.0	192.8

[a] Units: $\Delta H^{\circ}_{\mathrm{dim,TAM}}$, $\Delta G^{\circ}_{\mathrm{dim,TAM}}$ and $T\Delta S^{\circ}_{\mathrm{dim,TAM}}$ in kJ$\cdot$ mol^{-1}

6.3.2 Resorcin[4]arene interactions

Considering the dilution experiments results, additions of a solution of ca. 11.5 mM of Na_4TES to a solution of ca. 2.0 mM of $TAM \cdot (HCl)_4$ in the same solvent mixture were done to study the interactions between $TAM \cdot H^{4+}$ and TES^{4-}. Figure D.2 shows that for samples with a mass composition of DMSO below 80% showed exothermic heats, while for 80% onwards the process is endothermic. Integration

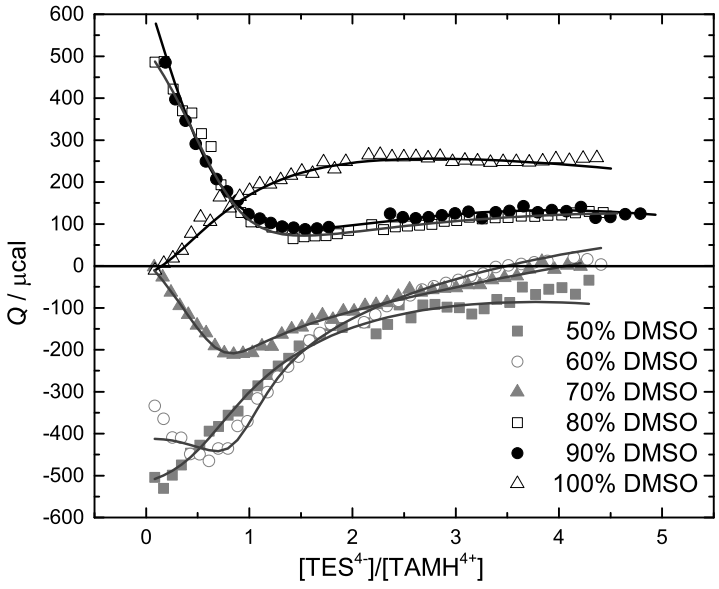

Figure 6.2: Enthalpograms as function of molar ratio for the titration of $\sim$ 11.5 mM Na_4TES and $\sim$ 2.0 mM $TAM \cdot (HCl)_4$ solutions in different mixtures of DMSO-Water at 298.15 K. Lines represent fits with the selected models (See text).

of signal peaks gave injections heats with correlation to the mole ratio between $TAM \cdot H^{4+}$ and TES^{4-}. This is shown in Figure 6.2, where the analysis of the obtained heats is presented. Different models using the "model-builder" from the software AFFINImeter where tried. The selected model considered formation of the expected ionic aggregate $[TES^{4-} \cdot (TAM \cdot H^{4+})]$, as previously suggested[4], among with the dimer formation of each ionic resorcin[4]arene:

$$TAMH^{4+} + TES^{4-} \overset{K_{IA}}{\rightleftharpoons} TAMH \cdot TES \tag{6.3}$$

$$TAMH^{4+} + TAMH^{4+} \overset{K_{dim,TAM}}{\rightleftharpoons} (TAMH^{4+})_2 \tag{6.4}$$

$$TES^{4-} + TES^{4-} \overset{K_{dim,TES}}{\rightleftharpoons} (TES^{4-})_2 \tag{6.5}$$

Formation of the $TAM \cdot H^{4+}$ dimer, $(TAM \cdot H^{4+})_2$, is expected from the results of the dilution experiments. The same experiments did not show formation of the TES^{4-} dimer; however, its inclusion improved the fit as visually seen in Figure D.3. This difference with dilution experiments might arise from the fact that titration of Na_4TES into $TAM \cdot (HCl)_4$ consisted in twice the amount of injections, reaching larger concentrations. Additionally, this model is consistent with other studies of the formation of heterodimers[15].

The model according to eq. (6.3)-(6.5) can be clearly illustrated by the resolved species diagram (Figure 6.3), where it can be seen that the dimer $(TAM \cdot H^{4+})_2$ is dissociated upon addition of TES^{4-}, leading to the formation of $[TES^{4-} \cdot (TAM \cdot H^{4+})]$. Continuous addition of the TES^{4-} confirms the stoichiometry of the ionic aggregate

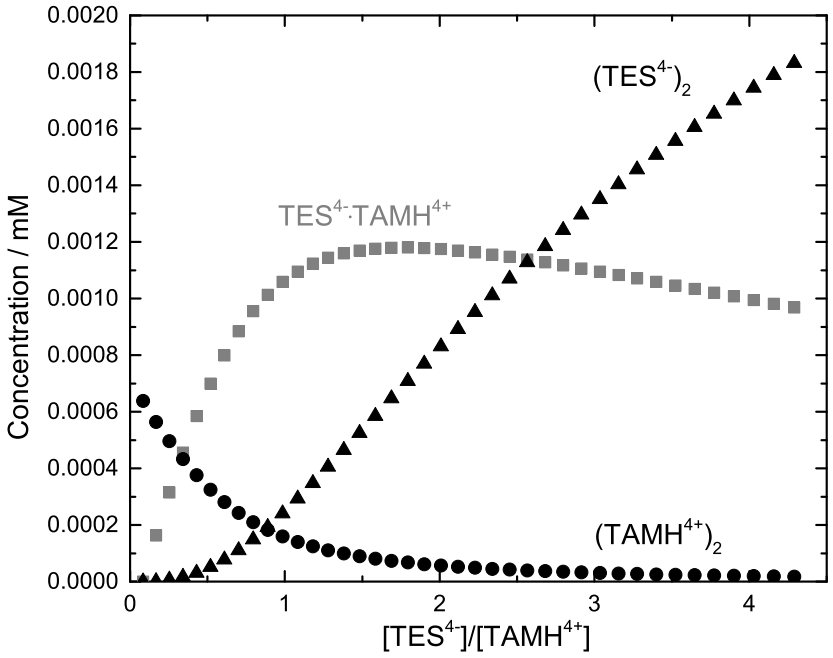

Figure 6.3: Species diagram for the titration of Na_4TES into $TAM \cdot (HCl)_4$ in DMSO 50% by mass solvent mixture with water.

since the maximum concentration of $[TES^{4-} \cdot (TAM \cdot H^{4+})]$ is reached when the molar ratio between ionic resorcin[4]arenes is 1:1. Afterwards, addition of TES^{4-} only promote the formation of $(TES^{4-})_2$.

Table 6.3 shows the resolved association constants and enthalpy changes, ΔH°, for the equilibria described in eq. (6.3)-(6.5) as a function of solvent composition. Best fit was achieve by fixing $K_{\mathrm{dim,TAM}}$ to the values obtained in the dilutions experiments (see Table 6.2). Unfortunately, resolved $\Delta H^\circ_{\mathrm{dim,TAM}}$ values only agree in the resolved sign (see tables 6.2 and 6.3). Consequently, determined association constants for the ionic aggregate $[TES^{4-} \cdot (TAM \cdot H^{4+})]$, K_{IA}, were obtained with a precision between 2% and 8%, while association constants for the TES^{4-} dimer formation, $K_{\mathrm{dim}}(TES^{4-})$ are between 3% and 27%. In the case of the enthalpy change, uncertainty is between 2% and 32%, being larger for the dimer formation equilibria, specially the $(TES^{4-})_2$.

Figure 6.4 shows the derived thermodynamic properties using equation (6.2). It can be said that only for the formation of $[TES^{4-} \cdot (TAM \cdot H^{4+})]$ simple trends with changing solvent composition were determined for the three derived thermodynamic quantities. The other two equilibria showed large uncertainties within the studied experimental conditions. However, it is important to mention that complex behavior of Thermodynamic quantities as function of medium composition has been reported previously [3].

Table 6.3: Resolved association constants, K_i, and Enthalpy Change, $\Delta H_{\mathrm{i}}^{\circ}$, with their uncertainties in brackets, and the calculated Gibbs free energy, $\Delta G_{\mathrm{i}}^{\circ}$, and enthalpy change, $T\Delta S_{\mathrm{i}}^{\circ}$ using equation (6.2) at $T = 298.15$ K for the formation of associates [$\mathrm{TES}^{4-}\cdot(\mathrm{TAM}\cdot\mathrm{H}^{4+})$] with ($K_{\mathrm{IA}}$, $\Delta H_{\mathrm{IA}}^{\circ}$), $(\mathrm{TES}^{4-})_2$ ($K_{\mathrm{dim,TES}}$, $\Delta H_{\mathrm{dim,TES}}^{\circ}$), and $(\mathrm{TAM}\cdot\mathrm{H}^{4+})_2$ ($K_{\mathrm{dim,TAM}}$ [a], $\Delta H_{\mathrm{dim,TAM}}^{\circ}$) as function of mass fraction of DMSO, w_{DMSO}, in DMSO-Water mixtures.[b]

Equilibrium	w_{DMSO}	$K_i(10^4)$	ΔH_i°	ΔG_i°	$T\Delta S_i^{\circ}$
Eq. (6.3)	0.50	11.1(±0.1)	-0.5(±0.1)	-12.5	12.0
	0.60	10.4(±0.8)	-4.1(±0.7)	-12.4	8.3
	0.70	9.1(±0.2)	-3.9(±0.1)	-12.3	8.4
	0.80	7.7(±8.6)	-6.8(±1.5)	-12.1	5.4
	0.90	6.9(±0.6)	-8.7(±2.8)	-12.0	3.3
	1.00	3.6(±1.3)	-11.5(±2.5)	-11.3	-0.2
Eq. (6.5)	0.50	38.7(±2.3)	8.6(±0.6)	-13.9	22.5
	0.60	3.1(±0.1)	1.8(±0.1)	-11.1	13.0
	0.70	15.3(±1.7)	-3.1(±0.3)	-12.9	9.8
	0.80	5.8(±1.6)	2.8(±0.5)	-11.8	14.7
	0.90	10.9(±2.2)	9.8(±1.5)	-12.5	22.3
	1.00	3.0(±0.1)	4.4(±0.7)	-11.1	15.4
Eq. (6.4)	0.50	0.11[a]	-9.9(±0.8)	-7.5	-2.3
	0.60	0.16[a]	-11.4(±0.2)	-7.9	-3.5
	0.70	0.24[a]	-11.2(±0.4)	-8.4	-2.8
	0.80	0.28[a]	-23.8(±1.8)	-8.6	-15.2
	0.90	0.34[a]	-38.0(±2.6)	-8.8	-29.3
	1.00	0.42[a]	-26.8(±0.9)	-9.0	-17.8

[a]Association constants for (6.4) were taken from Table 6.2(See text). [b]Units: ΔH_i°, ΔG_i° and $T\Delta S_i^{\circ}$ in kJ$\cdot$ mol^{-1}

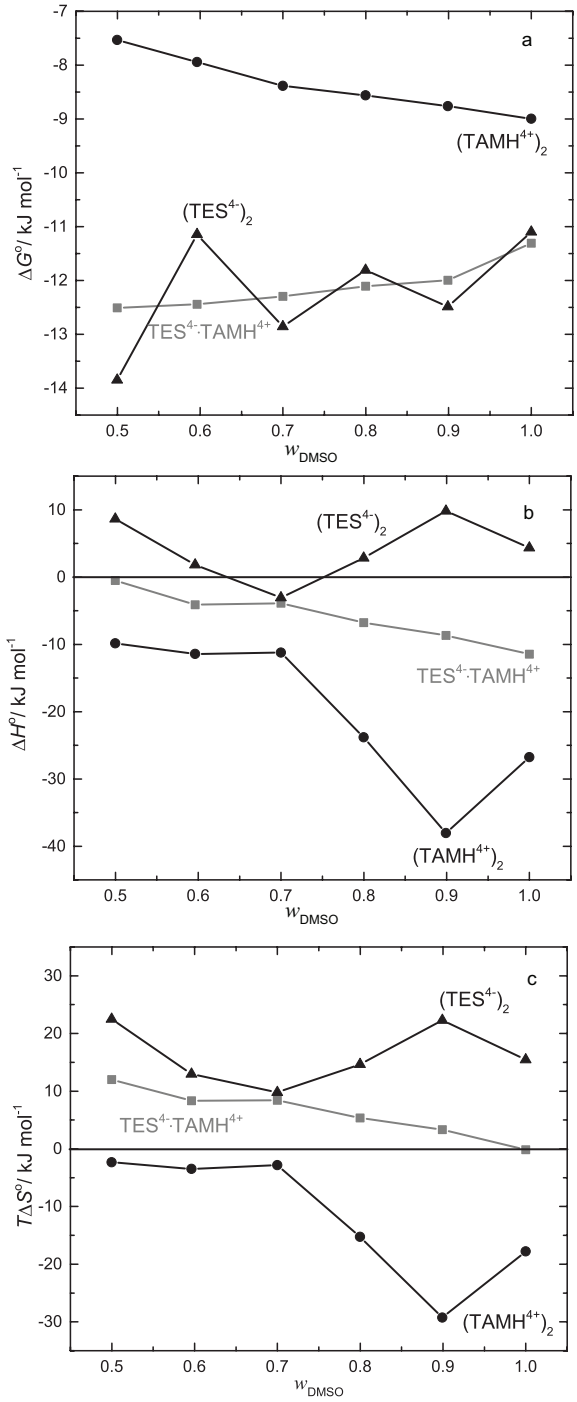

Figure 6.4: Thermodynamic profile for the titration of Na_4TES into $TAM \cdot (HCl)_4$ at 298.15 K as function of DMSO mass fraction, w_{DMSO}. Panel (a) show the Gibbs free energy, panel (b) the resolved enthalpy change and panel (c) the change in entropy as $T\Delta S^o$ for the different process considered in equilibria (6.3-6.5.)

6.3.3 Interactions with Cadmium and Choline ions

To evaluate the possible inclusion of a guest within the [TES^{4-}·($TAM \cdot H^{4+}$)] capsule, studies using Cadmium Perchlorate and Choline Chloride were carried out at constant solvent composition of 50% DMSO by weight. Figure 6.5 shows the experiments in presence of Cadmium ion. It can be seen that the presence of Cd^{2+} drastically change the isotherm behavior. When Cd^{2+} ion is present, the measured heats are endothermic and tend to decrease upon addition of TES^{4-}. Analysis of the isotherms using AFFINImeter software, showed that the main interaction is between TES^{4-} and Cd^{2+} according to:

$$TAMH^{4+} + TES^{4-} \overset{K_{IA,Cd}}{\rightleftharpoons} TAMH \cdot TES \tag{6.6}$$

which is accompanied with the stepwise formation of [TES·Cd_2]:

$$TES^{4-} + Cd^{2+} \overset{K_{TES,1Cd}}{\rightleftharpoons} Cd \cdot TES + Cd^{2+} \overset{K_{TES,2Cd}}{\rightleftharpoons} Cd_2 \cdot TES \tag{6.7}$$

In the case of the titration of Cadmium ion with Na_4TES (Fig. 6.5, TES^{4-} + Cd^{2+}) a simple model indicating the concerted formation of the complex Cd_2TES where enough to describe the data:

$$TES^{4-} + 2\,Cd^{2+} \overset{K_{Cd2,TES}}{\rightleftharpoons} Cd_2TES \tag{6.8}$$

Table 6.4 shows the obtained association constant along with the corresponding resolved enthalpy changes and derived thermodynamic profile using equation (6.2). Figures D.4 and D.5 shows the adjust isotherms with the models describe above.

Table 6.4: Resolved association constants, $\log K_i$, enthalpy change, ΔH_i^o, with their uncertainties in brackets, and derived Gibbs Free Energy, ΔG_i^o, and change in Entropy, $T\Delta S_i^o$, for the equilibrium process in the ITC titration including Cadmium ion at DMSO mass fraction of $w_{DMSO} = 0.5$.[a]

Equilibrium	$\log K_i$	ΔH_i^o	ΔG_i^o	$T\Delta S_i^o$
Eq. (6.6)	6.44(±0.03)	220.(±42.)	-16.0	-235.5
Eq. (6.7, TES,1Cd)	6.57(±0.03)	-181.(±16.)	-16.3	164.7
Eq. (6.7, TES,2Cd)	1.7(±0.2)	78.(±23.)	-4.2	-82.3
Eq. (6.8)	4.64(±0.08)	143.(±8.)	-11.5	-154.4

[a] Units: ΔH_i°, ΔG_i° and $T\Delta S_i^\circ$ in kJ· mol^{-1}

Figure 6.6, shows a titration in the presence of Choline Chloride. It is interesting to see that a similar isotherm is obtained for the system TES^{4-} + Choline and TES^{4-} + $TAM \cdot H^{4+}$ + Choline. Unfortunately, from the obtained isotherms it was not possible to perform a quantitative analysis. However, comparison with Na_4TES dilution and titration of TES^{4-} with $TAM \cdot H^{4+}$ seems to indicate that no interaction between resorcin[4]arene when choline is present. Previously it was reported[16] that TES^{4-} weakly interacts with Choline ion in aqueous solutions, thus indicating that this interaction prevent the formation of the [TES^{4-}·($TAM \cdot H^{4+}$)] associate.

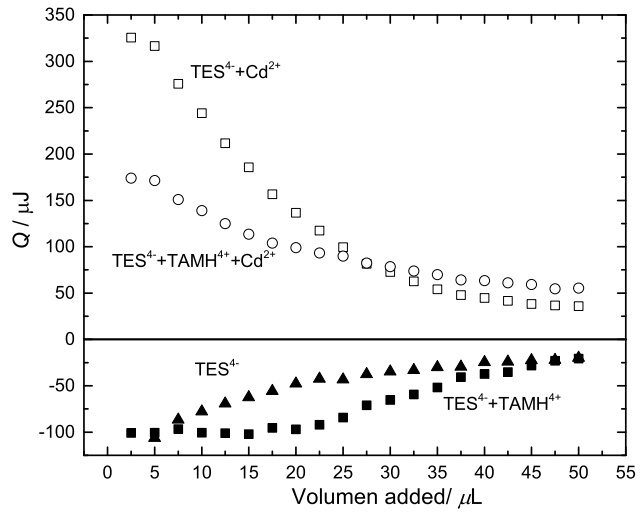

Figure 6.5: Enthalpograms for the dilution of Na_4TES (TES^{4-}), titration of Na_4TES into $TAM \cdot (HCl)_4$ (TES^{4-} + $TAMH^{4+}$), Na_4TES into Cadmium Perchlorate (TES^{4-} + Cd^{2+}), and Na_4TES into $TAM \cdot (HCl)_4$ in the presence of Cadmium perchlorate (TES^{4-} + $TAMH^{4+}$ + Cd^{2+}) in DMSO-Water mixture with DMSO mass fraction $w_{DMSO} = 0.5$ at 298.15 K.

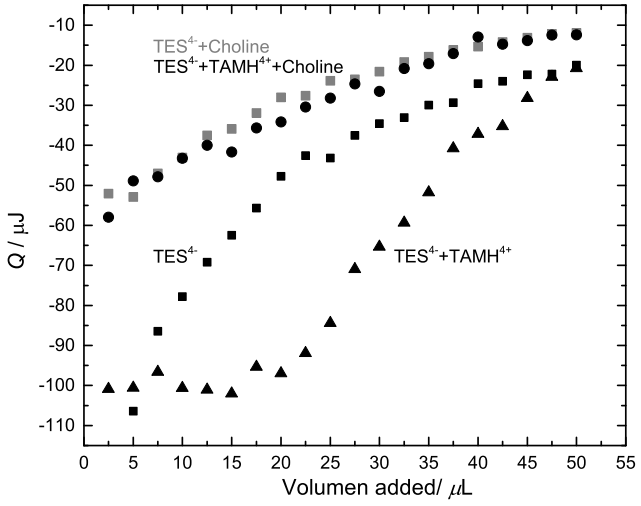

Figure 6.6: Enthalpograms for the dilution of Na_4TES (TES^{4-}), titration of Na_4TES into $TAM \cdot (HCl)_4$ (TES^{4-} + $TAMH^{4+}$), Na_4TES into Choline Chloride (TES^{4-} + Choline), and Na_4TES into $TAM \cdot (HCl)_4$ in the presence of Choline Chloride (TES^{4-} + $TAMH^{4+}$ + Choline) in DMSO-Water mixture with DMSO mass fraction $w_{DMSO} = 0.5$ at 298.15 K.

6.4 Discussion

It was previously reported[4] that formation of [TES^{4-}·($TAM \cdot H^{4+}$)], which is insoluble in aqueous solutions, can be carried out by combining aqueous solutions of Na_4TES and $TAM \cdot (HCl)_4$. It was also mentioned that combination of DMSO solutions of the ionic resorcin[4]arenes did not form the ionic aggregate, most likely due to ion pair formation[4]. Contrary to this finding, as seen in Figure 6.4a, the ionic aggregate is formed in DMSO solution with an association constant $K_a = 3.6 \times 10^4$. It was further found that the formation of the [TES^{4-}·($TAM \cdot H^{4+}$)] associate also takes place in DMSO-Water mixtures with DMSO mass fraction $0.5 \leq w_{DMSO}$. When $w_{DMSO} \leq 0.5$, the associate is insoluble. Among the studied media, in neat DMSO the formation process of associate [TES^{4-}·($TAM \cdot H^{4+}$)] has the lowest association constant (Table 6.3). Comparison with the previously determined counter ion association constants in pure DMSO ($K_{IP}(Na_4TES)$=52 and $K_{IP}(TAM \cdot (HCl)_4)$=134, see chapters 3 and 5) with $K_{IA} = 3.7 \times 10^5$ suggest that ion pairing may not be a cause that prevents the [TES^{4-}·($TAM \cdot H^{4+}$)] formation.

Measured association constants, K_{IA}, showed in table 6.3, indicate that association strength decreases with decreasing water content in the solvent mixture. Interestingly, although the water content decrement goes along with a reduction of the static permittivity, ε, of the mixture[17], the association constant, K_{IA}, decreases despite the interaction between TES^{4-} and $TAM \cdot H^{4+}$ ions is electrostatic. This is observed from the reported 2D NOESY experiments which suggest a "head-to-head" formation[4]. According to ion association theory[18], it should be expected an increment of K_{IA} with the reciprocal of ε. Since this is not the case for [TES^{4-}·($TAM \cdot H^{4+}$)], it could be state that association is not solely determined by the capacity of the medium to screen charges, but also by solvation phenomena.

The previous solvation studies presented in Chapter 3 and 4 indicate that TES^{4-} and $TAM \cdot H^{4+}$ solvation is predominantly via solvophobic mechanism in DMSO while in water solvophilicity plays and important role. However, solvation in solvent mixtures might be additionally affected by preferential solvation. In this context, understanding of the solvent structure might bring clarity on how the solvation process is taking place. Studies of DMSO-Water mixtures using vibrational spectroscopy[19] suggest that the solvent structure is composition dependent since a hydrogen bonding network, including DMSO and Water molecules, increases it extend upon water addition, being more evident for solvent compositions with molar fraction of DMSO $x_{DMSO} < 0.5$. Considering that the present study covers mixtures with w_{DMSO} between 0.5 and 1 ($0.2 < x_{DMSO}/\text{mol mol}^{-1} < 1$), the extend of the hydrogen bond decreases as the number of DMSO molecules is increased. On the other hand, it has been mentioned before that hydrogen bonded solvents promote solvophobic effects[20] allowing to state that the main driving force behind the formation of [TES^{4-}·($TAM \cdot H^{4+}$)] might be a solvophobic effect, since the changing hydrogen bonding network in the medium, upon decrease of DMSO content, promote association. This may also explain why there is a larger association constant with increasing polarity in the present work and previous observations[6,8].

Figures 6.4b and c shows that formation of the ionic associate is entropically favored upon increment of DMSO content. Addition of DMSO cause an increment in

enthalpy change while for the entropy change a reduction is observed. Interestingly, at a mass fraction of $w_{\mathrm{DMSO}} = 0.5$ the process is practically entropy driven while in pure DMSO the process is closely dominated by the change in enthalpy. From the previous calculated solvation numbers (see chapter 3 and 4), it can be said that the studied resorcin[4]arenes in this work are preferably surrounded by water than DMSO. Thus it can be considered that the increment of $T\Delta S$ with w_{water} is correlated with an increment of the entropy of desolvation, a hallmark of the solvophobic effect[9,11].

Despite the studies with cadmium and choline did not yield a clear evidence of formation of an inclusion complex within $[TES^{4-}\cdot(TAM\cdot H^{4+})]$, valuable information is still obtained. In both cases, competition between $[TES^{4-}\cdot(TAM\cdot H^{4+})]$ formation and TES^{4-}-Guest association was observed, suggesting that the competition scenario is taking place. A previous study attempting the encapsulation with different possible ionic guests using the $[TES^{4-}\cdot(TAM\cdot H^{4+})]$ associate yielded no evidence of encapsulation[4]. To achieve encapsulation, such study tried forming first a TES^{4-}-Guest complex with a subsequent addition of the $TAM\cdot H^{4+}$ to close the capsule. As a result, a release of the guest molecule with a concomitant precipitation of $[TES^{4-}\cdot(TAM\cdot H^{4+})]$ was observed[4], supporting the idea that competence between the formation of different process is responsible for the no formation of the complex between $[TES^{4-}\cdot(TAM\cdot H^{4+})]$ and a guest molecule.

One reason that might explain why competence is preventing the encapsulation of a guest species is the opposing driving forces guiding the formation of associates. It has been mentioned before that complexation of ionic species and hydrophobic guests often show opposite polarity dependencies[9]. An example that may illustrate this is the interactions between TES^{4-}, $TAM\cdot H^{4+}$ and Cadmium ion. In this case, formation of the TES^{4-}-Cd^{2+} associate, is favored by polarity conditions that reduce the formation of the $[TES^{4-}\cdot(TAM\cdot H^{4+})]$ associate since the first process is promoted by electrostatic attraction while the second by a solvophobic effect. In the case of interactions with Choline ion, additional steric factors might be also involved. This can also be extended to the already reported observations in reference[4], where the formation the TES^{4-}-guest and addition of $TAM\cdot H^{4+}$ in aqueous solutions most likely promoted the formation of $[TES^{4-}\cdot(TAM\cdot H^{4+})]$ due to the large hydrophobic effect induced by the medium.

6.5 Conclusions

Experiments using isothermal titration calorimetry, ITC, helped to elucidate the main processes governing the interactions between TES^{4-} and $TAM\cdot H^{4+}$ in mixtures of DMSO-Water at 298.15 K. Although previous studies indicate that ion-pairing is present, when combined the two structures in solution all possible dimers (homodimers and heterodimer) are formed with a larger association constants than ion pairing. Within the studied experimental conditions, data was good enough to quantify the interaction between TES^{4-} and $TAM\cdot H^{4+}$ in solution. In the case of side process as resorcin[4]arene dimer dissociation data has a larger uncertainty.

Dependence of the association constant with solvent composition indicate that formation of the heterodimer $[TES^{4-}\cdot(TAM\cdot H^{4+})]$ is promoted by solvophobic

effect. Studies including ionic third species showed that encapsulation using the $[TES^{4-} \cdot (TAM \cdot H^{4+})]$ associate has not been achieved mostly due to the differences in solvation and nature of the interaction mediating the ensemble.

Bibliography

[1] Corbellini, F.; Fiammengo, R.; Timmerman, P.; Crego-Calama, M.; Versluis, K.; Heck, A. J.; Luyten, I.; Reinhoudt, D. N. *Journal of the American Chemical Society* **2002**, *124*, 6569–6575.

[2] Corbellini, F.; Di Costanzo, L.; Crego-Calama, M.; Geremia, S.; Reinhoudt, D. N. *Journal of the American Chemical Society* **2003**, *125*, 9946–9947.

[3] Sommer, F.; Marcus, Y.; Kubik, S. *ACS Omega* **2017**, *2*, 3669–3680.

[4] Morozova, Y. E.; Shalaeva, Y. V.; Makarova, N. A.; Syakaev, V. V.; Kazakova, E. K.; Konovalov, A. I. *Russ. Chem. Bull.* **2009**, *58*, 95–100.

[5] Gaynanova, G. A.; Bekmukhametova, A. M.; Kashapov, R. R.; Ziganshina, A. Y.; Zakharova, L. Y. *Chemical Physics Letters* **2016**, *652*, 190–194.

[6] Smithrud, D. B.; Diederich, F. *Journal of the American Chemical Society* **1990**, *112*, 339–343.

[7] Mizutani, T.; Wada, K.; Kitagawa, S. *The Journal of organic chemistry* **2000**, *65*, 6097–6106.

[8] Wittenberg, J. B.; Isaacs, L. *Supramolecular Chemistry: From Molecules to Nanomaterials* **2012**,

[9] Rekharsky, M.; Inoue, Y. *Supramolecular Chemistry: From Molecules to Nanomaterials* **2012**,

[10] Schmidtchen, F. P. *Analytical Methods in Supramolecular Chemistry* **2007**, 55–78.

[11] Gibb, C. L.; Gibb, B. C. *Supramolecular Chemistry: From Molecules to Nanomaterials* **2012**,

[12] Loh, W.; Brinatti, C.; Tam, K. C. *Biochimica et Biophysica Acta (BBA)-General Subjects* **2016**, *1860*, 999–1016.

[13] Bharti, S. K.; Roy, R. *TrAC Trends in Analytical Chemistry* **2012**, *35*, 5–26.

[14] McPhail, D.; Cooper, A. *Journal of the Chemical Society, Faraday Transactions* **1997**, *93*, 2283–2289.

[15] Geer, M. F.; Shimizu, L. S. *Supramolecular Chemistry: From Molecules to Nanomaterials* **2012**,

[16] Syakaev, V.; Shalaeva, Y. V.; Kazakova, E. K.; Morozova, Y. E.; Makarova, N.; Konovalov, A. *Colloid Journal* **2012**, *74*, 346–355.

[17] Plowas, I.; Swiergiel, J.; Jadzyn, J. *Journal of Chemical & Engineering Data* **2013**, *58*, 1741–1746.

[18] Barthel, J.; Krienke, H.; Kunz, W. *Physical chemistry of electrolyte solutions: modern aspects*; Springer Science & Business Media, 1998; Vol. 5.

[19] Wong, D. B.; Sokolowsky, K. P.; El-Barghouthi, M. I.; Fenn, E. E.; Giammanco, C. H.; Sturlaugson, A. L.; Fayer, M. D. *The Journal of Physical Chemistry B* **2012**, *116*, 5479–5490.

[20] Rodnikova, M. *Journal of Molecular Liquids* **2007**, *136*, 211–213.

Chapter 7

Summary and Conclusion

Two ionic *C*-methylresorcin[4]arenes with opposite charges in the upper rim where studied in aqueous and DMSO solutions. Positively charged *C*-methylresorcin[4]arene, $TAM \cdot (HCl)_4$, has dialkylaminomethylated hydrochloride residues ($-CH_2(CH_3)_2NH{\cdot}Cl$) while negatively charged *C*-methyresorcin[4]arene, Na_4TES, has sodium ethylsulphonate groups ($-CH_2SO_3Na$). The studies presented in this work where carried out to understand the relation between solvation and capsule formation between the two mentioned *C*-methylresorcin[4]arenes in polar media. For this purpose, different experimental techniques were used showing that Na_4TES and $TAM \cdot (HCl)_4$ in solution have differences in solvation and counter-ion association.

First, studies using Dielectric Relaxation Spectroscopy (see Chapter 3) showed that each *C*-methylresorcin[4]arene affects in different manners the dynamics of water molecules. Aqueous solutions of $TAM \cdot (HCl)_4$ have both moderate retardation and complete immobilization of water molecules, while for solutions of Na_4TES only the latter was observed. This pattern suggest that Na_4TES solvation is driven by hydrophilicity while for $TAM \cdot H^{4+}$ hydrophobicity is also present. A similar analysis showed that in DMSO solutions also both mechanisms are present but in a lesser extent. Further information on solvation and the effect of temperature was assessed by analysis of the standard molar volumes and isentropic compressibilities (see Chapter 4). The changes presented by these quantities and properties derived thereof suggest that in water the solute-solvent interactions are sensitive to the change of temperature and to the solute structural features. On the contrary, in DMSO no significant effect of temperature or solute structure was observed, suggesting that in DMSO, although present, solute-solvent interactions are not the main driving force behind solvation but possibly solvent-solvent interactions which change in accordance to surround solute molecules. Complementary information was provided from the analysis of limiting ionic conductivities (see Chapter 5) which showed that *C*-methylresorcin[4]arenes moves with a loose solvation shell, and such mobility is larger in water than in DMSO.

Secondly, from the analysis of DRS data evidence of counter-ion association with rather larger values for the binding constant was detected. In the case of Na_4TES solutions the medium did not show large influence on the ion association strength, while for $TAM \cdot (HCl)_4$ solutions the solvent nature played a significant contribution. Measurements of the electrical molar conductivity as a function of temperature, allowed to further study the strength of counter-ion association. The

determined constants showed that the association process is temperature independent, and corroborated the medium influence observed in DRS data. Analysis of the thermodynamic properties of ion association showed that the process is driven by the change in entropy.

The interaction between the two ionic *C*-methylresorcin[4]arenes in mixtures of water and DMSO at 298.15 K was studied using isothermal titration calorimetry (see Chapter 6). Solvent mixtures were selected considering that the $[TES^{4-} \cdot (TAM \cdot H^{4+})]$ 'capsule' solubility is appreciable only in mixtures with a DMSO mass fraction larger than 0.5. This indicate that preferential solvation might play a role. Analysis of binding isotherms suggested that the capsule formation is not prevented by counterion association since the measured association constants for the capsule formation are larger. Additionally, it was observed that the association constant increased with increasing polarity of the solvent mixture, despite association being mediated mediated by ionic interactions. This result indicate that solvophobic effect is the main driving force behind the association. Additionally, association strength seems to be tunable by changing the solvent composition, which in turn changes the extend of the hydrogen bonding network which promote the association. Lastly, attempts to encapsulate guest molecules where unsuccessful, most likely due to the differences in solvation between the counterparts of the capsule and the guest.

Finally it can be said that the capsule formation between the two ionic *C*-methylresorcin[4]arenes is promoted mainly by the solvent and complemented by the ionic interactions. Thus, in order to encapsulate guest molecules in polar media using ionic resorcin[4]arenes, the process should consider features that take advantage of the solvophobic effect.

Appendices

Appendix A

Supporting Information: Solvation and Counter-Ion Binding of Ionic Resorcin[4]arenes

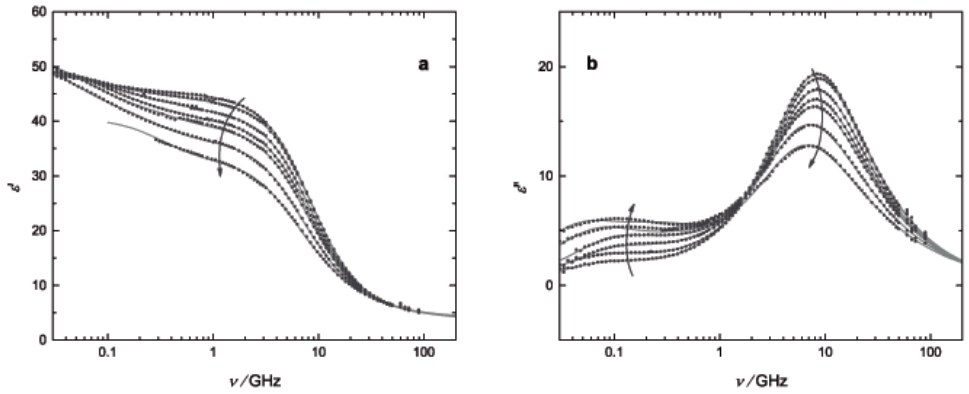

Figure A.1: Recorded (a) Static permittivity, $\varepsilon'(\nu)$, and (b) dielectric loss, $\varepsilon''(\nu)$, spectra of Na_4TES in DMSO. Arrows indicated increasing concentration

Table A.1: Parameters of the 2D+CD model for the dielectric spectra of Na_4TES DMSO solutions of concentration, c, at 298.15 K: static permittivity, ε; amplitudes, S_j and relaxation times, τ_j, of the resolved modes, $j = 1 \ldots 3$; and high-frequency permittivity, ε_∞. Also included are data for density, ρ, and conductivity, κ.[a]

c	ρ	κ^b	ε	S_1	τ_1	S_2	τ_2	S_3	τ_3	β_3	ε_∞
0.0000[c]	1.095470	0.073	46.50					42.36	20.7	0.885	4.14
0.0142	1.100868	0.073	48.85	3.30	2080	0.88	320	40.75	20.8	0.87883	3.92
0.0247	1.104824	0.102	49.73	4.53	2100	1.52	353	39.67	20.3	0.8841	4.01
0.0519	1.115009	0.151	49.29	5.26	1650	2.38	321	37.65	21.1	0.86507	4.00
0.0757	1.123791	0.177	49.71	6.94	1640	2.75	346	36.14	22.1	0.84205	3.88
0.0958	1.131346	0.183	51.34	8.53	2420	3.90	420	35.36	23.5	0.80912	3.54
0.1416	1.152584	0.165	51.62	9.08	3440	6.28	562	32.86	27.2	0.75144	3.40
0.1846	1.173013	0.195	40.45			7.73	500F	28.53	28.0	0.72597	3.22

[a] Units: c in M; ρ in $\mathrm{kg\,L^{-1}}$; κ in $\mathrm{S\,m^{-1}}$; τ_j in 10^{-12} s. [b] Obtained from fit.[c] Taken from Ref(?).Parameter values followed by the letter F were not adjusted in the fitting procedure.

Table A.2: Parameters of the 3D model for the dielectric spectra of aqueous Na_4TES solutions of concentration, c, at 298.15 K: static permittivity, ε; amplitudes, S_j and relaxation times, τ_j, of the resolved modes, $j = 1 \ldots 3$; and high-frequency permittivity, ε_∞. Also included are data for density, ρ, and conductivity, κ.[a]

c	ρ^b	κ	ε	S_1	τ_1	S_2	τ_2	S_3	τ_3	ε_∞
0.0000[c]	0.997047		78.37					74.85	8.32	3.52
0.0100	1.001444	0.488	81.90	4.47	556	0.57	60.0F	71.01	8.27	5.85
0.0244	1.007969	1.033	81.38	5.69	301	0.87	60.0F	68.80	8.23	6.03
0.0488	1.019547	1.844	80.56	6.93	293	1.94	60.0F	65.42	8.23	6.26
0.0722	1.031324	2.515	79.27	6.71	247	3.77	60.0F	62.44	8.07	6.36
0.0819	1.036412	2.762	78.80	7.01	250	4.32	60.0F	61.14	7.96	6.32
0.1307	1.063694	3.804	76.54	7.39	335	6.02	60.0F	56.80	8.18	6.33
0.1841	1.096924	4.624	73.39	6.89	353	8.18	60.0F	51.71	8.19	6.61
0.2263	1.125676	5.131	69.14	5.56	322	8.36	60.0F	48.07	8.29	7.16

[a] Units: c in M; ρ in $\mathrm{kg\,L^{-1}}$; κ in $\mathrm{S\,m^{-1}}$; τ_j in 10^{-12} s. [b] Interpolated. Taken from Ref(?).Parameter values followed by the letter F were not adjusted in the fitting procedure.

Table A.3: Parameters of the CC+D model for the dielectric spectra of aqueous Na_4TES solutions of concentration, c, at 298.15 K: static permittivity, ε; amplitudes, S_j and relaxation times, τ_j, of the resolved modes, $j = 1 \ldots 3$; and high-frequency permittivity, ε_∞. Also included are data for density, ρ, and conductivity, κ.[a]

c	ρ^b	κ	S_2	τ_2	S_1	τ_1	α_1	ε_∞
0.0100	1.001444	0.488	71.18	8.30	4.95	518	0.05F	5.90
0.0245	1.007969	1.033	68.72	8.23	7.57	305	0.13	6.02
0.0488	1.019547	1.844	65.23	8.24	10.70	276	0.19	6.23
0.0722	1.031324	2.515	61.63	8.06	13.25	175	0.24	6.21
0.0819	1.036412	2.762	60.36	7.95	13.81	164	0.23	6.18
0.1307	1.063694	3.804	54.07	8.18	21.42	180	0.42	5.50
0.1841	1.096924	4.624	47.30	8.21	24.59	104	0.43	5.22
0.2263	1.125676	5.131	42.85	8.30	23.79	72.6	0.42	5.59

[a] Units: c in M; ρ in $\mathrm{kg\,L^{-1}}$; κ in $\mathrm{S\,m^{-1}}$; τ_j in 10^{-12} s. [b] Interpolated. Parameter values followed by the letter F were not adjusted in the fitting procedure.

Table A.4: Parameters of the 3D model for the dielectric spectra of aqueous $TAM \cdot (HCl)_4$ solutions of concentration, c, at 298.15 K: static permittivity, ε; amplitudes, S_j and relaxation times, τ_j, of the resolved modes, $j = 1 \ldots 3$; and high-frequency permittivity, ε_∞. Also included are data for density, ρ, and conductivity, κ.[a]

c	ρ^b	κ	ε	S_1	τ_1	S_2	τ_2	S_3	τ_3	ε_∞
0.0000	0.997047		78.37					74.85	8.32	3.52
0.0101	0.99937	0.495	80.77	2.45	475	1.17	28.3	71.49	8.25F	5.66
0.0194	1.00154	0.827	80.67	3.13	404	0.81	48.7	71.10	8.35F	5.62
0.0296	1.00391	1.145	80.33	3.94	321	0.62	43.7	69.94	8.38F	5.83
0.0388	1.00608	1.437	79.74	4.39	266	1.14	23.3	68.41	8.40	5.81
0.0474	1.00810	1.649	79.14	4.92	232	1.68	20.4	66.57	8.44	5.97
0.0569	1.01035	1.922	78.68	5.25	219	2.19	20.2	65.24	8.30F	6.00
0.0681	1.01303	2.155	78.02	5.32	226	1.45	38.7	65.14	8.51F	6.11
0.0769	1.01514	2.415	77.39	5.81	203	1.93	30.0	63.37	8.54F	6.28
0.0848	1.01704	2.545	76.84	6.00	194	2.62	20.7	61.91	8.57F	6.31
0.0937	1.01919	2.754	75.98	5.95	188	3.18	20.1	60.57	8.56	6.27
0.1346	1.02918	2.686	71.80	5.61	183	3.42	27.1	56.71	8.73	6.05
0.1734	1.03883	3.084	69.46	5.70	229	4.39	33.6	53.22	8.84	6.14
0.2139	1.04905	4.614	66.39	6.92	138	6.95	14.0	45.69	9.00F	6.83

[a] Units: c in M; ρ in $\mathrm{kg\,L^{-1}}$; κ in $\mathrm{S\,m^{-1}}$; τ_j in 10^{-12} s. [b] Interpolated. Parameter values followed by the letter F were not adjusted in the fitting procedure.

Table A.5: Parameters of the 5D model for the dielectric spectra of TAM · $(HCl)_4$ in DMSO-Water(10.9% w) solutions of concentration, c, at 298.15 K: static permittivity, ε; amplitudes, S_j and relaxation times, τ_j, of the resolved modes, $j = 1 \ldots 3$; and high-frequency permittivity, ε_∞. Also included are data for density, ρ, and conductivity, κ.[a]

c	ρ	κ^b	ε	S_1	τ_1	S_2	τ_2	S_3	τ_3	S_4	τ_4	S_5	τ_5	ε_∞
0.0000	1.098638	-0.002	57.08					37.25	40.5	13.19	16.9	2.37	2.32	4.27
0.0295	1.104436	0.101	57.05	1.58	1650	0.54F	450F	30.53	47.2	17.31	20.0	2.91	2.69	4.19
0.0552	1.109257	0.144	57.08	2.58	1230	1.05	412F	26.90	52.0	19.05	22.5	3.02	3.22	4.47
0.0852	1.114789	0.178	56.19	3.07	1150	1.67	387	25.73	55.5	17.91	23.5	3.27	3.66	4.54
0.1112	1.119502	0.196	55.79	4.44	1220	2.10	194	25.83	56.6	15.50	22.8	3.29	3.85	4.62
0.1374	1.124153	0.207	55.27	4.99	1290	2.65	223	24.73	60.0	14.93	23.4	3.29	3.89	4.67
0.1727	1.130475	0.215	53.92	5.18	1250	3.53	230	24.14	63.5	13.09	23.4	3.24	4.02	4.74

[a] Units: c in M; ρ in $\mathrm{kg\,L^{-1}}$; κ in $\mathrm{S\,m^{-1}}$; τ_j in 10^{-12} s. [b] Obtained from fit. Parameter values followed by the letter F were not adjusted in the fitting procedure.

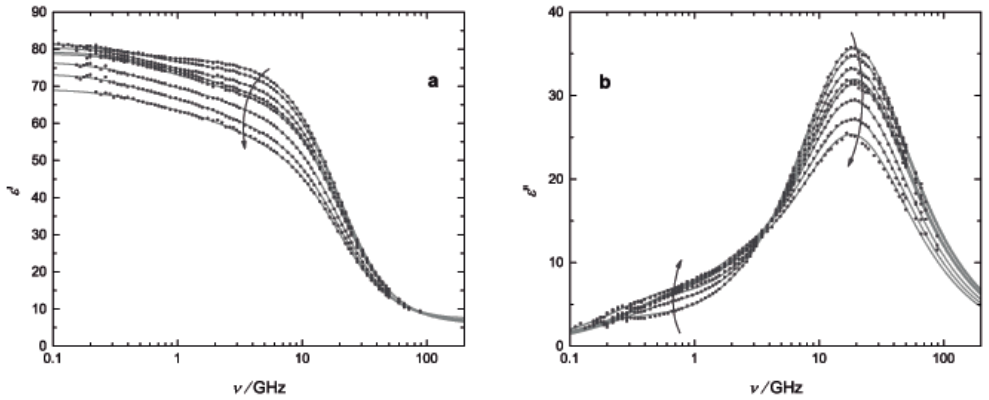

Figure A.2: Recorded (a) Static permittivity, $\varepsilon'(\nu)$, and (b) dielectric loss, $\varepsilon''(\nu)$, spectra of Na_4TES in water. Arrows indicated increasing concentration

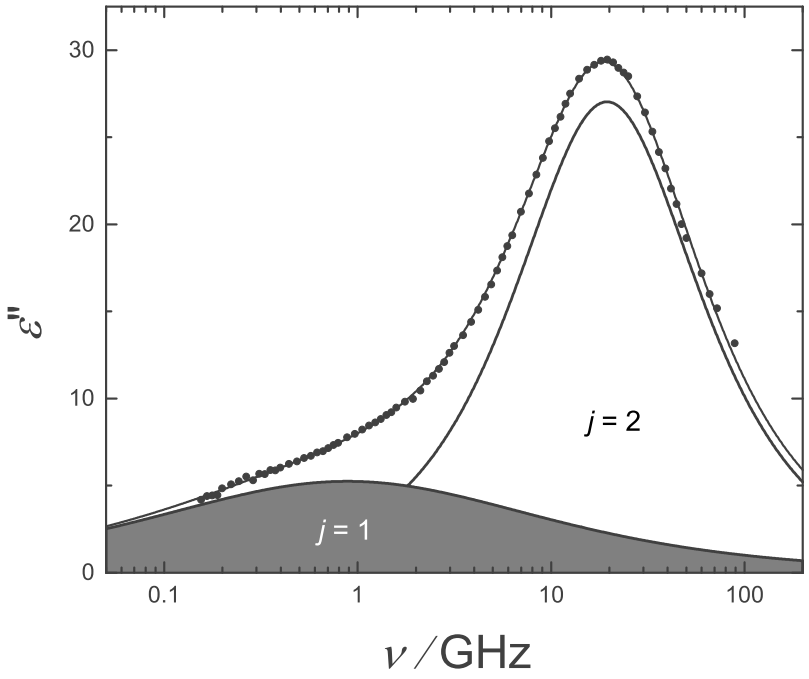

Figure A.3: Dielectric loss of Na_4TES in water fitted with a CC+D model. Contribution $j = 1$ represents the CC mode. Details see table S3.

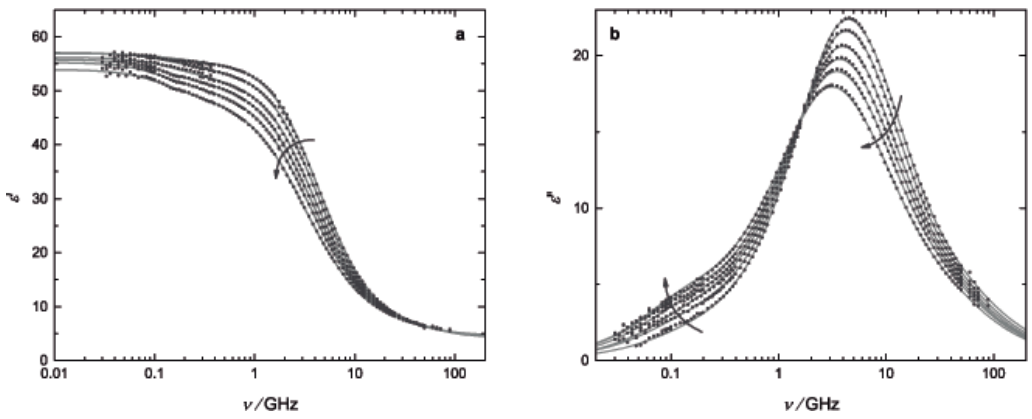

Figure A.4: Recorded (a) Static permittivity, $\varepsilon'(\nu)$, and (b) dielectric loss, $\varepsilon''(\nu)$, spectra of $TAM \cdot (HCl)_4$ in DMSO-Water(10.9% w). Arrows indicated increasing concentration

Appendix B

Supporting Information: Temperature Effect on the Solvation of Two ionic Resorcin[4]arenes from Volumetric and Acoustic Properties in Polar Media

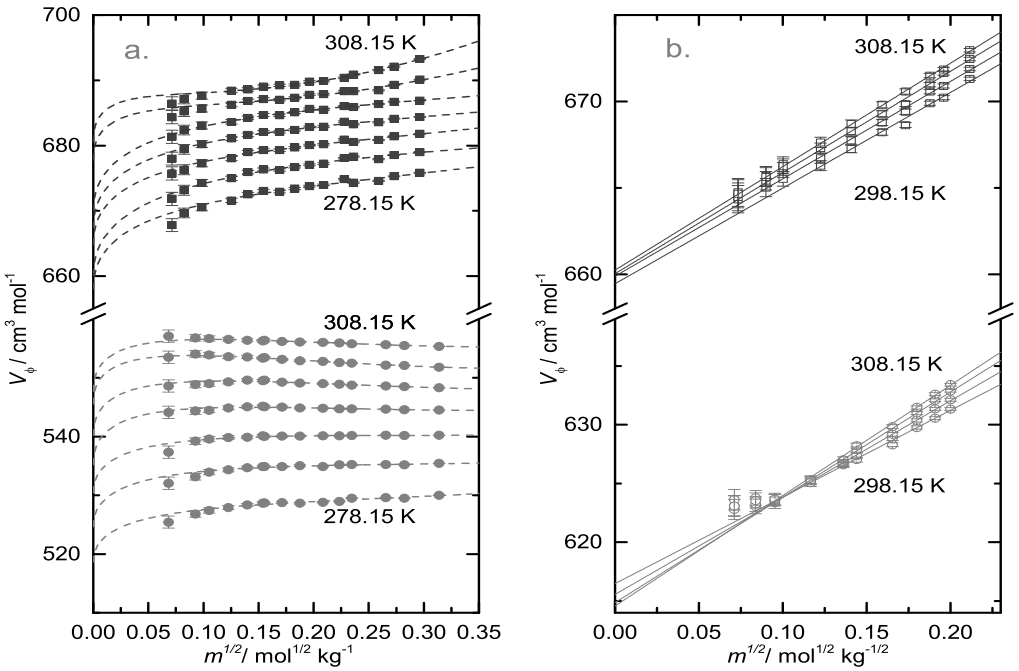

Figure B.1: Apparent molal volumes, V_ϕ, as a function of the square root of the molal, m, concentration at different temperatures. Panel a. shows the V_ϕ of aqueous solutions of Na_4TES (circles) and $TAM \cdot (HCl)_4$ (Squares). Dashed lines represents the fits using eq. (4.2). Panel b. shows the V_ϕ for the solutions in DMSO of Na_4TES(empty squares) and $TAM \cdot (HCl)_4$ (empty circles) at different temperatures. Continuous lines represents fits using eq. (4.4).

Table B.1: Densities, ρ, and apparent molal volumes, V_ϕ, with their uncertainties, u_{V_ϕ}, as function of molal concentration,m, at different temperatures of aqueous solutions of Na_4TES.[a]

T	m	ρ	$V_\phi(\pm u_{V_\phi})$	T	m	ρ	$V_\phi(\pm u_{V_\phi})$	T	m	ρ	$V_\phi(\pm u_{V_\phi})$	T	m	ρ	$V_\phi(\pm u_{V_\phi})$
278.15	0.004680	1.002221	525.4(±1.0)	283.15	0.004680	1.001926	532.1(±1.0)	288.15	0.004680	1.001302	537.3(±1.0)	293.15	0.004680	1.00038	544.1(±1.0)
	0.008558	1.004071	526.8(±0.6)		0.008558	1.003753	533.1(±0.6)		0.008558	1.003102	539.2(±0.6)		0.008558	1.00216	544.4(±0.6)
	0.011036	1.005247	527.4(±0.4)		0.011036	1.004911	533.9(±0.4)		0.011036	1.004250	539.6(±0.4)		0.011036	1.00330	544.5(±0.4)
	0.015053	1.007147	527.9(±0.3)		0.015053	1.006787	534.3(±0.3)		0.015053	1.006105	539.9(±0.3)		0.015053	1.00514	544.9(±0.3)
	0.019513	1.009245	528.4(±0.2)		0.019513	1.008858	534.7(±0.2)		0.019513	1.008158	539.9(±0.2)		0.019513	1.00716	545.1(±0.2)
	0.023651	1.011182	528.7(±0.2)		0.023651	1.010771	534.9(±0.2)		0.023651	1.010049	540.1(±0.2)		0.023651	1.00904	545.2(±0.2)
	0.024180	1.011429	528.7(±0.2)		0.024180	1.011015	534.9(±0.2)		0.024180	1.010293	540.03(±0.2)		0.024180	1.00928	545.1(±0.2)
	0.029350	1.013841	528.7(±0.2)		0.029350	1.013398	534.9(±0.2)		0.029350	1.012648	540.1(±0.2)		0.029350	1.01161	545.0(±0.2)
	0.035171	1.016546	528.6(±0.1)		0.035171	1.016058	535.1(±0.1)		0.035171	1.015283	540.1(±0.1)		0.035171	1.01422	544.9(±0.1)
	0.043364	1.020316	528.8(±0.1)		0.043364	1.019789	534.9(±0.1)		0.043364	1.018965	540.1(±0.1)		0.043364	1.01787	544.8(±0.1)
	0.049848	1.023272	529.0(±0.1)		0.049848	1.022701	535.2(±0.1)		0.049848	1.021859	540.1(±0.1)		0.049848	1.02074	544.7(±0.1)
	0.055077	1.025618	529.5(±0.1)		0.055077	1.025042	535.2(±0.1)		0.055077	1.024174	540.2(±0.1)		0.055077	1.02304	544.7(±0.1)
	0.070481	1.032529	529.6(±0.1)		0.070481	1.031871	535.2(±0.1)		0.070481	1.030926	540.2(±0.1)		0.070481	1.02973	544.6(±0.1)
	0.079764	1.036652	529.5(±0.1)		0.079764	1.035938	535.2(±0.1)		0.079764	1.034949	540.2(±0.1)		0.079764	1.03371	544.6(±0.1)
	0.098550	1.044817	529.98(±0.04)		0.098550	1.044024	535.41(±0.04)		0.098550	1.042962	540.2(±0.04)		0.098550	1.04166	544.49(±0.04)
298.15	0.004680	0.999197	548.6(±1.0)	303.15	0.004680	0.997778	553.5(±1.0)	308.15	0.004680	0.996143	557.1(±1.1)				
	0.008558	1.000968	548.9(±0.6)		0.008558	0.999528	554.1(±0.6)		0.008558	0.997887	556.8(±0.6)				
	0.011036	1.002095	549.0(±0.4)		0.011036	1.000646	553.9(±0.4)		0.011036	0.998998	556.7(±0.4)				
	0.015053	1.003913	549.3(±0.3)		0.015053	1.002454	553.6(±0.3)		0.015053	1.000793	556.6(±0.3)				
	0.019513	1.005920	549.6(±0.2)		0.019513	1.004449	553.5(±0.2)		0.019513	1.002778	556.4(±0.2)				
	0.023651	1.007779	549.5(±0.2)		0.023651	1.006296	553.3(±0.2)		0.023651	1.004612	556.3(±0.2)				
	0.024180	1.008014	549.6(±0.2)		0.024180	1.006528	553.5(±0.2)		0.024180	1.004843	556.4(±0.2)				
	0.029350	1.010332	549.2(±0.2)		0.029350	1.008826	553.1(±0.2)		0.029350	1.007123	556.2(±0.2)				
	0.035171	1.012922	549.1(±0.1)		0.035171	1.011397	552.9(±0.1)		0.035171	1.009673	556.1(±0.1)				
	0.043364	1.016539	549.0(±0.1)		0.043364	1.014985	552.8(±0.1)		0.043364	1.013235	556.0(±0.1)				
	0.049848	1.019381	548.9(±0.1)		0.049848	1.017809	552.6(±0.1)		0.049848	1.016032	556.0(±0.1)				
	0.055077	1.021662	548.8(±0.1)		0.055077	1.020068	552.5(±0.1)		0.055077	1.018280	555.8(±0.1)				
	0.070481	1.028302	548.6(±0.1)		0.070481	1.026667	552.2(±0.1)		0.070481	1.024820	555.6(±0.1)				
	0.079764	1.032252	548.5(±0.1)		0.079764	1.030585	552.1(±0.1)		0.079764	1.028714	555.5(±0.1)				
	0.098550	1.040142	548.29(±0.04)		0.098550	1.038420	551.8(±0.04)		0.098550	1.036475	555.36(±0.04)				

[a] Units: T in K; m in mol kg^{-}1; ρ in kg L^{-1}; V_ϕ and in cm^3 mol^{-1}. Pressure atmospheric, $p = 0.07466$ MPa. Standard uncertainties, u, are $u(T) = 0.005$ K; $u(p) = 1$ kPa.

Table B.2: Densities, ρ, and apparent molal volumes, V_ϕ, with their uncertainties, u_{V_ϕ}, as function of molal concentration,m, at different temperatures of aqueous solutions of TAM $\cdot$ $(HCl)_4$.[a]

T	m	ρ	$V_\phi(\pm u_{V_\phi})$	T	m	ρ	$V_\phi(\pm u_{V_\phi})$	T	m	ρ	$V_\phi(\pm u_{V_\phi})$	T	m	ρ	$V_\phi(\pm u_{V_\phi})$
278.15	0.005096	1.001239	667.8(±1.0)	283.15	0.005096	1.000955	671.8(±1.0)	288.15	0.005096	1.000337	675.7(±1.0)	293.15	0.005096	0.999433	678.0(±1.0)
	0.007057	1.001648	669.7(±0.8)		0.007057	1.001361	673.2(±0.8)		0.007057	1.000742	676.3(±0.8)		0.007057	0.999829	679.4(±0.7)
	0.010080	1.002356	670.6(±0.5)		0.010080	1.002057	674.3(±0.5)		0.010080	1.001431	677.3(±0.5)		0.010080	1.000512	680.2(±0.5)
	0.016319	1.003804	671.6(±0.3)		0.016319	1.003489	675.0(±0.3)		0.016319	1.002846	678.0(±0.3)		0.016319	1.001910	681.1(±0.3)
	0.020473	1.004750	672.5(±0.3)		0.020473	1.004421	676.0(±0.3)		0.020473	1.003767	679.0(±0.3)		0.020473	1.002829	681.6(±0.3)
	0.024764	1.005723	673.1(±0.2)		0.024764	1.005385	676.3(±0.2)		0.024764	1.004722	679.3(±0.2)		0.024764	1.003771	682.1(±0.2)
	0.029770	1.006868	672.9(±0.2)		0.029770	1.006514	676.2(±0.2)		0.029770	1.005836	679.3(±0.2)		0.029770	1.004874	682.1(±0.2)
	0.034711	1.007972	673.4(±0.2)		0.034711	1.007603	676.7(±0.2)		0.034711	1.006914	679.7(±0.2)		0.034711	1.005944	682.4(±0.2)
	0.040044	1.009155	673.8(±0.1)		0.040044	1.008772	677.1(±0.1)		0.040044	1.008068	680.1(±0.1)		0.040044	1.007084	682.9(±0.1)
	0.045411	1.010342	674.0(±0.1)		0.045411	1.009943	677.2(±0.1)		0.045411	1.009229	680.2(±0.1)		0.045411	1.008236	682.9(±0.1)
	0.054013	1.012194	674.8(±0.1)		0.054013	1.011772	678.1(±0.1)		0.054013	1.011041	680.9(±0.1)		0.054013	1.010028	683.7(±0.1)
	0.055720	1.013096	674.3(±0.1)		0.055720	1.012620	678.3(±0.1)		0.055720	1.011914	680.5(±0.1)		0.055720	1.010895	683.2(±0.1)
	0.067107	1.015644	674.6(±0.1)		0.067107	1.015171	677.9(±0.1)		0.067107	1.014398	680.9(±0.1)		0.067107	1.013353	683.6(±0.1)
	0.074508	1.017241	675.3(±0.1)		0.074508	1.016750	678.6(±0.1)		0.074508	1.015963	681.4(±0.1)		0.074508	1.014903	684.1(±0.1)
	0.087733	1.020091	675.8(±0.1)		0.087733	1.019569	679.0(±0.1)		0.087733	1.018755	681.8(±0.1)		0.087733	1.017678	684.4(±0.1)
298.15	0.005096	0.998260	681.4(±1.0)	303.15	0.005096	0.996851	684.4(±1.0)	308.15	0.005096	0.995225	686.5(±1.0)				
	0.007057	0.998654	682.4(±0.8)		0.007057	0.997242	685.2(±0.8)		0.007057	0.995615	687.2(±0.8)				
	0.010080	0.999331	683.1(±0.5)		0.010080	0.997915	685.7(±0.5)		0.010080	0.996284	687.7(±0.5)				
	0.016319	1.000720	683.6(±0.3)		0.016319	0.999292	686.3(±0.3)		0.016319	0.997651	688.4(±0.3)				
	0.020473	1.001630	684.2(±0.3)		0.020473	1.000195	686.8(±0.3)		0.020473	0.998556	688.6(±0.3)				
	0.024764	1.002564	684.7(±0.2)		0.024764	1.001125	687.1(±0.2)		0.024764	0.999478	689.0(±0.2)				
	0.029770	1.003658	684.6(±0.2)		0.029770	1.002212	687.0(±0.2)		0.029770	1.000552	689.2(±0.2)				
	0.034711	1.004715	685.1(±0.2)		0.034711	1.003265	687.3(±0.2)		0.034711	1.001606	689.3(±0.2)				
	0.040044	1.005841	685.6(±0.1)		0.040044	1.004386	687.8(±0.1)		0.040044	1.002720	689.8(±0.1)				
	0.045411	1.006989	685.5(±0.1)		0.045411	1.005518	687.9(±0.1)		0.045411	1.003845	689.9(±0.1)				
	0.054013	1.008777	686.0(±0.1)		0.054013	1.007297	688.3(±0.1)		0.054013	1.005612	690.4(±0.1)				
	0.055720	1.009622	685.9(±0.1)		0.055720	1.008128	688.3(±0.1)		0.055720	1.006411	690.9(±0.1)				
	0.067107	1.012047	686.4(±0.1)		0.067107	1.010556	688.5(±0.1)		0.067107	1.008785	691.6(±0.1)				
	0.074508	1.013596	686.7(±0.1)		0.074508	1.012060	689.3(±0.1)		0.074508	1.010296	692.1(±0.1)				
	0.087733	1.016353	686.9(±0.1)		0.087733	1.014741	690.1(±0.1)		0.087733	1.012292	693.3(±0.1)				

[a] Units: T in K; m in mol kg^{-}1; ρ in kg L^{-1}; V_ϕ and in cm^3 mol^{-1}. Pressure atmospheric, $p = 0.07466$ MPa. Standard uncertainties, u, are $u(T) = 0.005$ K; $u(p) = 1$ kPa.

Table B.3: Densities, ρ, and apparent molal volumes, V_ϕ, with their uncertainties, u_{V_ϕ}, as function of molal concentration,m, at different temperatures of DMSO solutions of $Na_4TES$and $TAM \cdot (HCl)_4$.[a]

T	Solute	m	ρ	$V_\phi(\pm u_{V_\phi})$	T	Solute	m	ρ	$V_\phi(\pm u_{V_\phi})$	T	Solute	m	ρ	$V_\phi(\pm u_{V_\phi})$	T	Solute	m	ρ	$V_\phi(\pm u_{V_\phi})$
293.15	Na_4TES	0.005065	1.102279	623.1(±0.9)	298.15	Na_4TES	0.005065	1.097276	622.8(±0.9)	303.15	Na_4TES	0.005065	1.092269	623.6(±0.9)	308.15	Na_4TES	0.005065	1.087271	623.1(±0.9)
		0.007014	1.102967	623.1(±0.6)			0.007014	1.097964	623.2(±0.6)			0.007014	1.092961	623.8(±0.6)			0.007014	1.087965	623.6(±0.6)
		0.009096	1.103696	623.4(±0.5)			0.009096	1.098696	623.6(±0.5)			0.009096	1.093701	623.6(±0.5)			0.009096	1.088706	623.7(±0.5)
		0.013614	1.105245	625.3(±0.3)			0.013614	1.100257	625.2(±0.3)			0.013614	1.095273	625.1(±0.3)			0.013614	1.090283	625.3(±0.3)
		0.018511	1.106907	626.6(±0.2)			0.018511	1.101925	626.7(±0.2)			0.018511	1.096945	626.8(±0.2)			0.018511	1.091963	627.0(±0.2)
		0.020780	1.107672	627.0(±0.2)			0.020780	1.102688	627.4(±0.2)			0.020780	1.097702	627.9(±0.2)			0.020780	1.092721	628.2(±0.2)
		0.027337	1.109857	628.3(±0.2)			0.027337	1.104876	628.8(±0.2)			0.027337	1.099904	629.2(±0.2)			0.027337	1.094922	629.8(±0.2)
		0.032364	1.111486	629.8(±0.1)			0.032364	1.106509	630.4(±0.1)			0.032364	1.101534	631.0(±0.1)			0.032364	1.096565	631.5(±0.1)
		0.036459	1.112809	630.6(±0.1)			0.036459	1.107829	631.4(±0.1)			0.036459	1.102855	632.1(±0.1)			0.036459	1.09789	632.6(±0.1)
		0.040007	1.113939	631.3(±0.1)			0.040007	1.108963	632.1(±0.1)			0.040007	1.103991	632.9(±0.1)			0.040007	1.099029	633.4(±0.1)
	$TAM \cdot (HCl)_4$	0.005379	1.101591	664.3(±0.8)		$TAM \cdot (HCl)_4$	0.005379	1.096589	664.7(±0.8)		$TAM \cdot (HCl)_4$	0.005379	1.091594	664.5(±0.8)		$TAM \cdot (HCl)_4$	0.005379	1.086592	665.5(±0.8)
		0.008080	1.102137	665.0(±0.5)			0.008080	1.097141	665.4(±0.5)			0.008080	1.092149	665.7(±0.5)			0.008080	1.087154	666.4(±0.5)
		0.010041	1.102529	665.5(±0.4)			0.010041	1.097536	666.0(±0.4)			0.010041	1.092548	666.4(±0.4)			0.010041	1.087559	666.8(±0.4)
		0.015043	1.103523	666.3(±0.3)			0.015043	1.098532	667.3(±0.3)			0.015043	1.093561	667.3(±0.3)			0.015043	1.088579	668.0(±0.3)
		0.019854	1.104458	667.2(±0.2)			0.019854	1.099486	667.8(±0.2)			0.019854	1.094516	668.3(±0.2)			0.019854	1.089546	668.8(±0.2)
		0.025342	1.105507	668.2(±0.2)			0.025342	1.100545	668.8(±0.2)			0.025342	1.095587	669.3(±0.2)			0.025342	1.090623	670.0(±0.2)
		0.030033	1.106402	668.7(±0.1)			0.030033	1.101432	669.7(±0.1)			0.030033	1.096496	669.9(±0.1)			0.030033	1.091538	670.7(±0.1)
		0.035230	1.107347	669.9(±0.1)			0.035230	1.102401	670.6(±0.1)			0.035230	1.097468	671.0(±0.1)			0.035230	1.092541	671.2(±0.1)
		0.038390	1.107931	670.2(±0.1)			0.038390	1.102991	670.9(±0.1)			0.038390	1.098050	671.6(±0.1)			0.038390	1.093111	672.4(±0.1)
		0.044763	1.109070	671.3(±0.1)			0.044763	1.104118	672.5(±0.1)			0.044763	1.099198	673.0(±0.1)			0.044763	1.094271	673.7(±0.1)

[a] Units: T in K; m in mol $kg^{-}1$; ρ in kg L^{-1}; V_ϕ and in cm^3 mol^{-1}. Pressure atmospheric, $p = 0.07466$ MPa. Standard uncertainties, u, are $u(T) = 0.005$ K; $u(p) = 1$ kPa.

Table B.4: Calculated ionic standard expansibility, $E^o(\mathrm{R[4]A}^{4z})$, and parameter b, with their uncertainties u, from the fit of $V^o(\mathrm{R[4]A}^{4z})$ with temperature T using eq. (4.9).[a]

Solute	Solvent	$E^o(\mathrm{R[4]A}^{4z})$	$u_{E^o(\mathrm{R[4]A}^{4z})}$	b	u_b
$\mathrm{TAM \cdot H}^{4+}$	DMSO	0.05	±0.01	609.	±3.
	Water	0.35	±0.01	483.	±4.
TES^{4-}	DMSO	0.15	±0.05	551.	±15.
	Water	0.75	±0.03	346.	±9.

[a] Units: $E^o(\mathrm{R[4]A}^{4z})$ in $\mathrm{cm^3 \cdot mol^{-1}\ K^{-1}}$; b in $\mathrm{cm^3 \cdot mol^{-1}}$

Table B.5: Speed of sound, v, isentropic compressibility, κ_s and solvation number, n and their uncertainties in brackets for the aqueous solutions of Na_4TES at different temperatures.[a]

T	m	v	$10^{14}\kappa_s(\pm u_{\kappa_s})$	$n(\pm u_n)$	T	m	v	$10^{14}\kappa_s(\pm u_{\kappa_s})$	$n(\pm u_n)$	T	m	v	$10^{14}\kappa_s(\pm u_{\kappa_s})$	$n(\pm u_n)$	T	m	v	$10^{14}\kappa_s(\pm u_{\kappa_s})$	$n(\pm u_n)$
278.15	0.004680	1429.0	4.8859(±0.0007)	56.2(±3.4)	283.15	0.004680	1450.3	4.7451(±0.0007)	61.7(±3.4)	288.15	0.004680	1468.1	4.6334(±0.0007)	49.9(±3.3)	293.15	0.004680	1484.4	4.5364(±0.0006)	49.5(±3.3)
	0.008558	1431.2	4.8625(±0.0007)	61.7(±1.9)		0.008558	1451.9	4.7262(±0.0007)	59.4(±1.8)		0.008558	1470.1	4.6128(±0.0007)	56.1(±1.8)		0.008558	1486.0	4.5189(±0.0006)	52.0(±1.8)
	0.011036	1432.1	4.8508(±0.0007)	59.8(±1.4)		0.011036	1453.0	4.7133(±0.0007)	59.6(±1.4)		0.011036	1471.2	4.6006(±0.0006)	56.6(±1.4)		0.011036	1486.9	4.5080(±0.0006)	52.3(±1.4)
	0.015053	1434.2	4.8271(±0.0007)	61.6(±1.1)		0.015053	1454.7	4.6936(±0.0007)	59.0(±1.0)		0.015053	1472.8	4.5824(±0.0006)	55.9(±1.0)		0.015053	1488.7	4.4893(±0.0006)	53.5(±1.0)
	0.019513	1436.2	4.8038(±0.0007)	61.1(±0.8)		0.019513	1456.6	4.6719(±0.0007)	58.5(±0.8)		0.019513	1474.6	4.5615(±0.0006)	55.9(±0.8)		0.019513	1490.3	4.4703(±0.0006)	53.1(±0.8)
	0.023651	1437.3	4.7874(±0.0007)	58.2(±0.7)		0.023651	1457.7	4.6563(±0.0007)	55.9(±0.7)		0.023651	1475.8	4.5460(±0.0006)	54.0(±0.6)		0.023651	1491.5	4.4549(±0.0006)	51.8(±0.6)
	0.024180	1437.6	4.7838(±0.0007)	58.6(±0.6)		0.024180	1458.5	4.6501(±0.0007)	57.7(±0.6)		0.024180	1476.3	4.5419(±0.0006)	54.8(±0.6)		0.024180	1491.9	4.4516(±0.0006)	52.3(±0.6)
	0.029350	1440.3	4.7547(±0.0007)	59.5(±0.5)		0.029350	1460.4	4.6270(±0.0007)	56.7(±0.5)		0.029350	1478.3	4.5185(±0.0006)	54.7(±0.5)		0.029350	1493.8	4.4301(±0.0006)	52.0(±0.5)
	0.035171	1443.0	4.7241(±0.0007)	59.5(±0.4)		0.035171	1462.7	4.6000(±0.0007)	56.2(±0.4)		0.035171	1480.6	4.4929(±0.0006)	54.3(±0.4)		0.035171	1496.1	4.4051(±0.0006)	52.1(±0.4)
	0.043364	1446.3	4.6857(±0.0007)	58.3(±0.4)		0.043364	1466.4	4.5604(±0.0006)	56.2(±0.4)		0.043364	1483.8	4.4576(±0.0006)	53.8(±0.3)		0.043364	1499.0	4.3723(±0.0006)	51.5(±0.3)
	0.049848	1448.5	4.6575(±0.0007)	57.1(±0.3)		0.049848	1468.3	4.5354(±0.0006)	54.7(±0.3)		0.049848	1486.2	4.4303(±0.0006)	53.3(±0.3)		0.049848	1501.3	4.3464(±0.0006)	51.1(±0.3)
	0.055077	1449.2	4.6424(±0.0007)	54.8(±0.3)		0.055077	1469.0	4.5207(±0.0006)	52.7(±0.3)		0.055077	1486.4	4.4192(±0.0006)	50.6(±0.3)		0.055077	1501.6	4.3349(±0.0006)	48.8(±0.3)
	0.070481	1456.3	4.5664(±0.0007)	55.0(±0.2)		0.070481	1475.7	4.4502(±0.0006)	52.8(±0.2)		0.070481	1492.7	4.3537(±0.0006)	50.7(±0.2)		0.070481	1507.6	4.2729(±0.0006)	48.8(±0.2)
	0.079764	1461.2	4.5178(±0.0006)	55.5(±0.2)		0.079764	1480.5	4.4040(±0.0006)	53.4(±0.2)		0.079764	1497.1	4.3109(±0.0006)	51.2(±0.2)		0.079764	1511.6	4.2336(±0.0006)	49.2(±0.2)
	0.098550	1467.6	4.4436(±0.0006)	53.4(±0.1)		0.098550	1486.4	4.3355(±0.0006)	51.3(±0.1)		0.098550	1502.8	4.2454(±0.0006)	49.3(±0.1)		0.098550	1517.1	4.1713(±0.0006)	47.5(±0.1)
298.15	0.004680	1498.9	4.4547(±0.0006)	51.9(±3.3)	303.15	0.004680	1511.2	4.3883(±0.0006)	51.8(±3.2)	308.15	0.004680	1521.7	4.3353(±0.0006)	48.9(±3.2)					
	0.008558	1500.1	4.4397(±0.0006)	50.1(±1.8)		0.008558	1512.4	4.3742(±0.0006)	49.1(±1.8)		0.008558	1522.8	4.3217(±0.0006)	47.1(±1.8)					
	0.011036	1501.0	4.4292(±0.0006)	50.7(±1.4)		0.011036	1513.1	4.3648(±0.0006)	48.8(±1.4)		0.011036	1523.6	4.3121(±0.0006)	47.6(±1.4)					
	0.015053	1502.6	4.4118(±0.0006)	51.5(±1.0)		0.015053	1514.4	4.3495(±0.0006)	48.5(±1.0)		0.015053	1524.9	4.2969(±0.0006)	47.8(±1.0)					
	0.019513	1504.2	4.3939(±0.0006)	51.1(±0.8)		0.019513	1516.1	4.3311(±0.0006)	49.4(±0.8)		0.019513	1526.5	4.2794(±0.0006)	48.3(±0.8)					
	0.023651	1505.3	4.3793(±0.0006)	49.8(±0.6)		0.023651	1517.3	4.3168(±0.0006)	48.3(±0.6)		0.023651	1527.8	4.2648(±0.0006)	47.7(±0.6)					
	0.024180	1505.7	4.3761(±0.0006)	50.4(±0.6)		0.024180	1517.5	4.3141(±0.0006)	48.7(±0.6)		0.024180	1527.8	4.2637(±0.0006)	47.2(±0.6)					
	0.029350	1507.5	4.3551(±0.0006)	50.4(±0.5)		0.029350	1519.3	4.2942(±0.0006)	48.7(±0.5)		0.029350	1529.1	4.2464(±0.0006)	46.4(±0.5)					
	0.035171	1509.6	4.3322(±0.0006)	50.1(±0.4)		0.035171	1521.3	4.2723(±0.0006)	48.4(±0.4)		0.035171	1531.2	4.2245(±0.0006)	46.7(±0.4)					
	0.043364	1512.4	4.3010(±0.0006)	49.6(±0.3)		0.043364	1523.9	4.2427(±0.0006)	47.9(±0.3)		0.043364	1533.6	4.1962(±0.0006)	46.2(±0.3)					
	0.049848	1514.7	4.2760(±0.0006)	49.4(±0.3)		0.049848	1526.1	4.2186(±0.0006)	47.7(±0.3)		0.049848	1535.8	4.1728(±0.0006)	46.2(±0.3)					
	0.055077	1515.6	4.2611(±0.0006)	48.0(±0.3)		0.055077	1526.2	4.2087(±0.0006)	45.5(±0.3)		0.055077	1536.9	4.1578(±0.0006)	45.3(±0.3)					
	0.070481	1520.5	4.2066(±0.0006)	47.1(±0.2)		0.070481	1531.5	4.1525(±0.0006)	45.6(±0.2)		0.070481	1541.5	4.1065(±0.0006)	44.6(±0.2)					
	0.079764	1524.3	4.1695(±0.0006)	47.4(±0.2)		0.079764	1535.2	4.1173(±0.0006)	45.8(±0.2)		0.079764	1544.5	4.0751(±0.0005)	44.5(±0.2)					
	0.098550	1529.3	4.1105(±0.0006)	45.8(±0.1)		0.098550	1540.0	4.0605(±0.0006)	44.4(±0.1)		0.098550	1549.6	4.0179(±0.0005)	43.4(±0.1)					

[a] Units: T in K; m in mol kg^{-1}; v in m s^{-1}; κ_s in Pa^{-1}. Pressure atmospheric, $p = 0.07466$ MPa. Standard uncertainties are $u(v) = 0.1$ m s^{-1}; $u(T) = 0.005$ K; $u(p) = 1$ kPa.

Table B.6: Speed of sound, v, isentropic compressibility, κ_s and solvation number, n and their uncertainties in brackets for the aqueous solutions of TAM $\cdot$ $(HCl)_4$ at different temperatures.[a]

T	m	v	$10^{14}\kappa_s(\pm u_{\kappa_s})$	$n(\pm u_n)$	T	m	v	$10^{14}\kappa_s(\pm u_{\kappa_s})$	$n(\pm u_n)$	T	m	v	$10^{14}\kappa_s(\pm u_{\kappa_s})$	$n(\pm u_n)$	T	m	v	$10^{14}\kappa_s(\pm u_{\kappa_s})$	$n(\pm u_n)$
278.15	0.005096	1429.6	4.8872(±0.0007)	48.8(±3.1)	283.15	0.005096	1450.4	4.7494(±0.0007)	46.8(±3.1)	288.15	0.005096	1468.7	4.6341(±0.0007)	44.1(±3.1)	293.15	0.005096	1484.9	4.5376(±0.0006)	42.5(±3.0)
	0.007057	1430.4	4.8794(±0.0007)	49.5(±2.4)		0.007057	1451.2	4.7421(±0.0007)	47.6(±2.3)		0.007057	1469.4	4.6278(±0.0007)	44.3(±2.3)		0.007057	1485.6	4.5319(±0.0006)	42.3(±2.3)
	0.010080	1431.6	4.8678(±0.0007)	48.2(±1.6)		0.010080	1452.6	4.7298(±0.0007)	48.1(±1.6)		0.010080	1470.8	4.6163(±0.0007)	45.1(±1.6)		0.010080	1486.5	4.5235(±0.0006)	40.1(±1.6)
	0.016319	1434.6	4.8405(±0.0007)	49.5(±1.0)		0.016319	1455.1	4.7065(±0.0007)	47.0(±1.0)		0.016319	1473.2	4.5946(±0.0006)	44.4(±1.0)		0.016319	1489.1	4.5010(±0.0006)	42.3(±1.0)
	0.020473	1436.3	4.8248(±0.0007)	48.5(±0.8)		0.020473	1457.0	4.6901(±0.0007)	47.2(±0.8)		0.020473	1475.0	4.5791(±0.0006)	44.8(±0.8)		0.020473	1490.7	4.4871(±0.0006)	42.3(±0.8)
	0.024764	1438.6	4.8043(±0.0007)	49.8(±0.7)		0.024764	1459.0	4.6728(±0.0007)	47.4(±0.7)		0.024764	1476.8	4.5634(±0.0006)	44.9(±0.6)		0.024764	1492.5	4.4721(±0.0006)	42.6(±0.6)
	0.029770	1440.8	4.7845(±0.0007)	49.3(±0.5)		0.029770	1461.0	4.6548(±0.0007)	46.8(±0.5)		0.029770	1478.7	4.5467(±0.0006)	44.3(±0.5)		0.029770	1494.4	4.4563(±0.0006)	42.2(±0.5)
	0.034711	1443.1	4.7639(±0.0007)	49.2(±0.5)		0.034711	1463.2	4.6358(±0.0007)	46.8(±0.5)		0.034711	1480.8	4.5290(±0.0006)	44.3(±0.5)		0.034711	1496.3	4.4400(±0.0006)	42.2(±0.5)
	0.040044	1445.3	4.7439(±0.0007)	48.6(±0.4)		0.040044	1465.3	4.6173(±0.0007)	46.2(±0.4)		0.040044	1482.8	4.5115(±0.0006)	43.9(±0.4)		0.040044	1498.5	4.4221(±0.0006)	42.2(±0.4)
	0.045411	1447.8	4.7216(±0.0007)	48.6(±0.4)		0.045411	1467.7	4.5967(±0.0007)	46.2(±0.3)		0.045411	1485.1	4.4924(±0.0006)	43.9(±0.3)		0.045411	1500.5	4.4053(±0.0006)	41.9(±0.3)
	0.054013	1450.8	4.6940(±0.0007)	46.9(±0.3)		0.054013	1470.7	4.5698(±0.0006)	44.9(±0.3)		0.054013	1487.9	4.4678(±0.0006)	42.6(±0.3)		0.054013	1503.1	4.3821(±0.0006)	40.7(±0.3)
	0.055720	1452.9	4.6762(±0.0007)	47.3(±0.3)		0.055720	1472.6	4.5537(±0.0006)	45.2(±0.3)		0.055720	1489.8	4.4527(±0.0006)	42.9(±0.3)		0.055720	1504.8	4.3687(±0.0006)	40.8(±0.3)
	0.067107	1457.5	4.6352(±0.0007)	46.2(±0.2)		0.067107	1477.0	4.5154(±0.0006)	44.1(±0.2)		0.067107	1493.9	4.4172(±0.0006)	41.9(±0.2)		0.067107	1508.7	4.3357(±0.0006)	39.9(±0.2)
	0.074508	1460.8	4.6069(±0.0007)	45.9(±0.2)		0.074508	1480.1	4.4893(±0.0006)	43.8(±0.2)		0.074508	1496.9	4.3929(±0.0006)	41.6(±0.2)		0.074508	1511.5	4.3126(±0.0006)	39.7(±0.2)
	0.087733	1466.7	4.5571(±0.0006)	45.4(±0.2)		0.087733	1485.5	4.4446(±0.0006)	43.1(±0.2)		0.087733	1502.0	4.3511(±0.0006)	41.0(±0.2)		0.087733	1516.4	4.2734(±0.0006)	39.2(±0.2)
298.15	0.005096	1499.1	4.4574(±0.0006)	41.2(±3.0)	303.15	0.005096	1511.4	4.3913(±0.0006)	40.2(±3.0)	308.15	0.005096	1522.0	4.3378(±0.0006)	38.6(±3.0)					
	0.007057	1499.7	4.4520(±0.0006)	40.8(±2.3)		0.007057	1512.0	4.3863(±0.0006)	39.5(±2.2)		0.007057	1522.5	4.3333(±0.0006)	37.4(±2.2)					
	0.010080	1500.8	4.4426(±0.0006)	40.5(±1.6)		0.010080	1513.0	4.3776(±0.0006)	38.9(±1.6)		0.010080	1523.4	4.3250(±0.0006)	37.1(±1.6)					
	0.016319	1503.2	4.4227(±0.0006)	40.8(±1.0)		0.016319	1515.3	4.3581(±0.0006)	39.7(±1.0)		0.016319	1525.6	4.3064(±0.0006)	38.1(±1.0)					
	0.020473	1504.6	4.4103(±0.0006)	40.3(±0.8)		0.020473	1516.6	4.3470(±0.0006)	38.8(±0.8)		0.020473	1526.8	4.2963(±0.0006)	36.9(±0.8)					
	0.024764	1506.3	4.3960(±0.0006)	40.8(±0.6)		0.024764	1518.3	4.3334(±0.0006)	39.2(±0.6)		0.024764	1528.4	4.2833(±0.0006)	37.5(±0.6)					
	0.029770	1508.1	4.3810(±0.0006)	40.5(±0.5)		0.029770	1519.9	4.3192(±0.0006)	38.9(±0.5)		0.029770	1530.0	4.2693(±0.0006)	37.4(±0.5)					
	0.034711	1509.8	4.3663(±0.0006)	40.2(±0.4)		0.034711	1521.6	4.3052(±0.0006)	38.6(±0.4)		0.034711	1531.5	4.2564(±0.0006)	37.0(±0.4)					
	0.040044	1512.1	4.3483(±0.0006)	40.6(±0.4)		0.040044	1523.8	4.2881(±0.0006)	39.1(±0.4)		0.040044	1533.5	4.2410(±0.0006)	37.2(±0.4)					
	0.045411	1514.0	4.3326(±0.0006)	40.3(±0.3)		0.045411	1525.6	4.2732(±0.0006)	38.8(±0.3)		0.045411	1535.4	4.2255(±0.0006)	37.4(±0.3)					
	0.054013	1516.4	4.3109(±0.0006)	39.1(±0.3)		0.054013	1527.9	4.2526(±0.0006)	37.6(±0.3)		0.054013	1537.6	4.2060(±0.0006)	36.2(±0.3)					
	0.055720	1517.9	4.2988(±0.0006)	39.1(±0.3)		0.055720	1529.2	4.2416(±0.0006)	37.5(±0.3)		0.055720	1538.8	4.1962(±0.0006)	35.9(±0.3)					
	0.067107	1521.5	4.2682(±0.0006)	38.1(±0.2)		0.067107	1532.8	4.2120(±0.0006)	36.7(±0.2)		0.067107	1542.2	4.1678(±0.0006)	35.2(±0.2)					
	0.074508	1524.3	4.2460(±0.0006)	38.0(±0.2)		0.074508	1535.3	4.1917(±0.0006)	36.5(±0.2)		0.074508	1544.7	4.1485(±0.0006)	35.0(±0.2)					
	0.087733	1528.9	4.2090(±0.0006)	37.5(±0.2)		0.087733	1539.7	4.1569(±0.0006)	36.0(±0.2)		0.087733	1549.0	4.1170(±0.0006)	34.3(±0.2)					

[a] Units: T in K; m in mol kg^{-1}; v in m s^{-1}; κ_s in Pa^{-1}. Pressure atmospheric, $p = 0.07466$ MPa. Standard uncertainties are $u(v) = 0.1$ m s^{-1}; $u(T) = 0.005$ K; $u(p) = 1$ kPa.

Table B.7: Speed of sound, v, isentropic compressibility, κ_s and solvation number, n, and their uncertainties in brackets for the solutions in DMSO of Na_4TES and $TAM \cdot (HCl)_4$ at different temperatures.[a]

T	Solute	m	v	$10^{14}\kappa_s(\pm u_{\kappa_s})$	$n(\pm u_n)$	T	Solute	m	v	$10^{14}\kappa_s(\pm u_{\kappa_s})$	$n(\pm u_n)$
293.15	$TAM \cdot (HCl)_4$	0.005379	1506.4	4.0003(±0.0006)	7.8(±0.7)	298.15	$TAM \cdot (HCl)_4$	0.005379	1489.4	4.1111(±0.0006)	7.9(±0.7)
		0.008080	1507.4	3.9931(±0.0006)	8.0(±0.4)			0.008080	1490.3	4.1037(±0.0006)	8.1(±0.4)
		0.010041	1507.9	3.9890(±0.0006)	7.8(±0.4)			0.010041	1490.8	4.0995(±0.0006)	7.8(±0.4)
		0.015043	1509.4	3.9774(±0.0006)	7.6(±0.2)			0.015043	1492.3	4.0877(±0.0006)	7.7(±0.2)
		0.019854	1510.8	3.9668(±0.0006)	7.5(±0.2)			0.019854	1493.7	4.0765(±0.0006)	7.6(±0.2)
		0.025342	1513.0	3.9515(±0.0005)	7.8(±0.1)			0.025342	1495.9	4.0606(±0.0006)	7.9(±0.1)
		0.030033	1513.7	3.9445(±0.0005)	7.3(±0.1)			0.030033	1496.6	4.0535(±0.0006)	7.4(±0.1)
		0.035230	1515.1	3.9340(±0.0005)	7.2(±0.1)			0.035230	1498.0	4.0425(±0.0006)	7.3(±0.1)
		0.038390	1515.8	3.9284(±0.0005)	7.1(±0.1)			0.038390	1498.7	4.0365(±0.0006)	7.1(±0.1)
		0.044763	1518.1	3.9125(±0.0005)	7.2(±0.1)			0.044763	1501.0	4.0202(±0.0006)	7.3(±0.1)
	Na_4TES	0.005065	1506.2	3.9987(±0.0006)	9.2(±0.7)		Na_4TES	0.005065	1489.2	4.1092(±0.0006)	9.6(±0.7)
		0.007014	1506.8	3.9933(±0.0006)	9.1(±0.5)			0.007014	1489.6	4.1045(±0.0006)	9.0(±0.5)
		0.009096	1507.4	3.9875(±0.0006)	9.1(±0.4)			0.009096	1490.3	4.0982(±0.0006)	9.1(±0.4)
		0.013614	1508.6	3.9755(±0.0006)	8.9(±0.3)			0.013614	1491.4	4.0860(±0.0006)	8.9(±0.3)
		0.018511	1509.8	3.9631(±0.0006)	8.7(±0.2)			0.018511	1493.1	4.0708(±0.0006)	9.1(±0.2)
		0.020780	1510.6	3.9564(±0.0006)	8.7(±0.2)			0.020780	1493.6	4.0650(±0.0006)	8.9(±0.2)
		0.027337	1512.2	3.9403(±0.0005)	8.5(±0.1)			0.027337	1495.6	4.0462(±0.0006)	8.9(±0.1)
		0.032364	1513.5	3.9274(±0.0005)	8.5(±0.1)			0.032364	1496.8	4.0340(±0.0006)	8.7(±0.1)
		0.036459	1514.8	3.9163(±0.0005)	8.5(±0.1)			0.036459	1498.0	4.0228(±0.0006)	8.7(±0.1)
		0.040007	1515.5	3.9085(±0.0005)	8.4(±0.1)			0.040007	1498.8	4.0141(±0.0006)	8.6(±0.1)
303.15	$TAM \cdot (HCl)_4$	0.005379	1472.4	4.2259(±0.0006)	7.9(±0.7)	308.15	$TAM \cdot (HCl)_4$	0.005379	1455.6	4.3438(±0.0006)	7.9(±0.7)
		0.008080	1473.3	4.2181(±0.0006)	8.2(±0.4)			0.008080	1456.6	4.3355(±0.0006)	8.3(±0.5)
		0.010041	1473.8	4.2138(±0.0006)	7.9(±0.4)			0.010041	1457.1	4.3310(±0.0006)	8.0(±0.4)
		0.015043	1475.3	4.2015(±0.0006)	7.7(±0.2)			0.015043	1458.5	4.3186(±0.0006)	7.8(±0.2)
		0.019854	1476.7	4.1897(±0.0006)	7.6(±0.2)			0.019854	1459.9	4.3065(±0.0006)	7.7(±0.2)
		0.025342	1478.9	4.1732(±0.0006)	7.9(±0.1)			0.025342	1462.1	4.2889(±0.0006)	8.0(±0.1)
		0.030033	1479.6	4.1659(±0.0006)	7.4(±0.1)			0.030033	1462.8	4.2813(±0.0006)	7.5(±0.1)
		0.035230	1480.9	4.1546(±0.0006)	7.3(±0.1)			0.035230	1464.1	4.2700(±0.0006)	7.4(±0.1)
		0.038390	1481.7	4.1482(±0.0006)	7.2(±0.1)			0.038390	1464.9	4.2628(±0.0006)	7.3(±0.1)
		0.044763	1483.9	4.1315(±0.0006)	7.3(±0.1)			0.044763	1467.1	4.2459(±0.0006)	7.4(±0.1)
	Na_4TES	0.005065	1472.2	4.2243(±0.0006)	9.3(±0.7)		Na_4TES	0.005065	1455.4	4.3419(±0.0006)	9.5(±0.7)
		0.007014	1472.7	4.2184(±0.0006)	9.2(±0.5)			0.007014	1456.2	4.3345(±0.0006)	10.0(±0.5)
		0.009096	1473.6	4.2104(±0.0006)	9.8(±0.4)			0.009096	1456.9	4.3276(±0.0006)	9.9(±0.4)
		0.013614	1474.8	4.1975(±0.0006)	9.4(±0.3)			0.013614	1458.3	4.3128(±0.0006)	9.8(±0.3)
		0.018511	1476.2	4.1831(±0.0006)	9.3(±0.2)			0.018511	1459.8	4.2975(±0.0006)	9.7(±0.2)
		0.020780	1476.8	4.1772(±0.0006)	9.1(±0.2)			0.020780	1460.6	4.2896(±0.0006)	9.7(±0.2)
		0.027337	1478.8	4.1576(±0.0006)	9.1(±0.1)			0.027337	1462.6	4.2696(±0.0006)	9.5(±0.1)
		0.032364	1480.4	4.1423(±0.0006)	9.1(±0.1)			0.032364	1464.2	4.2540(±0.0006)	9.5(±0.1)
		0.036459	1481.7	4.1299(±0.0006)	9.1(±0.1)			0.036459	1465.6	4.2407(±0.0006)	9.5(±0.1)
		0.040007	1482.5	4.1213(±0.0006)	8.9(±0.1)			0.040007	1467.0	4.2282(±0.0006)	9.6(±0.1)

[a] Units: T in K; m in mol kg^{-}1; v in m s^{-1}; κ_s in Pa^{-1}. Pressure atmospheric, $p = 0.07466$ MPa. Standard uncertainties are $u(v) = 0.1$ m s^{-1}; $u(T) = 0.005$ K; $u(p) = 1$ kPa.

Table B.8: Pure solvent values for the solvent density, ρ_o, and speed of sound, v, at different values.[a]

Solvent	T	ρ_o	v_o
Water[b]	278.15	0.9999641	1427.26
	283.15	0.9997000	1448.14
	288.15	0.9991005	1466.66
	293.15	0.9982058	1482.95
	298.15	0.9970474	1497.20
	303.15	0.9956504	1509.55
	308.15	0.9940313	1520.17
DMSO	293.15	1.100484	1504.71
	298.15	1.095470	1487.63
	303.15	1.090459	1470.68
	308.15	1.085449	1453.90

[a] Units: T in K; ρ_o in kg L^{-1}; v in m s^{-1}. Pressure atmospheric, p = 0.07466 MPa. Standard uncertainties are $u(\rho_o)$ =5 x 10^{-6} kg L$^-$1; $u(v) = 0.1$ m s^{-1}; $u(T) = 0.005$ K; $u(p) = 1$ kPa.[b] Pure water ρ_o values were taken from Ref.[(1)] and v_o from Ref.[(2)]

Bibliography

[1] Kell, G. *Journal of Chemical and Engineering data* **1967**, *12*, 66–69.

[2] Del Grosso, V.; Mader, C. *The Journal of the Acoustical Society of America* **1972**, *52*, 1442–1446.

Appendix C

Supporting Information: Electric Molar Conductivity of Two Ionic Resorcin[4]arenes

Table C.1: Electrical molar conductivity, Λ, for the aqueous solutions of Na_4TES at different temperatures T.[a]

$10^3 m$	T =278.15	T =283.15	T =288.15	T =293.15	T =298.15	T =303.15	T =308.15
0.04051	295.1	341.4	397.6	449.3	503.4	559.6	618.7
0.08309	295.4	341.4	390.0	441.1	494.3	549.6	606.4
0.16472	290.0	334.1	381.8	432.6	486.7	539.3	595.2
0.20445	287.7	331.5	378.3	427.5	479.0	532.8	587.3
0.24705	284.4	328.8	375.6	424.6	475.8	529.0	583.9
0.28748	282.1	326.4	372.9	421.4	472.1	524.9	579.0
0.32725	281.0	324.8	370.9	419.3	470.2	522.9	577.0
0.40726	277.6	320.8	366.3	414.3	464.1	516.2	570.0
1.23481	255.3	299.0	340.5	384.6	431.6	479.8	568.4
2.14952	245.6	283.5	323.9	366.6	411.5	458.3	530.5
2.93682	230.1	266.3	304.5	344.7	387.0	431.2	506.5
3.61978	220.8	255.5	291.9	330.4	370.6	412.5	476.7
4.18862	216.7	250.7	286.6	324.4	364.0	405.0	455.5
4.87160	208.8	241.6	276.1	312.5	350.7	390.1	447.2
5.54371	204.8	236.8	270.5	306.1	343.6	382.4	430.5
6.08865	201.4	233.2	266.7	302.0	339.0	377.5	422.3
6.75745	197.0	228.0	260.8	295.2	331.4	369.0	416.9

[a] Units: m in mol kg^{-1}; Λ in S cm^{-1} mol^{-1}; T in K.

Table C.2: Electrical molar conductivity, Λ, for the DMSO solutions of Na_4TES at different temperatures T.[a]

$10^3 m$	T =293.15	T =298.15	T =303.15	T =308.15
0.44103	72.0	80.3	89.0	97.8
1.03141	67.9	75.7	83.9	92.3
1.76357	61.2	68.3	75.6	83.2
2.25817	58.7	65.5	72.6	79.9
2.80300	56.1	62.6	69.4	76.4
3.45386	53.5	59.7	66.2	72.9
3.91858	52.3	58.3	64.7	71.2
4.40452	50.9	56.9	63.0	69.4
4.89774	49.9	55.6	61.7	67.9
5.38144	48.8	54.5	60.4	66.6
5.84393	48.2	53.9	59.7	65.8
6.32897	47.4	52.9	58.7	64.6
6.79298	46.6	52.1	57.8	63.6
7.25651	46.2	51.6	57.2	63.0
7.62350	45.7	51.1	56.7	62.4

[a] Units: m in mol kg^{-1}; Λ in S cm^{-1} mol^{-1}; T in K.

Table C.3: Electrical molar conductivity, Λ, for the aqueous solutions of TAM $\cdot$ $(HCl)_4$ at different temperatures T.[a]

$10^3 m$	T =278.15	T =283.15	T =288.15	T =293.15	T =298.15	T =303.15	T =308.15
2.14298	372.9	423.9	476.7	531.2	587.5	644.9	704.5
2.96417	364.0	413.7	464.9	517.8	572.2	627.9	686.0
3.89899	355.4	403.6	453.5	504.3	560.1	611.8	667.9
4.86213	349.8	397.4	446.5	497.0	549.0	602.2	657.3
5.75270	344.7	391.6	440.2	490.8	542.1	594.6	648.9
6.59003	340.2	386.4	434.0	483.0	533.3	584.9	638.4
7.42781	337.3	383.0	430.2	478.7	528.7	579.6	632.3
8.19092	335.2	380.1	426.7	474.7	524.3	574.9	626.9
8.80957	331.7	376.7	423.0	470.5	519.5	569.5	621.7

[a] Units: m in mol kg^{-1}; Λ in S cm^{-1} mol^{-1}; T in K.

Table C.4: Electrical molar conductivity, Λ, for the DMSO solutions of TAM $\cdot$ $(HCl)_4$ as at different temperatures T.[a]

$10^3 m$	T =293.15	T =298.15	T =303.15	T =308.15
0.51783	95.1	105.4	116.3	127.6
1.09710	78.4	86.9	95.7	104.9
1.65674	70.4	78.0	85.8	93.8
2.21573	65.1	72.0	79.1	86.5
2.73586	61.5	68.0	74.7	81.7
3.28961	58.3	64.4	70.7	77.3
3.87559	55.5	61.3	67.3	73.5
4.42547	53.7	59.4	65.1	71.2
4.97921	52.0	57.5	63.0	68.8
5.54985	50.3	55.5	61.0	66.6
6.09307	48.8	53.9	59.2	64.7
6.57973	47.7	52.6	57.8	63.1
6.99118	47.8	52.8	58.0	63.4
7.10856	48.0	53.0	58.3	63.7

[a] Units: m in mol kg^{-1}; Λ in S cm^{-1} mol^{-1}; T in K.

Appendix D

Supporting Information: Solvation and Ionic Association of Resorcin[4]arenes in polar media

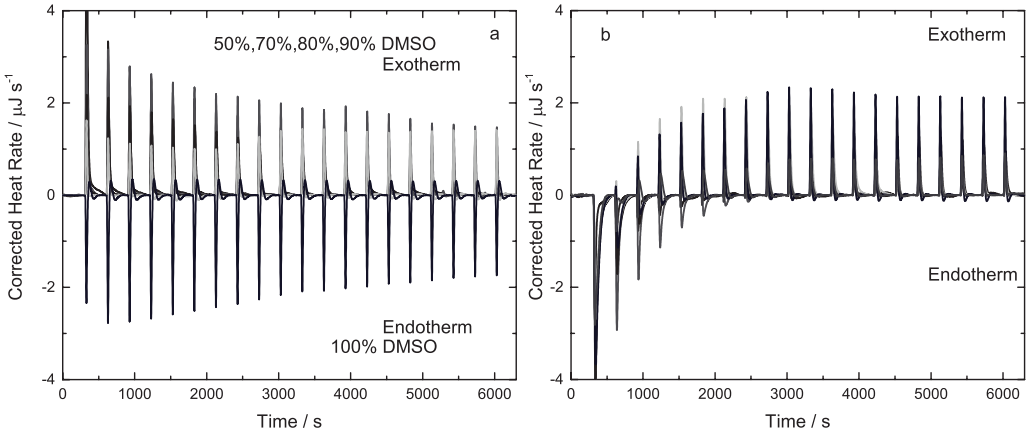

Figure D.1: Dilution titration of $\sim$ 11.5 mM (a) Na_4TES and (b) $TAM \cdot (HCl)_4$ solutions in different mixtures of DMSO-Water at 298.15 K.

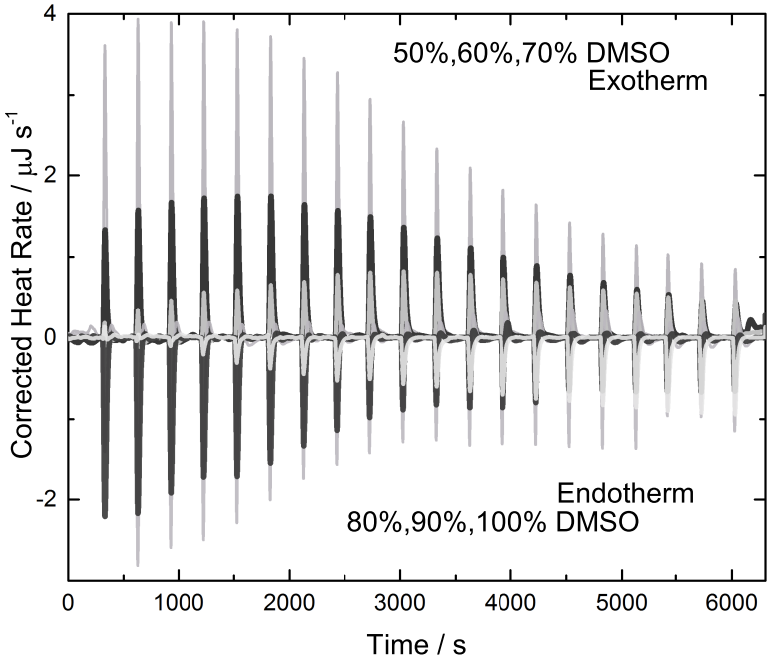

Figure D.2: ITC titration of $\sim$ 11.5 mM Na_4TES into $\sim$ 2.0 mM $TAM \cdot (HCl)_4$ solutions in different mixtures of DMSO-Water at 298.15 K.

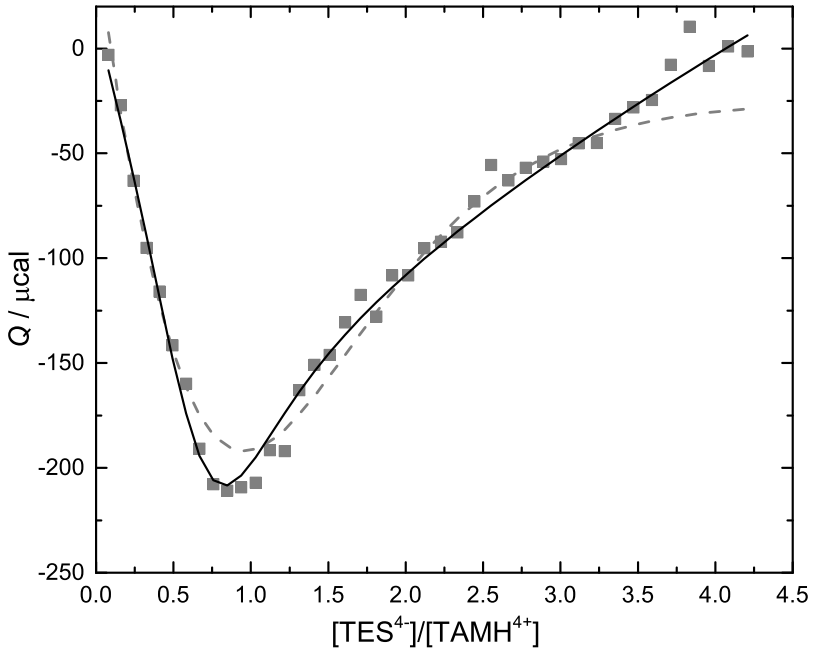

Figure D.3: ITC titration of 11.5 mM Na_4TES into 2.0 mM $TAM \cdot (HCl)_4$ in a mixture of DMSO-Water $w_{DMSO} = 0.7$ at 298.15 K. The dashed line is the fit considering only equilibria (6.3-6.4) and full line represents the model equilibria (6.3-6.5)

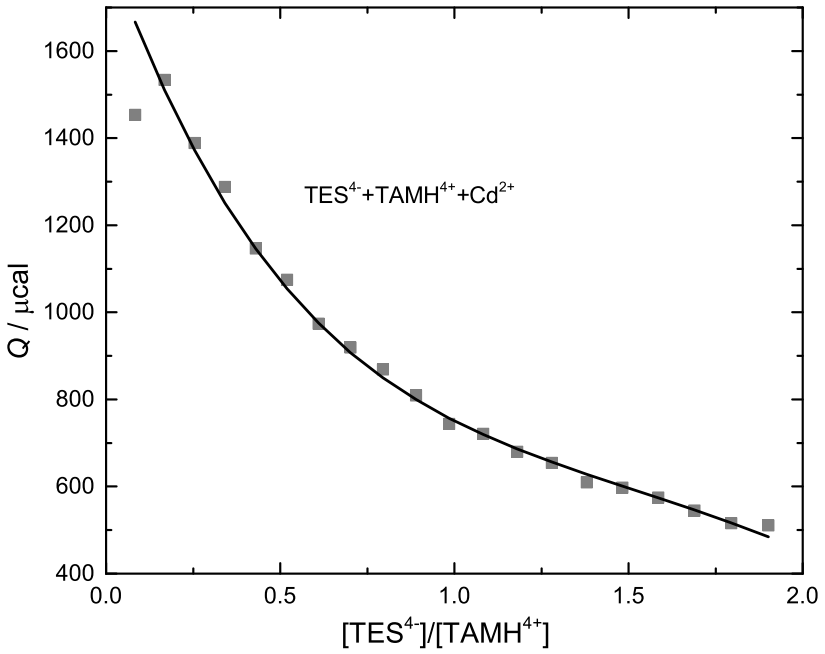

Figure D.4: ITC titration of 11.5 mM Na_4TES into 2.0 mM $TAM \cdot (HCl)_4$ with Cd^{2+} 6.6 mM solutions in different a mixture of DMSO-Water $w_{DMSO} = 0.5$ at 298.15 K .

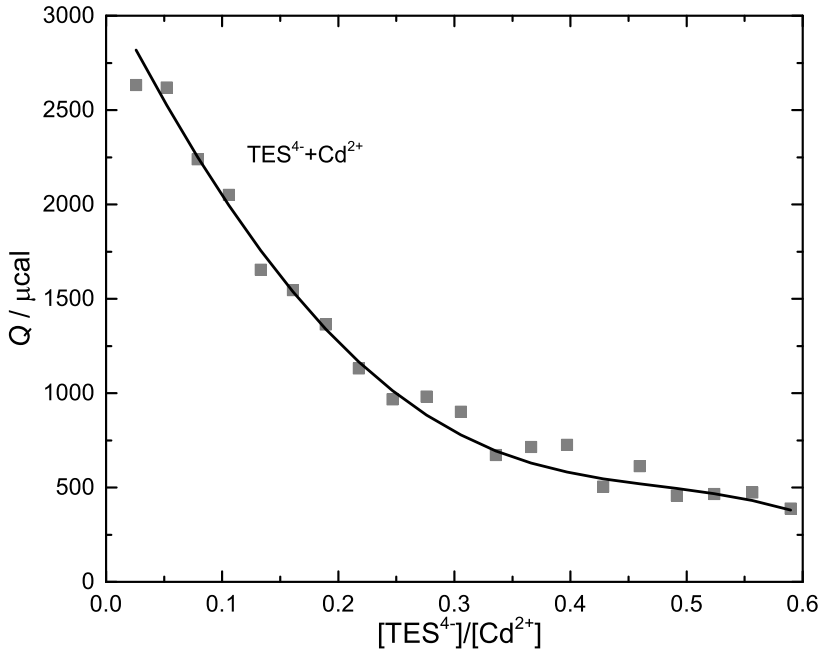

Figure D.5: ITC titration of 11.5 mM Na_4TES into Cd^{2+} 6.6 mM solutions in different a mixture of DMSO-Water $w_{DMSO} = 0.5$ at 298.15 K .